Process Intensification in a Liquid Biphasic Reaction System by Application of an External Electric Field

By

Nan Wang
Ph.D., University of Kansas, 2021

Submitted to the graduate degree program in Chemical Engineering and the Graduate Faculty of the University of Kansas in partial fulfillment of the requirements for the degree of Doctor of Philosophy.

_____

Chair: Laurence R. Weatherley

_____

Raghunath V. Chaudhari

_____

Mark B. Shiflett

_____

Kevin C. Leonard

_____

Michael Rubin

_____

Alan M. Allgeier

Date Defended: 10 May 2021

The dissertation committee for Nan Wang certifies that this is the approved version of the following dissertation:

Process Intensification in a Liquid Biphasic Reaction System by Application of an External Electric Field

Chair: Laurence R. Weatherley

Date Approved: 14 May 2021

ABSTRACT

Due to the increasing concerns on global warming and depletion of fossil fuels, sustainable chemistry and engineering has been a research focus in the 21st century. Tremendous efforts have been devoted to designing inherently safe chemicals and processes with minimal waste emission and energy consumption. Among the many ongoing technologies, conducting chemistry in liquid biphasic systems is a promising approach and has found many successful applications in organic synthesis, biocatalysis, biomass pretreatment, etc. The development of green solvents, such as ionic liquids, further extends the scope of liquid biphasic systems for investigation of sustainable chemistry. While liquid biphasic systems feature many advantages, reactions in those systems usually suffer from mass transfer limitation. To facilitate mass transfer across the interfacial boundary, conventional methods, such as vigorous mechanical agitation or organic additions (e.g., phase transfer catalysts, or surfactants) are being extensively used. These methods, however, require significant energy input, increase the complexity of the reaction systems, and add to environmental concerns. To address this challenge, an intensification method achieved by application of external electric fields is proposed in this thesis. The electrostatic intensification in reaction performance in a liquid biphasic system was studied in two aspects: 1) controlling the migration of reactive species in a batch system, 2) increasing interfacial areas and reaction rates by application of an electrospray in a continuous system. This approach is easy to apply with relatively low energy consumption, thus showing great potential for a wide range of applications.

Chapter I is an introduction of the research background. It discussed the importance and challenges of liquid biphasic systems in the development of sustainable chemistry and engineering. Three typical applications of liquid biphasic reaction systems, phase transfer catalysis, aqueous biphasic systems, and biomass processing, were discussed in terms of their

abilities to achieve sustainability in chemistry and engineering. Recent advances in intensification methods in liquid biphasic systems were discussed with continuous flow processes, including microfluidic systems, and application of external electric fields as representatives. Afterwards, the model reaction system was discussed, followed by the proposals of research motivations and goals.

In Chapter II, the roles of external electric fields in the batch reaction system were examined. It was demonstrated that water participated in the transfer hydrogenation of acetophenone when aqueous sodium formate was employed as hydrogen source. The external electric field was found to act as promoter or inhibitor for the phase transfer hydrogenation depending on the orientation of the electric field, which suggests the great potential of external electric fields in controlling reaction rates.

In Chapter III, the ability of external electric fields to control reaction rates was further explored. It was found that the reaction performance was not linearly dependent on the applied voltages when the reaction time increased. The application of a negative voltage may result in the decomposition of the catalyst, which led to the decreased product enantioselectivity. It was also demonstrated that the reaction could be externally controlled by simply switching the applied electric potential over the course of the reaction.

In Chapter IV, a continuous reaction system based on electrospray was established to further intensify mass transfer and reaction rates. Unlike the observations in Chapter II and III, the orientation of external electric fields was found to show no effects on the reaction performance. The induced electric current in the reaction system due to the increased conductivity of the continuous phase was proposed correlated to the improved conversion and yields. In this

electrospray system, 71% conversion could be achieved in 1 h with a 13-fold increase in throughput compared to that in the batch system studied in Chapter II and III.

In Chapter V, the importance of this work in understanding the roles of external electric fields in organic synthesis and catalysis was summarized. Further research directions and some new ideas were also proposed as complement to this thesis.

Acknowledgements

First of all, I would like to express my sincere gratitude to my advisor Dr. Laurence R. Weatherley, distinguished professor at the Department of Chemical and Petroleum Engineering. I am very grateful to him for taking me as his student when I switched the research group. By the time I joined his group in the Fall of 2017, I was totally new to this area. His kindly guidance and support walked me through my PhD study. The encouragement and inspiration that I obtained from his attitude and enthusiasm in science and research will always inspire me in my scientific career.

I am sincerely grateful to Dr. Alan M. Allgeier for his valuable input and advice on both my research and job searching. His generosity of sharing lab equipment and materials and his friendliness and patience are deeply appreciated. I also benefit from his unique view in science.

I would like to thank my other committee members, Dr. Raghunath V. Chaudhari, Dr. Mark B. Shiflett, Dr. Kevin C. Leonard, and Dr. Michael Rubin for their precious time and valuable suggestions during my preliminary and comprehensive examination and on my research. Special thanks to Dr. Michael Rubin for sharing chemicals from his lab.

I am also grateful for my graduate fellows from the department, Kyle Stephens, Anoop Uchagawkar, Akash Anand, Dr. Luan Nguyen, Yuting Li, Simon Velasquez Morales, for their great help and support in my research and life at KU.

I would like to acknowledge Martha Kehr for her great support on the graduate affairs. Her help with smile and patience is very much appreciated. I am also thankful to Jeff Worth and Scott Ramskill for their help in assisting the lab setup, which creates a much easier environment for

me to conduct research. Great thanks to Jim Hodgson from the Kansas State University for making those excellent glass reactors for my research.

I would like to express my deepest thanks to my parents, my family for their unconditional care, support, and faith in me over the course of my oversea study.

Finally, I want to thank myself for the efforts that I put in over the past 5 years. It is a great experience and memory to study and live in Lawrence. A PhD degree is a milestone that I am achieving in my life, and it is never the end. I am ready to move forward and take the next challenges.

Table of Contents

ABSTRACT ..... **iii**

Acknowledgements ..... **vi**

List of Figures ..... **xiii**

List of Tables ..... **xvi**

Chapter I: Process Intensification in Liquid Biphasic Reaction Systems: Challenges and Opportunities **1**

1.1 Applications of liquid biphasic reaction systems 1

1.1.1 Phase transfer catalysis 2

1.1.2 Aqueous biphasic system 4

1.1.3 Biomass processing reaction 5

1.1.4 Summary 6

1.2 Process intensification in liquid biphasic reaction systems 7

1.2.1 Microreactors 8

1.2.2 Other continuous flow processes 14

1.2.3 Application of external electric fields (EEFs) 17

1.2.4 Summary 23

1.3 Model reaction system 24

1.4 Research motivation 27

1.5 Research goals 29

Chapter II: Enhanced Catalytic Phase Transfer Hydrogenation of Acetophenone by Application of a Low External Electric Field 30

2.1 Introduction 30

2.2 Experimental section 31

2.2.1 Materials 31

2.2.2 Experimental apparatus 31

2.2.3 Experimental procedure 32

2.2.4 Analytical methods and characterizations 33

2.3 Results and discussion 34

2.3.1 Reaction stoichiometry 34

2.3.2 Direction of EEF 36

2.3.2 Possible mechanism 37

2.3.3 Organic solvents 39

2.3.4 Potential of EEF 42

2.4 Conclusions 43

Chapter III: Controlling Reaction Rate of Phase Transfer Hydrogenation of Acetophenone by Application of a Low External Electric Field 45

3.1 Introduction 45

3.2 Experimental section 46

3.2.1 Materials 46

3.2.2 Experimental apparatus and procedure 47

3.2.3 Analytical methods and characterizations 48

3.3 Theoretical modeling and simulation 49

3.4 Results and discussion 51

3.4.1 Solvent effects 51

3.4.2 Electric field potential 53

3.4.3 Proposed mechanism and kinetics study 59

3.4.4 Electric field polarity and product enantioselectivity 61

3.5 Conclusions 64

Chapter IV: An Electrospray-Based Flow Reaction System for Intensified Transfer Hydrogenation of Acetophenone 67

4.1 Introduction 67

4.2 Experimental Section 68

4.2.1 Materials 68

4.2.2 Experiment apparatus 68

4.2.3 Experimental procedure 70

4.2.4 Analytical methods and characterizations 71

4.3 Results and discussion 71

4.3.1 Magnitude and polarity of applied electric fields 71

4.3.2 Flow rates and concentration of dispersed phase 73

4.3.3 Composition of continuous phase 76

4.3.4 Catalyst activity 79

4.4 Conclusions 80

Chapter V: Conclusions and Perspectives of Future Work 82

5.1 Conclusions 82

5.2 Further work 83

5.2.1 Droplet size and charge measurements in an electrospray system 83

5.2.2 Evaluation of the importance of current flow 84

5.2.3 Extension of reaction scopes 85

5.2.4 New reactor design 86

Reference 88

Appendix I: Retention times for different compounds in a nonchiral GC column. 103

Appendix II: GC spectrum of a 24 h reaction sample from a batch reactor with 1-butanol as organic solvent. 104

Appendix III: GC spectrum of a 1 h reaction sample from the electrospray system with 20 mL of organic phase (10 mL toluene and 10 mL 1-butanol) and 2 kV of voltage applied. 105

Appendix IV: XFR analysis data of the black slurry from stainless steel electrode decomposition. 106

Appendix V: Reactor used for the batch reactions in Chapter II and III. 107

Appendix VI: Reactor used for the continuous reaction in Chapter IV..... 108

List of Publications, Presentations and Awards..... 116

List of Figures

Figure 1.1 Representative system and mechanism of a PTC reaction with aqueous anions. 3

Figure 1. 2 Process intensification and its components. 8

Figure 1. 3 Flow patterns in liquid-liquid system, (a) parallel flow, (b) segmented flow. 10

Figure 1.4 Geometries for production of droplets. a) T-junction, b) flow focusing, c) co-flowing, d) membrane. 12

Figure 1.5 (a) Schematic view of a Corning advanced flow reactor, (b) flow patterns of hexane/water within a Corning advanced flow reactor..... 15

Figure 1.6 a) Schematic drawing of the reactor column, b) design of a single stage. 16

Figure 1.7 (a) Possible forces that are imposed on a positively charged liquid entity in a fluid continuum, (b) distribution of electrostatic force on a positively charged liquid entity..... 19

Figure 1.8 Development of a charged droplet formation under an external electric field..... 20

Figure 1.9 Electrostatic dispersion in a liquid-liquid system..... 20

Figure 1.10 Mechanism of asymmetric transfer hydrogenation of acetophenone with 2-propanol catalyzed by chiral RuCl(p-cymene)[Ts-DPEN] complex. 25

Figure 2.1 (a) Sketch of experiment set-up, (b) orientations of the positive and negative electric fields, (c) experiment apparatus with a 15 V of positive electric field applied. 32

Figure 2.2 (a) FTIR spectra for the solid sample, (b) FTIR spectra for the 1:1 mixture of standard sodium formate and sodium bicarbonate, (c) FTIR spectra for the standard sodium bicarbonate, (d) FTIR spectra for the standard sodium formate..... 35

Figure 2.3 Yields of 1-phenylethanol under different electric field conditions (15 V positive OEEF, 15 V negative OEEF, and no OEEF). 37

Figure 2.4 Proposed distribution and migration of ions/species in the two phases under a positive EEF. 39

Figure 2.5 The (a) protonated 16-electron Ru complex and (b)18-electron Ru complex..... 39

Figure 2.6 Yields and selectivity of 1-phenylethanol with different solvents used and 15 V of positive EEF applied. 41

Figure 2.7 Yield and selectivity of 1-phenylethanol under different positive EEF potential with chloroform as solvent. 43

Figure 3.1 Model geometry. L = 0.5 cm. ACP is short for acetophenone. 50

Figure 3.2 Acetophenone conversion (mol%) and 1-phenelethanol yields (mol%) under 0 V or 15 V of positive external electric field for 24 h with different organic solvents and stainless steel electrodes. 52

Figure 3.3 Acetophenone conversion (mol%) under different positive external electric field for 24 h with stainless steel electrodes and 1-butanol as solvent. 54

Figure 3.4 Simulated concentration profiles at the interface under various electric fields. (a) concentration profile of formate ions, (b) concentration profile of Ru catalyst. 56

Figure 3.5 Proposed mechanism for the phase transfer hydrogenation of acetophenone with aqueous formate as hydrogen source and Ru-TsDPEN catalyst. **1**: neutral Ru pre-catalyst (RuCl(p-cymene)[(S-S)-Ts-DPEN]), **2**: cationic Ru catalyst (Ru^{+}(p-cymene)[(S-S)-Ts-DPEN]), **3**: Ru-hydride catalyst (RuH(p-cymene)[(S-S)-Ts-DPEN]), **4**: acetophenone, **5**: corresponding alkoxide of acetophenone, **6**: 1-phenylethanol. 60

Figure 3.6 Current flow at different reaction time under various negative external electric fields. 62

Figure 3.7 Stack plot of 1D 1H NMR spectra of samples 1 (A), 2 (B), 3 (C) and 4 (D). To highlight the minor species, spectra B was expanded vertically by 8 times, and spectra C and D were expanded by 24 times. 64

Figure 4.1 Sketch of the experiment setup for the continuous electrospray reaction system. 69

Figure 4.2 Reaction conversions and product yields under various electric field conditions. The concentration of sodium formate solution was 0.0025 mol/mL, and the flow rate of dispersed phase was 0.82 mL/min. 73

Figure 4.3 (a) Reaction conversion at various flow rates of the dispersed phase. Reactions were conducted with 3 kV applied with sodium formate solution of 0.0025 mol/mL and 30 mL of organic solvent consisting of 16.7% v/v 1-butanol in toluene. (b) reaction conversion with different concentration of sodium formate in the dispersed phase. Reactions were conducted with 3 kV applied with the flow rate of dispersed phase as 0.82 mL/min and 30 mL of organic solvent consisting of 16.7% v/v 1-butanol in toluene. 75

Figure 5.1 Experimental setup for droplet charge, size, and velocity measurement. 84

Figure 5.2 A list of ketone substrates. 85

Figure 5.3 Experiment setup for the electrified coaxial liquid jet. 87

List of Tables

Table 2.1 Physical properties of the studied organic solvents 42

Table 3.1 Properties of the studied organic solvents..... 53

Table 3.2 Summary of experiments under various positive external electric fields. 58

Table 3. 3 Summary for experiments with various negative external electric fields applied. 62

Table 4.1 Reaction performance with different organic composition and reaction conditions. .. 79

Table 4.2 Reaction performance in an electrospray system and a batch system at different reaction times. 80

Chapter I: Process Intensification in Liquid Biphasic Reaction Systems: Challenges and Opportunities

Liquid-liquid processes are essential and crucial in process engineering and have found wide industrial applications.[1] A typical liquid biphasic system involves two immiscible liquid phases and has served as an extraction technique for separation and purification in various industries,[2,3] including petrochemical, pharmaceutical, food and metal industries. On the other hand, liquid biphasic systems have been employed as novel reaction systems for pursuing sustainable chemistry and engineering due to the increasing concerns in energy consumption and environmental impacts.[4]

1.1 Applications of liquid biphasic reaction systems

Solvents play an important role in chemical reactions for their abilities to facilitate mixing, to stabilize reactive intermediates and to influence reaction reactivity and rates.[5,6] While the appropriate selection of solvents can greatly facilitate reaction efficiency, many of the current commercial chemical processes, especially for production of pharmaceuticals, involve large excess of organic solvents that are volatile, toxic, or flammable, which consumes significant amount of energy for recycling and poses negative environmental impacts. With the development of green chemistry, tremendous efforts are being devoted to developing sustainable alternative pathways and processes for chemical synthesis that consume less energy, operate under mild reaction conditions, use benign solvents, and incorporate inherently safe design.[7,8] Liquid-liquid biphasic reaction systems may provide a promising solution to address this challenge. Due to the advantages of being cheap, abundant, safe, and environmentally friendly, water is widely used to generate liquid biphasic reaction systems with other liquids, which

significantly reduces the usage of organic solvents and features feasible separation of products and catalysts. Water based liquid phasic systems have been widely employed in organic synthesis, biocatalysis, biomass processing, among others. Furthermore, the development of green solvents, such as ionic liquids, offers more possibilities for the constitution of liquid biphasic systems.[9,10] In this thesis, phase transfer catalysis for organic synthesis, aqueous biphasic systems for integration of biocatalysis and bioseparation, and aqueous-organic biphasic systems for biomass processing will be discussed as representatives to show the importance of liquid biphasic reaction systems in the developments of sustainable chemistry and engineering.

1.1.1 Phase transfer catalysis

Phase transfer catalysis (PTC) is one of the examples of applying liquid biphasic system as a green methodology for organic synthesis.[11] PTC was introduced in 1965-1971 by Makosza,[12] Brandstrom, and Starks.[13] Since then, it has been recognized as a powerful methodology in organic synthesis for achieving high reactivity and selectivity with operational simplicity, low energy consumption, mild reaction conditions, and environmentally benign reaction systems.[11,12,14,15] In 1989, O'Donnell et al. reported the pioneering study of highly enantioselective alkylation promoted by chiral phase transfer catalysts,[16] which leads to the enormous development of PTC as a powerful and practical method for the pursuit of green chemistry in asymmetric transformations,[17,18] which is important for the pharmaceutical industry.

A typical PTC system consists of an aqueous phase being a reservoir of reaction anions or base for generation of organic anions and an organic phase in which organic reactants and catalysts are located,[12] as shown in **Figure 1.1**. The reacting anions (Y^-) are continuously transferred into the organic phase by a phase transfer catalyst (Q^+X^-), normally onium salts or complexing agents, in the form of lipophilic ion pairs (Q^+Y^-) produced according to the ion

exchange equilibrium, followed by a rapid reaction with the organic substrate (R-X) in organic phase with releasing the catalyst cation (Q^+).

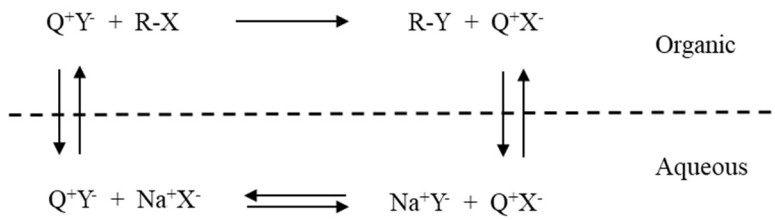

Figure 1.1 Representative system and mechanism of a PTC reaction with aqueous anions.[15]

In an asymmetric PTC system, the reactions generally follow an interfacial mechanism, in which the organic substrate undergoes deprotonation at the interface by reacting with a base located in the aqueous phase.[17] Subsequent ion-exchange of the formed reactant anions with the chiral catalyst leads to the generation of a lipophilic chiral intermediate which reacts further with the other substrate in organic phase to form product compounds. Ideal chiral catalysts will result in the fast ion-exchange with the reactant anions meanwhile shield one of the two enantiotopic faces of the anions, therefore achieving a high enantioselectivity.[17]

Over the past three decades, notable achievements have been made in asymmetric phase transfer catalysis. Recent advances of PTC have been focused on the rational design of new chiral phase transfer catalysts toward understanding the relationship between the structure of the catalyst and their stereocontrolling abilities for asymmetric synthesis.[19] So far, asymmetric PTC has found a wide variety of successful synthetic applications,[17,18,20] such as alkylation, conjugate addition, aldol reaction, cyclization, hydroxylation, hydrolysis, oxidation, and many others. For instance, cinchona alkaloid or binaphthyl-derived quaternary ammonium salts catalysts have been developed for C-C bond formation,[21-23] and some of those mentioned reactions have been applied to asymmetric synthesis of biologically active compounds.[24] Furthermore,

pharmaceutical companies have demonstrated the practicability of asymmetric phase transfer reactions in the large scale of preparation of drugs.[25]

1.1.2 Aqueous biphasic system

Aqueous biphasic system (ABS), or commonly known as aqueous two-phase system (ATPS) is another example of liquid biphasic systems. Aqueous biphasic systems are formed when two incompatible aqueous solution are mixed at appropriate concentrations or at a particular temperature.[26] For instance, when mixing two different aqueous polymer solutions (e.g., polyethylene glycol and dextran), an aqueous medium containing two separable phases is generated.[27] The formation of the two phases results from the steric exclusion of the large polymer aggregates formed in the system. Similar phenomenon can be observed in a polymer-salt based aqueous mixture system.[28] The specialty of aqueous biphasic systems is that each of the two phases contains large amount of water while still maintaining an interfacial layer,[26] which shows great potential for sustainable chemistry and engineering applications.

Due to the gentle environment and the capability to acclimatize biomolecules to be partitioned to one of the phases by a physicochemical interaction, aqueous biphasic systems have been extensively studied for bioseparation and purification.[29] Advantages of ABS as a separation technique include environment friendly, low cost, rapid and efficient separation, and ease of scaling-up.[26,27] Further studies of ABS in separation are focused on the development of alternative phase-forming components, such as alcohols,[30] ionic liquids,[31] surfactants,[32] etc.

As a result of its novelty for feasible separation of biomolecules, ABS has been studied as a platform for integrated biocatalysis and separation, particularly in the design of reversible mono/biphasic system for sequential reaction and separation. For example, Freire and co-workers reported a switchable ionic liquids based aqueous biphasic system driven by pH change

to achieve simultaneous production and separation of 5-hydroxymethylfurfural from fructose.[33] The dehydration of fructose was promoted by the monophasic mixture of ionic liquid and acid. After reaction, a biphasic system was induced by increasing the pH, and the 5-hydroxymethylfurfural product was selectively recovered in the ionic liquid rich phase. In a recent study by Ferreira et al., a thermoreversible aqueous biphasic system composed of ammonium-based zwitterions and polymers was studied as an integration process for biocatalytic oxidation of 2,2'-azinobis(3-ethylbenzthiazoline-6-sulfonate) (ABTS) by laccase.[34] The oxidation reaction took place in an aqueous monophasic mixture composed of zwitterion and polyethylene glycol, followed by the phase separation through a temperature change to selectively recover the product and catalyst in different phases.

1.1.3 Biomass processing reaction

Liquid biphasic reaction systems have also been studied for biomass processing. Due to the increasing environmental concerns and demands for clean energy, biomass has been extensively studied as an alternative resource for sustainable production of chemicals and fuels.[35] One of the main challenges with current biorefinery technology is the high production cost. This could be overcome by producing valuable coproducts from hemicellulose or lignin, for example furfural, a high value-added chemical derived from hemicelluloses.[36] However, in a conventional biorefinery primarily targeting cellulose conversion, the valorization potential of hemicellulose and lignin is often sacrificed and plenty of non-cellulosic wastes are released.[37] To address this challenge, various liquid biphasic systems have been studied for efficient utilization of lignocellulose to achieve sustainability in biorefinery processes.[37-39]

Chen and co-workers studied an aqueous choline chloride/methyl isobutyl ketone biphasic liquid system for simultaneous lignocellulose fractionation and conversion.[37] In their study, the

fractionation of switchgrass biomass took place in the aqueous phase, followed by the acidic hydrolysis of hemicellulose into pentose which underwent further dehydration into furfural. Furfural was then simultaneously extracted to the methyl isobutyl ketone phase without further degradation. Meanwhile, high purity of high-quality lignin was obtained in the aqueous phase with digestible cellulose formed as solid residues. This study demonstrated the effectiveness of novel liquid biphasic system for integrated reaction and separation to produce value-added chemicals in biorefinery.

Zhang et al. studied a series of organic-aqueous biphasic systems to screen a highly efficient system for furfural production from xylose and *Eucalyptus*.[38] Among those studied systems, methyl isobutyl ketone and cyclopentyl methyl ether in combination with aqueous NaCl solution exhibited the best performance on furfural production from xylose with formic acid as catalyst. The methyl isobutyl ketone/NaCl-water biphasic system also showed promising performance on furfural production rates and cellulose enrichment from *Eucalyptus* under relatively mild conditions.

1.1.4 Summary

Apart from the above-described applications in asymmetric organic synthesis, biocatalysis and biomass processing, liquid biphasic reaction systems have also served as a powerful tool/technique in many other chemistry and chemical processes, such as hydrogen peroxide production,[40] gem-dichlorocyclopropanation of alkenes,[41] etc. Overall, liquid biphasic reaction systems offer a great potential and opportunity for the pursuit of sustainability in chemistry and engineering for various industrial applications.

1.2 Process intensification in liquid biphasic reaction systems

While liquid-liquid reaction systems have emerged as an effective methodology for achieving sustainable chemistry, these systems are often constrained by insufficient mixing and low mass transfer rates due to small interfacial areas. Reactions in liquid biphasic systems can take place either at the interface or in one of the bulk phases. For both cases, large interfacial area and efficient mixing are essential to promote mass transfer in the bulk phase or across the interface to achieve high reaction rates. For those biphasic reactions conducted in conventional batch systems, vigorous stirring is often required to achieve sufficient dispersion and interfacial contact of the two phases, which consumes huge energy and makes it difficult to operate on a large scale. Therefore, new technologies and tools are desired for process intensification in liquid biphasic reaction systems to intensify mixing while minimize energy consumption.

Generally, process intensification can be classified into two areas, novel equipment design and new methods (processes) design, as shown in **Figure 1.2**.[42] The aim of process intensification is to optimize driving forces through increased mass and heat transfer at all scales and thus promote reaction kinetics and achieve higher conversion and selectivity, which in turn would reduce energy consumption and reaction wastes.[43] In the cases of liquid-liquid processes, understanding the fluid mechanics, droplet size, droplet shape behaviors, and coalescence phenomena is the key to design novel equipment or methods for process intensification. Details of droplet behaviors and recent technologies for intensification in liquid-liquid processes can be found in a recent book by Weatherley.[44] In this thesis, only selected methodologies and techniques, e.g., continuous processes (including microflow systems), and application of electric fields, are discussed as representative equipment and methods for their successful applications in

liquid biphasic reaction systems for achieving high reaction efficiency while maintaining sustainability.

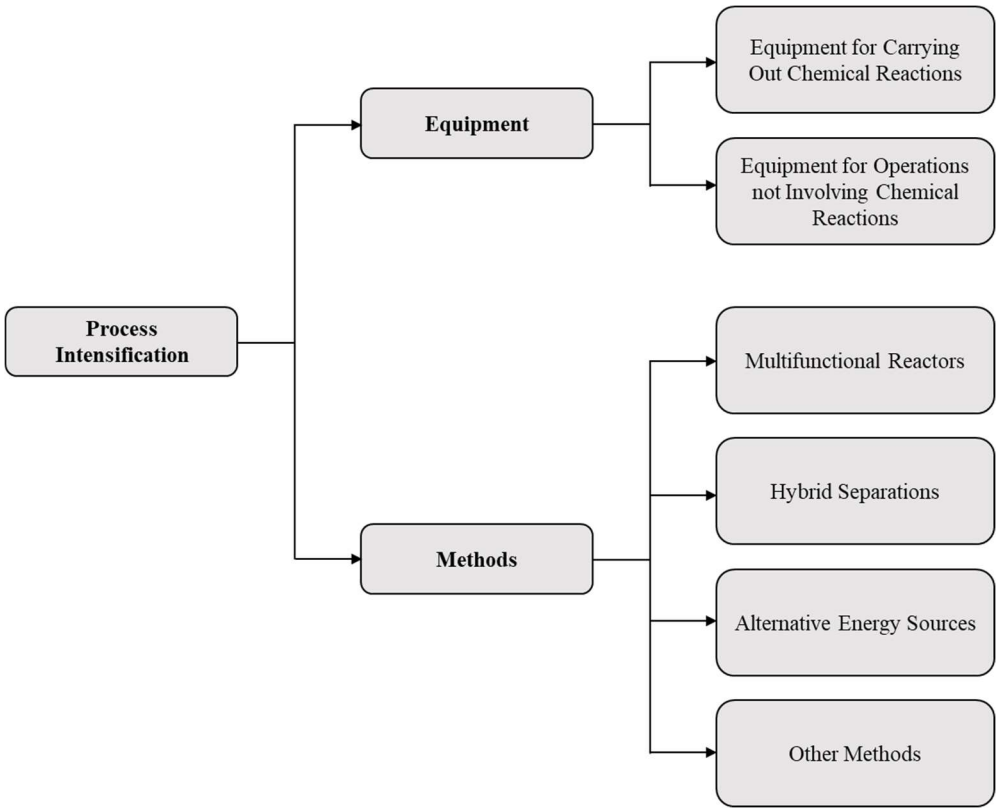

Figure 1. 2 Process intensification and its components.

1.2.1 Microreactors

A microreactor is generally defined as a series of interconnecting channels, typically from 10 to 300 microns in diameter, formed in a planar surface as a miniaturized reaction system.[45] In microreactors, the reactions can be manipulated by controlling the sequence of reagents introduced into the reactor and specifying the reaction time in a controlled condition. Products may then be analytically monitored in situ or separated for further reaction or testing.[45,46] Commonly used materials for fabrication of microreactors include silicon, glass, quartz, metals, and some polymers.[47] Microreactors offer many advantages over conventional scale reactors,

such as smaller amount of reagents used and most importantly the significantly increased surface areas. Due to the high surface to volume ratio, the heat, mass, and momentum transfer are dramatically facilitated, achieving high reaction rates. Meanwhile, it offers an opportunity for manipulation of reactions to eliminate side reactions, to increase safety for possible synthesis of hazardous materials, and to prevent potential accidents by means of heat removal control.[45-47]

On the other hand, microreactors could be employed as modular systems for large scale application. For instance, it has been shown that only 1000 micro reactors are required to operate continuously to produce 1 kg of material per day.[48] This suggested that the costly and time-consuming process of scaling up from lab to pilot plant to industrial production could be potentially by-passed by optimizing the reaction on a single chip and replicating it for 1000 times. This approach could not only eliminate the problems associated with the scaling up procedure, such as unexpected shut down if one unit fails, but also show the potential to maintain a high-level control of targeted reactions with much shorter timeframes for setup, testing and turnaround during scaling-up.[49]

Given the small dimensions, the flow regime of single phase in a microchannel is typically laminar, as the viscous forces dominate the inertial forces in the microchannel, resulting in a low Reynolds number. However, in a liquid-liquid system, the interfacial forces add complexity to the laminar flow, which may result in various flow patterns. The two-phase flow in microchannels is dominated by the balance of inertia, viscous, and interfacial tension, which can be characterized by dimensionless numbers called Capillary number (*Ca*) and Weber number (*We*).[50]

$$Ca = \mu v/\sigma \tag{1-1}$$

$$We = \rho u^2 d/\sigma \tag{1-2}$$

where μ is the viscosity, v is the velocity, σ is the interfacial tension, ρ is the fluid density, u is the fluid velocity, and d is the characteristic channel length.

The flow pattern formation depends on the flow rate, ratio of the phases, fluid properties, the channel geometry, and the construction materials.[4,46] In other words, by changing the fluid flow rates, using different construction materials, modifying the surface of the microchannel, adding surfactants into the fluids, or changing the inlet geometry, one could manipulate the two-phase flow in a microchannel.[51] Parallel flow and segmented flow, as shown in **Figure 1.3**,[46] are two typical flow patterns for a liquid-liquid system in a microchannel.

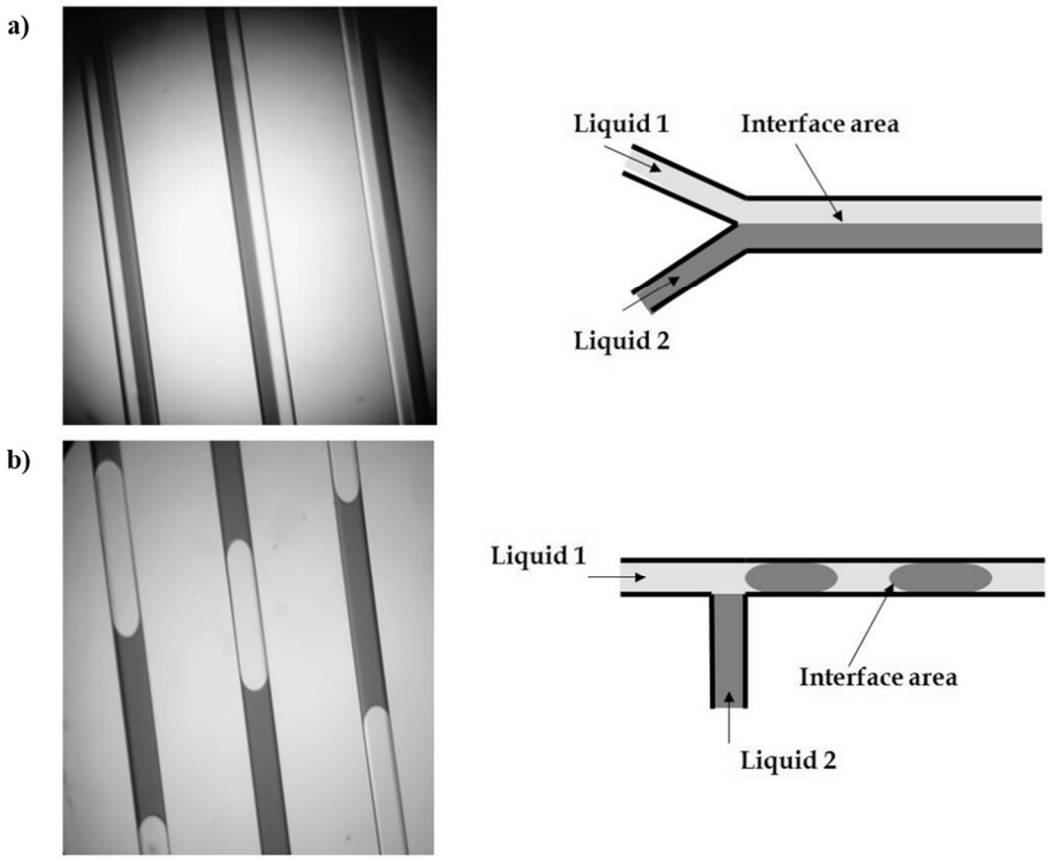

Figure 1. 3 Flow patterns in liquid-liquid system, (a) parallel flow, (b) segmented flow.

Flow behaviors of the two liquid phases are important for determining residence time, mixing, and mass/heat transfer, which make impacts on reaction conversion and product yield. In a stable parallel flow, mixing occurs via diffusion between the two phases, whereas in a segmented flow, internal vortices and recirculation inside the segment are created, which permits fast and efficient mixing of reactants[52]. Recent experiments have shown that segmented flow also allows precise matching of microliter amounts of reagents based on coalescence of droplets.[53] In addition, mass transfer of substance passing through interface is rapid according to several experiments.[54]

Efforts are also devoted to different designs of microchannels to increase mass transfer areas by producing smaller volume of one liquid phase (dispersed phase) in the other liquid phase (continuous phase), in other words, the generation of tiny droplets/emulsion in microfluidic systems. The resulting flow pattern is known as bubbly flow, in which those tiny droplets can act as individual microreactors. General geometries to produce droplets include T-junction, flow focusing, co-flowing, membrane, and step emulsification, as shown in **Figure 1.4**.[50] Details in the geometries, droplets size and breakup mechanism can be found in a recent review paper by Sattari et al.[50] Generally, the size of the droplets can be manipulated by the flow rate or inlet pressure in those systems. In addition to those passive control methods, external forces, such as electric forces, magnetic forces, laser, and ultrasonic fields, are also studied as active methods to manipulate the droplets formation.[50] The main advantage of active droplet generation methods is the capability to control particle size and production rate independently, which is almost impossible in passive particle generation methods. While those external forces provide more precise control on droplet formation and motion, it may require more sophisticated and specialized design of the microsystems, which limits their flexibility and versatility.

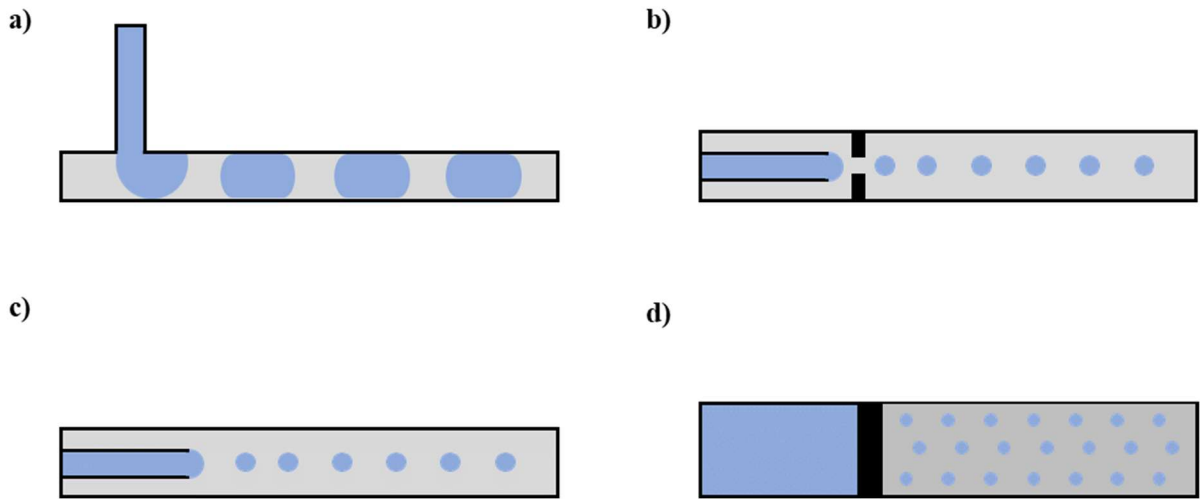

Figure 1.4 Geometries for production of droplets. a) T-junction, b) flow focusing, c) co-flowing, d) membrane.

Due to the inherent benefits of rapid reaction, efficient heat and mass transfer, fluidic control, and ease of scaling up, microreactors are now being extensively studied and successfully applied to liquid-liquid reaction systems for synthetic chemistry to achieve process intensification.[50,55] Peer et al. reported an intensified phase transfer catalysis reaction in a silicon Pyrex microreactor.[56] In the proposed system, 1-phenylethanol was oxidized by hydrogen peroxide with zinc-substituted polyoxotungstate as catalyst and tributylammonium hydrogen sulfate (TBAHS) as phase transfer catalyst. Conventional hydrogen peroxide oxidation of 1-phenelyethanol is performed in batch reactors, in which the reaction rate is limited by the low mass and heat transfer due to the low solubility of organic reactants in aqueous phase and the small interfacial area. In the microreactor, the segmented flow pattern in the microchannels significantly increased the interfacial area and promoted the transfer of active species, which resulted in a dramatical reduction in reaction time under the optimized reaction conditions compared to that when conventional reactors were used.

Shang et al. studied a packed bed microreactor for intensification of another phase transfer catalysis reaction.[57] In that study, the two immiscible liquid reactant streams were pumped into a

glass tube reactor packed with small inert glass beads for one step oxidation of cyclohexene by hydrogen peroxide with $[CH_3(C_8H_{12})_3N]HSO_4$ as phase transfer catalyst without additional solvent. The generated microchannels between those small beads dramatically increased the interfacial area and achieved a better mixing, which prevented the decomposition of hydrogen peroxide during the reaction and reduced the reaction time to 20 min compared to 8 h for batch reactors. On the other hand, this microreactor system offered a safe operation under high temperature (100 °C) which would pose safety issue, e.g., explosion, in batch systems.

Similar to the H_2O_2 oxidation reactions, some other phase transfer reactions, such as the etherification of benzyl bromide and phenoxide,[58] the esterification of sodium benzoate,[59] have also been improved with microflow reactions. As concluded from the above examples, micro reaction systems offer the advantages to employ green reagents (e.g., H_2O_2), reduce organic solvent usage, increase operational safety, reduce reaction time, and easily scale up, which can be employed as great approach to pursue sustainability in chemistry and engineering.

However, microreactors are not perfect. Frequently quoted disadvantages of microreactors are high fabrication cost, low throughput, incompatibility with solids and the omission of cost reduction by scale up effects which lead to still poor industrial acceptance.[46] On the other hand, low pulse or pulseless pumps are necessary to ensure stable flow in a microreactor, while pumps are one of the most expensive parts of the microreactor apparatus. Due to the small dimensions of microchannels, clogging is also one of the biggest problems in microreactors, which could be caused by flowing solids or highly viscous liquids. Additionally, when off-line analysis is used, it may take a very long time period to gather a sufficient amount of samples for performing the analysis. In regard to scale-up, numbering-up of hundreds or thousands of microreactors in

parallel or sequence will increase the complexity of the reactor network, and simultaneously controlling flows and temperatures in those microreactors is challenging.[60]

1.2.2 Other continuous flow processes

Continuous flow processes, including aforementioned microfluidic systems (microreactors), share the same benefits that the microflow systems possess, that are increased interfacial area, enhanced mixing and heat transfer, and efficient control of reaction conditions, and thus have been studied for intensification of liquid-liquid reactions. Noted that, flow in microchannels/microreactors is typically processed in small scales (e.g., microliters per minute or hour), and numbering-up of hundreds or thousands of microreactors for commercial-scale production is impractical in terms of simultaneously monitoring and controlling of the reactor network.[60] Therefore, larger continuous flow reactors that retain the mass and heat transfer performance are often preferred to produce large amounts of materials. In this section, continuous processes that are in different designs than microreactors or operate in relatively large scales, e.g., flow rates up to 100 mL/min, will be discussed.

Corning developed several models of glass fluidic reactors, and their hydraulic diameters were in the range of 0.3-4 mm with internal volumes from 0.5 to about 100 mL.[61] Corning flow reactors offer much higher productivity than microreactors. For instance, a Corning advanced flow reactor can be used for chemical processing with intermediate flow rates of 10-200 mL/min.[62] The heart shaped mixing cells and recombination of streams between cells in these reactors, as shown in **Figure 1.5**, force fluids to split and recombine, leading to enhanced mixing and improved mass transfer.[63] These reactors have been evidenced to yield large interfacial area in the range of 1000-10000 m^2/m^3 with flow rates from 10-80 mL/min, and the mass transfer coefficient values are within the range of 1.9-41 s^{-1}.[62] Zhang et al. reported a successful

application of using a Coring advanced flow reactor for a phase transfer catalysis reaction (oxidation of 1-phenylethanol by sodium hypochlorite) with flow rates more than 20 milliliters per minute.[63] The production rate was increased up to 700 times with higher yields of the desired products and shorter residence time compared to that using a spiral microreactor. Similarly, Peer et al. successfully scaled up a biphasic catalytic oxidation reaction by up to 650 times using a Corning advanced flow reactor without sacrificing conversion and yield.[56]

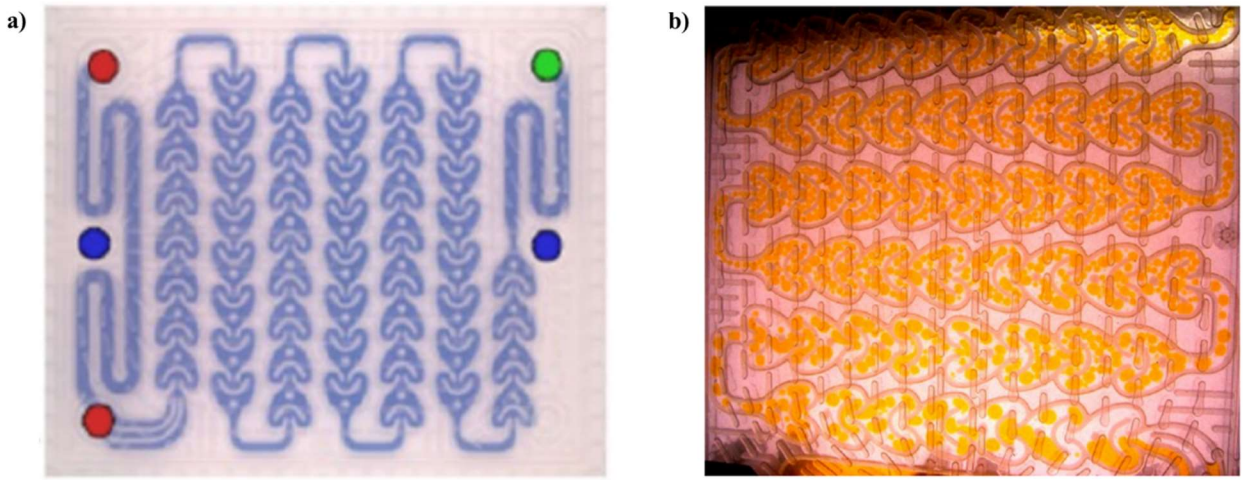

Figure 1.5 (a) Schematic view of a Corning advanced flow reactor, (b) flow patterns of hexane/water within a Corning advanced flow reactor.[62]

Mandrelli et al. reported a continuous reactor column design for the development and scale up of a liquid biphasic reaction (double alkylation of benzylamine with 1,5-dibromopentane catalyzed by aqueous sodium hydroxide) under super heating conditions.[64] This reactor consists of 13 stages of stirring chamber, as shown in **Figure 1.6**, enabling efficient mixing of the reaction mixture. Following entering the inlet at the bottom of the column, the reaction mixture progressed between each stage through a small opening, allowing the conversion to increase with each sequential stage. Phase accumulation and back mixing in the column could be minimized

by optimization of flow rate, stirring speed and stage opening size. It was proven that the proposed reactor eliminated mass transfer limitation for the studied reaction system and achieved a comparable performance to that in a microwave batch reactor, thus showing a superior potential for scale-up.

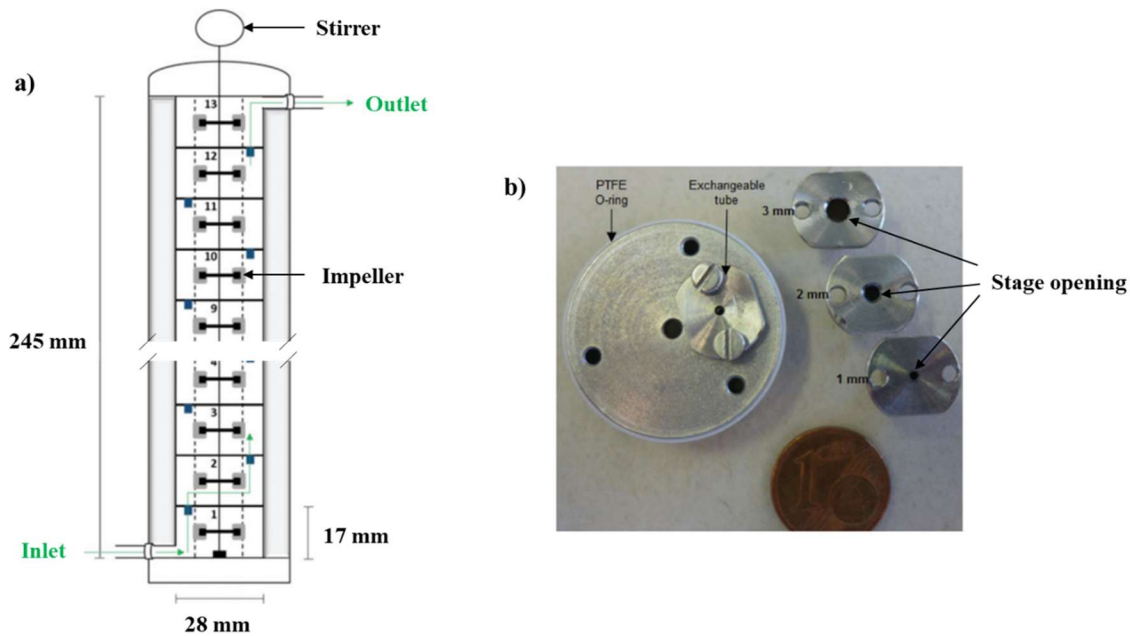

Figure 1.6 a) Schematic drawing of the reactor column, b) design of a single stage.

Efforts have also been devoted to other reactor designs, such as miniaturized continuous stirring tank reactor[65], and different process designs, such as continuous reaction with in-line separation to make the entire process fully continuous,[56] etc. Overall, continuous flow processes showed superior ability to eliminate mass transfer limitation for liquid biphasic reaction systems than conventional batch reactors and provide a sustainable alternative for organic synthesis which is particularly important for pharmaceutical applications.

1.2.3 Application of external electric fields (EEFs)

External electric fields (EEFs) have been studied and applied to liquid-liquid systems for many years. The action of electrical fields appears in different forms, ranging from electrically induced acceleration of ionic and other charged species through a fluid continuum, e.g., electrophoresis, to electrostatic dispersion and coalescence processes involving immiscible and partially miscible liquids, e.g., electrospray.[66] Advantages of applying electrical energy to liquid-liquid processes over conventionally used mechanical energy (stirring) include controllable droplet size, increased interfacial area, enhanced mixing, and higher mass/heat transfer rates,[67] which result from the fundamental interactions between electrostatic forces and liquid-liquid interfaces. In addition, the application of electric fields provides a more energy efficient way for process intensification than mechanical agitation, as the electrical energy supplied to the system interacts selectively with the liquid-liquid interface. Studies have suggested that energy required to create a dispersion by electric means can be up to two orders of magnitude less compared to mechanically agitated systems per unit volume of the dispersed phase.[68]

In the case of electrophoresis, the motion of charged particles in a fluid continuum is promoted by an electrostatic force. This phenomenon can be important in liquid-liquid systems in which externally applied electric fields may result in the enhanced transport of charged species/substrates to the liquid-liquid interface where the chemical reactions take place (e.g., phase transfer catalysis reactions). The enhanced diffusion of substrates to the interface could further influence reaction kinetics and conversion, which is particularly important for equilibrium reactions.

In the case of electrospray/electrostatic dispersion, there are two primary phenomena that need to be fundamentally understood. One is the disruption effect of electrostatic force on the

liquid interface, which causes breakup and formation of droplets and is important for droplet size control. The other one is the influence of electrical force on droplet behaviors, which is important for control of droplet motion and trajectory. To fully understand those phenomena, basic knowledge of electrostatics theory (e.g., Coulomb's law, Gauss's law, Poisson's law) and electrification of liquids is required, which can be found in detail in a book by Cross.[69]

To form droplets in an electrospray system, it usually requires the continuous phase to be of low conductivity to prevent charge leakage, while the dispersed phase should be highly conductive in order to facilitate charge acquisition from a charged source (usually a nozzle connected to an electrical power supply).[67] When the dispersed phase flows through the nozzle, it acquires surface charge. The charged droplet forms when the dispersed phase emerges from the nozzle to contact with the continuous phase. The electrostatic force imposed to the charged liquid interface will distort the shape of the interface together with other forces which are interfacial tension, gravity, buoyancy, inertial force, and other forces that are applied in the opposite or same direction, as shown in **Figure 1.7**. Noted that the electrostatic force is imposed perpendicularly to the interface directing from the conductive phase to the nonconductive phase.[70] As the charge is distributed on the whole droplet surface, the electrostatic force is applied in all directions. When the electric potential/voltage increases, the disruption becomes more significant, resulting in elongated meniscus followed with detachment of smaller droplets from the liquid filament. **Figure 1.8** illustrates the development of a charged droplet formation under an external electric field. By controlling the magnitude of the voltage, the droplet size can be manipulated. When the voltage increases to a certain point, droplets in the scale of microns are produced, forming electrostatic dispersion, as shown in **Figure 1.9**[71]. The droplet size has a significant impact on interfacial area and mass transfer, and it could further affect drop motion

and coalescence phenomenon. Extensive theoretical studies have been done to estimate the droplet size mathematically.[72,73] Recently, advanced technologies, such as particle dynamics analyzer, are being adopted to provide more precise in situ measurements of the droplet size distribution.[74]

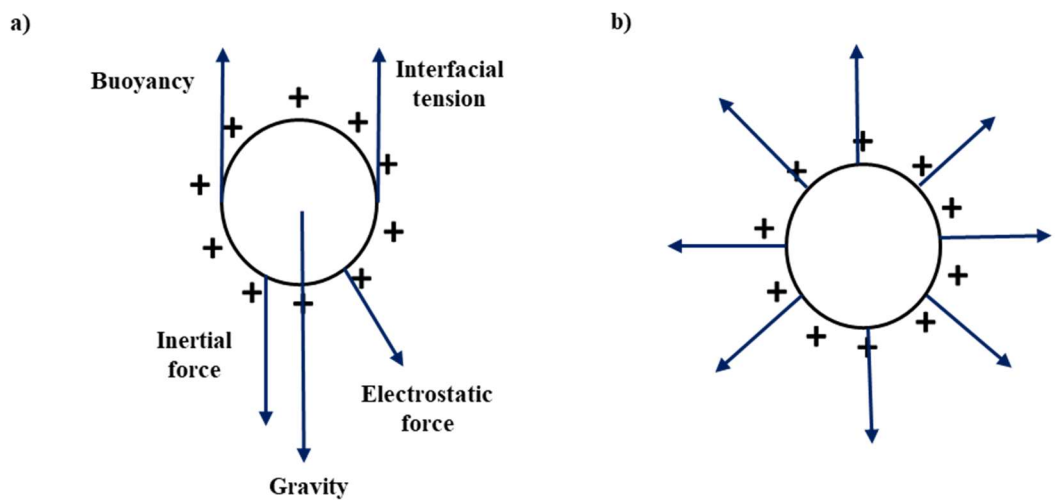

Figure 1.7 (a) Possible forces that are imposed on a positively charged liquid entity in a fluid continuum, (b) distribution of electrostatic force on a positively charged liquid entity.

Once the droplet is formed, it will move in the continuous phase under the influence of the electric field according to the direction of the field and the polarity of the charge on the droplet. The motion of droplets is governed by the sum of the forces (see **Figure 1.7**) acting on each droplet, in which the electrostatic force is the key component. As the electrostatic force is largely dependent on the electric field, the analysis of the electric field on space charge migration and calculation of electric field strength is crucial for understanding the drop motion. This problem was addressed in detail by Weatherley, Petera and co-workers.[71,75,76] Drop motion impacts residence time, mass transfer coefficients, and volumetric holdup of dispersed phase. In addition, the momentum transfer that occurs between moving droplets and the continuous phase could

create secondary flows in the continuous phase, which in turn impacts mass transfer and mixing phenomena. Drop motion in an electrically dispersed system is more complicated than the motion of discrete droplets. In the electrostatic dispersion condition, numerous droplets with smaller size are produced continuously. The interactions between droplets could promote collision and coalescence which results in the change of drop trajectory.

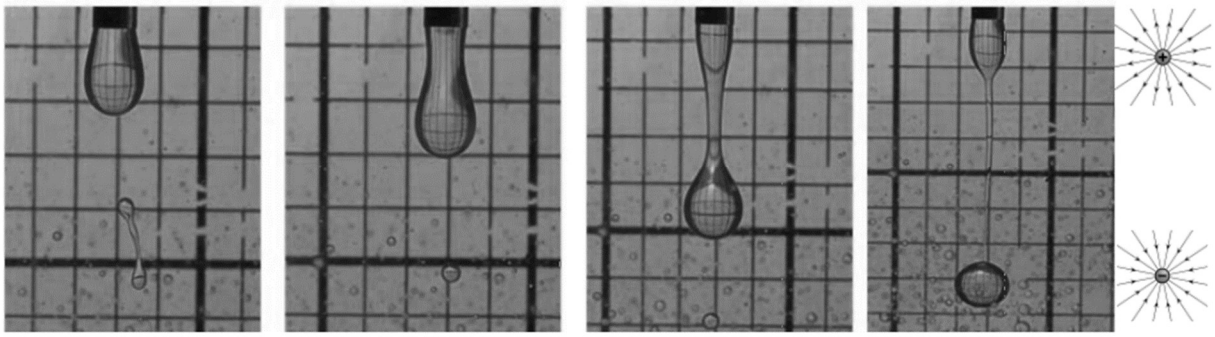

Figure 1.8 Development of a charged droplet formation under an external electric field.

Figure 1.9 Electrostatic dispersion in a liquid-liquid system.

Owing to the above-described formation of small drop size and accelerated drop motion, mass transfer in electrostatically intensified liquid-liquid systems is significantly intensified through the following mechanism: 1) increased interfacial area, 2) enhanced convection between dispersed and continuous phases, 3) induced interfacial disturbance, 4) promoted internal circulation within the droplets by oscillation.

Application of external electric fields has been widely studied as an efficient intensification technology in liquid-liquid systems. For example, electric field has been proved to be a useful tool for emulsion production.[77] It has been shown that the size of the generated droplets decreased with increased potential and decreased flow rates of dispersed phase.[77,78] In addition, electrostatic dispersion based liquid-liquid contactors was demonstrated efficient for extraction.[74] However, the study of electric fields in chemical reactions in liquid biphasic systems is rather limited.

Young et al. studied a photopolymerization reaction with combined electrospray and ultraviolet light to control the synthesis of hydrogel microspheres for cell delivery.[79] In their study, the electrospray was utilized as a tool for particle size control. Consistent results with other research were obtained in terms of decreased droplet size with increased voltages and reduced flow rates.

A few studies have investigated the effects of electric fields on biocatalytic processes.[80,81] Reactions employing biocatalysts are generally conducted in liquid biphasic systems under mild operating conditions and sufficient interfacial area is often required to achieve high reaction rates. The utilization of electrostatic dispersion offers a possibility to conduct biocatalysis with increased interfacial area while minimizing energy consumption. Kaufman et al. reported an electric field contactor for biodesulfurization of dibenzothiophene and crude oil.[80] In that system,

an emulsion of aqueous biocatalyst was generated in the organic phase by electric fields. Fine aqueous droplets of 5 μm in diameter could be produced which significantly increased the surface area with no increase in energy consumption compared to that in a batch system. Weatherley et al. investigated the hydrolysis of tri-glyceride ester in the presence of enzyme in an electrically sprayed reaction system and compared it with a stirred batch reactor.[81] It was shown that the reaction rate in the sprayed system was significantly enhanced when the applied electrical potential increased, which resulted from the increased interfacial area. A clear difference in the reaction rate was observed when the polarity of the electric field was reversed. More importantly, the reaction rate per unit interfacial area under electrical dispersion condition was dramatically increased compared to that in a stirred reactor, suggesting the possible influence of electric field on enzyme activity.

In a recent study by Wakisaka and co-workers, a so-called "femtoreactor" system based on electrospray was proposed.[82] In this work, the hydrolysis of dimethyldichlorosilane by water to form cyclosiloxanes was carried out in a liquid-liquid system, with the liquid reactants electrostatically sprayed into an organic phase through two inlets. It was suggested that the polarity of the electric field makes a difference on the droplet size. The reaction rate and yield of the kinetically favored product (hexamethylcyclotrisiloxane) increased with increased voltages. Those increases were attributed to the smaller droplet size under higher applied voltages, which increased the interfacial area and promoted the transfer of the cyclotrimer product to the organic phase before it further reacted to form the thermodynamically favored cyclotetramer product. This study demonstrated the enhanced reaction rate and selectivity achieved by increased interfacial areas due to the formation of electrostatically induced fine droplets.

Recently, controlling reaction rate and selectivity by applications of oriented external electric fields (OEEFs) has attracted plenty of attention.[83-85] It was proposed that an oriented external electric field could catalyze chemical reactions by lowering the activation energy barriers and stabilizing reactive species. Meir et al. reported that organic reactions can be theoretically accelerated when an external electric field is oriented along the "reaction axis" which enhances the electron flow, resulting in a lower reaction barrier and the stabilization of transition states.[86] Wang et al. predicted that the reaction enantioselectivity may be controlled by aligning the electric field along the dipole moment of the reactants.[87] Subsequent experimental studies proved the promoting ability of OEEF on organic reactions by aligning along the reaction coordinate at molecular level,[88,89] while there is no direct experimental evidence so far to support the idea of controlling chiral discrimination by OEEFs.

In conclusion, application of external electric fields to organic synthesis showed great benefits of mass transfer intensification and reaction control. While many of the scientifically intriguing questions raised by electric fields on reaction performance are not fully understood, further experimental and simulation studies would be worthy conducting for in-depth understanding of electrically intensified chemistry.

1.2.4 Summary

There is an ongoing effort to develop new technologies for process intensification in liquid-liquid reaction systems. Aims of those developed equipment or methods are focusing on intensified mass and heat transfer with efficient reaction control, lower energy consumption, and easy of scale-up. Among those, continuous flow processes in different scales, as discussed above, have been widely studied over the past decade, while application of external electric fields attracted less attention. However, by application of an electrospray, a continuous flow

process could also be established with comparable small droplet size. More importantly, employment of electrospray requires simpler reactor design which significantly reduces the fabrication cost, compared to the aforementioned flow processes. In addition, application of external electric fields to chemical reactions may promote the reactions in a way that not only increases interfacial area and promotes mass transfer but may also influence the kinetics. Therefore, it is worthy further exploring the potential of external electric fields in intensifying reactions in liquid-liquid systems.

1.3 Model reaction system

The reaction of choice for this study was the asymmetric transfer hydrogenation of acetophenone. The transfer hydrogenation of acetophenone is particularly important because of the industrial application of it two possible reaction products: 1-phenylethanol and 1-cyclohexylethanol. In fact, 1-cyclohexylethanol is used in the manufacture of some polymers and 1-phenylethanol is used in the pharmaceutical and perfume industries. On the other hand, acetophenone has also been regarded as a benchmark substrate for investigations of asymmetric transfer hydrogenation.

Asymmetric transfer hydrogenation of acetophenone has been extensively investigated with 2-propanol or formic acid as hydrogen source and chiral Ru complex as catalysts in homogeneous systems.[90-92] The high efficiency of the discovered chiral Ru catalysts (Noyori catalyst) enabled a yield of up to 99% and an enantioselectivity of up to 98% of the corresponding product enantiomer, which significantly promoted the development of asymmetric synthesis for medication applications. Subsequently, the mechanism of the reaction pathway was well presented by Noyori and co-workers,[93,94] as shown in **Figure 1.10**.

Briefly, the reduction of acetophenone by 2-propanol or formic acid follows a metal-ligand bifunctional mechanism.[95,96] The catalyst precursor (18 electron Ru complex **1**) undergoes facile elimination of HCl on treatment with one equivalent of a strong base to form the true catalyst, the 16 electron neutral Ru complex **2**. The catalyst **2** further reacts with 2-propanol to generate the Ru hydride complex **3** as an intermediate with the formation of acetone as byproduct. Upon reacting with the substrate, the hydride from RuH and a proton from NH_2 in complex **3** are simultaneously transferred to the C=O linkage via a six-membered pericyclic mechanism. It has been demonstrated that the reaction of catalyst **2** with 2-propanol is the turnover-limiting step in the steady-state hydrogen transfer.[91,93] With 2-propanol as hydrogen source, the Ru-catalyzed hydrogen transfer between alcohols and ketones occurs reversibly. In the case with formic acid as hydrogen source, CO_2 is produced as byproduct, which leads to full completion of the reaction.

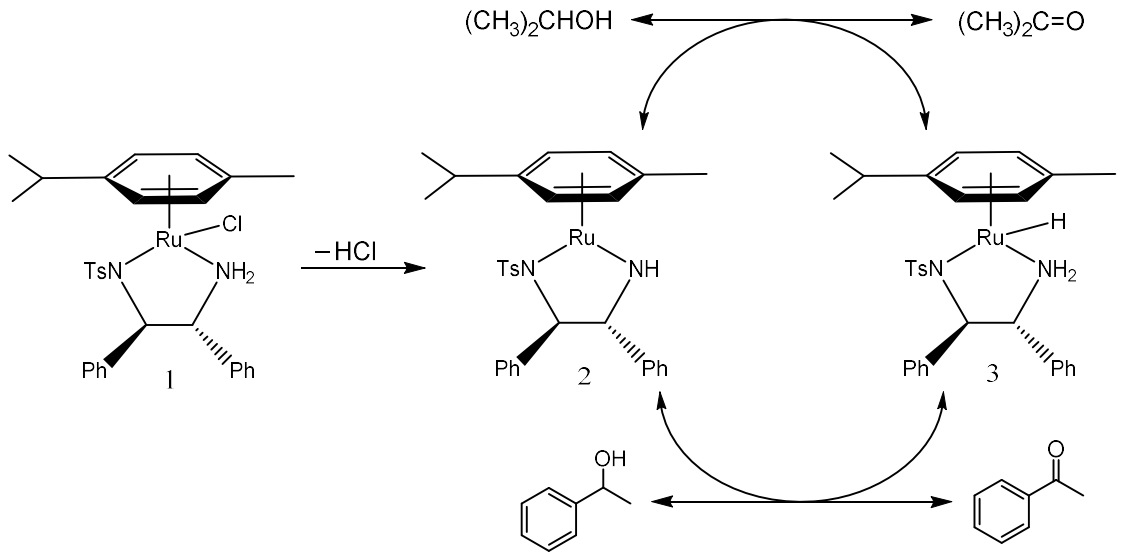

Figure 1.10 Mechanism of asymmetric transfer hydrogenation of acetophenone with 2-propanol catalyzed by chiral RuCl(p-cymene)[Ts-DPEN] complex.

Though with excellent activity, the Ru catalyst cannot be easily separated from products, as with most homogeneous catalysts. In the efforts to design immobilized Ru catalysts for better catalyst recovery, water was found to be an excellent solvent for the Ru-catalyzed transfer hydrogenation reaction with sodium formate as a reductant.[97-99] While facilitating the reaction rates, the presence of water further complicated the reaction mechanism by forming a biphasic system. On the other hand, vigorous agitation and a small volumetric ratio of organic substrate to water were required for efficient mixing. While surfactants or phase transfer catalysts may also be employed to promote the interfacial transfer of reactive species,[100] they could cause environmental concerns. Further mechanistic study suggested that the reaction rate was limited by the hydrogen transfer step (hydrogen transfer from catalyst to ketone substrate) when water was present, which is different from the limiting step in the asymmetric transfer hydrogenation of acetophenone with 2-propanol or formic acid presented. It was proposed that the mechanism of hydrogen transfer when water was present may be step-wise instead of concerted.[101] While water may significantly influence the reaction pathway, it role is not fully understood.

In conclusion, water plays an important role in the recovery of the chiral Ru catalyst and it may be involved in the transfer hydrogenation steps, yet the mechanism is not fully elucidated, which is worthy highlighting by further research. On the other hand, due to the formation of the liquid interface, mass transfer limitation becomes an issue, which requires vigorous agitation and a large excess of aqueous phase to promote mixing, limiting the practical application of this process. Therefore, the transfer hydrogenation of acetophenone with aqueous sodium formate as hydrogen source could serve as a great model system for evaluation of proposed intensification methods as well as for exploration of reaction mechanism with the presence of water.

1.4 Research motivation

Process intensification employing electric fields has been studied for decades, however, its application in liquid phase reaction systems, particularly for organic synthesis is rather limited. As has been discussed, application of liquid biphasic systems is important in chemical industry and offers a sustainable approach for organic synthesis. However, reactions in those systems often suffer from low mass transfer rates. Therefore, the initial purpose of this research is to establish a protocol of applying external electrical fields to intensify reactions in liquid biphasic systems for organic synthesis.

To achieve this goal, the transfer hydrogenation of acetophenone with aqueous sodium formate as hydrogen source catalyzed by the well-known chiral Ru catalyst (Noyori catalyst) was studied as a model reaction. By applying external electric fields, the reaction was studied in a batch system based on electrophoresis and in a continuous system based on electrospray. The innovation of this research is presented in the following three aspects:

1) The proposed reaction is a phase transfer reaction in principle, which takes place at the interface and is limited by mass transfer. By applying an external electric field to the reaction system, the charged reactive species, such as formate, could be transferred to the interface by the applied electrostatic forces through electrophoresis process. Enhanced transfer hydrogenation of acetophenone in an aqueous-organic liquid biphasic system by a cationic surfactant induced local electrostatic force was reported by Wang et al.,[102] which supports the idea of applying an external electric field to promote the reaction. On the other hand, with the application of external electric fields, phase transfer catalysts or surfactants are no longer required, thus avoiding lengthy design of new phase transfer catalysts and reducing complexity in the system.

2) The aqueous formate solution is highly conductive, while the organic phase containing acetophenone substrate is of low conductivity. By generating electrostatic dispersion of the aqueous phase into the organic phase, fine droplets could be produced to significantly increase interfacial area and eliminate mass transfer limitation in the reaction system. Furthermore, the energy consumption for generating an electrospray is significantly lower compared to that using mechanical mixing methods. While the aforementioned continuous flow processes, including microfluidic systems, could also intensify mass transfer between two liquid phases, they often require specialized design and the costs for fabrication or for pumps are very high. In contrast, electrostatic dispersion is feasible to set up and the cost is relatively low. Therefore, by applying an electrospray, a high-performance reaction system could be established with reduced energy consumption and costs.

3) Studies have shown that oriented external electric fields (OEEFs) could be employed for controlling reaction rate and selectivity via manipulation of activation energy barriers and stabilization of reactive species during the reactions. The influence of OEEFs upon chemical reaction performance has raised a number of scientifically interesting questions and increasing evidence has shown that OEEFs could be employed as smart reagents and catalysts in organic synthesis. However, those studies are limited in theoretical modeling or experiments that were conducted at the single molecule scale. The significance of OEEFs in experimentally controlling reaction rates and selectivity in bulk quantity reactions for organic synthesis remains understudied. Therefore, this research set out to explore the possibility of external electric fields being deployed to control synthesis of organics on a bulk scale and to shed light on the roles of external electric fields in synthetic chemistry and catalysis in liquid biphasic reaction systems.

1.5 Research goals

Based on the research motivations, there are several goals to be achieved in this research:

(1) Validate the idea of using an external electric field as a replacement of phase transfer catalysts in a batch reaction system.

(2) Explore the possibility of external electric fields in controlling chemical reactions, particularly for the proposed asymmetric transfer hydrogenation reaction, by means of influencing mass transfer, kinetic, and selectivity.

(3) Establish a flow reaction system based on electrospray to achieve fast and efficient reaction for potential large-scale applications.

Chapter II: Enhanced Catalytic Phase Transfer Hydrogenation of Acetophenone by Application of a Low External Electric Field

2.1 Introduction

As has been discussed in Chapter I, the asymmetric transfer hydrogenation of acetophenone with sodium formate as hydrogen source was studied as the model reaction in a liquid biphasic system to explore the possibility of applied external electric fields to intensify mass transfer and reaction performance. The reaction system consists of an aqueous phase in which sodium formate is located and an organic phase in which acetophenone substrate and Ru catalysts are dissolved. As the two reactants (acetophenone and formate) are separated in different phases, this reaction either requires a phase transfer catalyst to facilitate the transfer of formate species from the bulk aqueous phase to the interface or requires agitation for efficient mixing. Since the migration of negatively charged formate could be controlled by electrostatic forces, an external electric field was employed to facilitate mass transfer without mechanical mixing or addition of phase transfer catalysts. This is the first step to explore the roles of external electric fields in organic synthesis in liquid biphasic systems. The experiments were conducted in a batch system, in which the reactions took place in a quiescent hydrodynamic environment with low electric fields applied and no mechanical stirring employed. In this chapter, the reaction performance was evaluated based on the yields and selectivity of the desired products. Different parameters that could affect the reaction performance, such as electrical potential (direction and magnitude), choice of organic solvents, were investigated. The work in this chapter lays out the foundation of further exploration in this thesis on electrostatically intensified organic synthesis reactions in liquid biphasic systems, particularly for those with reactive ions involved.

2.2 Experimental section

2.2.1 Materials

All chemicals used in this work were purchased from commercial reagent suppliers and used without further purification: acetophenone (Sigma-Aldrich, ReagentPlus, 99%), sodium formate (SigmaAldrich, BioUltra, 99.0%), RuCl(p-cymene)[(S,S)-Ts-DPEN] (SigmaAldrich), pentane (Sigma-Aldrich, anhydrous, 99%), toluene (SigmaAldrich, anhydrous, 99.8%), chloroform (Sigma-Aldrich, ⩾99.5%), 1-cycolhexylethanol (Sigma-Aldrich, 97%), ethylbenzene (Sigma-Aldrich, anhydrous, 99.8%), 1-cyclohexylethanone (Sigma-Aldrich), ethylcyclohexane (Sigma-Aldrich, ⩾99%).

2.2.2 Experimental apparatus

The liquid biphasic system was set up with a sodium formate/water solution as the more dense aqueous phase and acetophenone as the less dense organic phase in which the Ru complex (RuCl(p-cymene)[TsDPEN]) was dissolved, as shown in **Figure 2.1**. A low voltage external electric field was applied across the two phases without any agitation. The reactor was constructed of highly insulating glass with a cylindrically symmetrical geometry. Two planar electrodes of equal dimensions were coaxially located at each end of the reactor. It was therefore assumed that the electrical field was linear and uniform in both radial and vertical direction with negligible space charge migration and wall effects under the low applied voltages which were used. The inner diameter of the reactor was 20 mm. The distance between the two electrodes was 10 mm. The orientations of the external electric fields are defined in **Figure 2.1 (b)**. Basically, a positive orientation in this work is defined as the direction of the electric field when the anode is placed in the organic phase with the cathode in the aqueous phase. A negative orientation is

defined as the direction of the electric field when the cathode is placed in the organic phase with the anode in the aqueous phase.

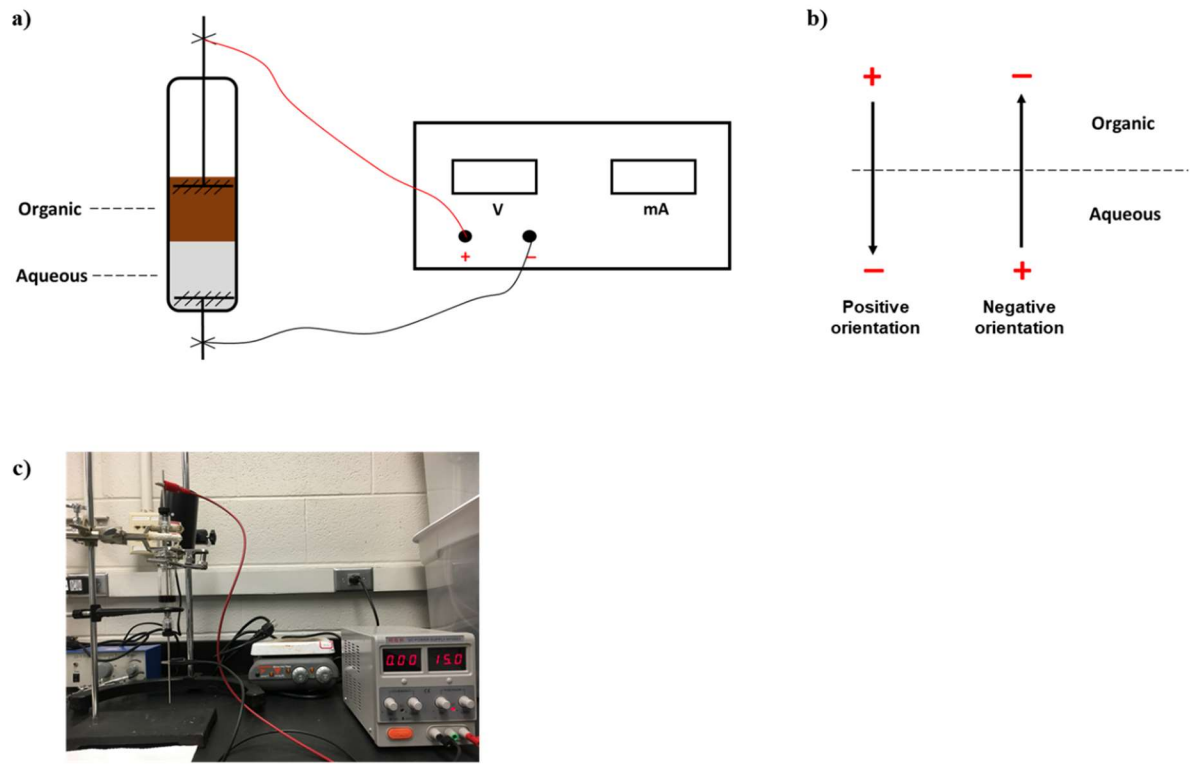

Figure 2.1 (a) Sketch of experiment set-up, (b) orientations of the positive and negative electric fields, (c) experiment apparatus with a 15 V of positive electric field applied.

2.2.3 Experimental procedure

Experiments were carried out in the glass reactor, as shown in **Figure 2.1**, with two adjustable electrodes on the ends. Experiments were conducted with or without the use of organic solvents. Organic solvents used were toluene, pentane, and chloroform.

When there was no organic solvent, experiments were conducted as follows: 0.8755 g of sodium formate was fully dissolved in 1.5 mL deionized water before transfer to the reactor, forming the bottom aqueous phase layer. Then 1.5 mL of acetophenone containing 0.0273 g of

dissolved Ru catalyst was added to the reactor, forming the top organic layer. The mole ratio of Ru catalyst: acetophenone: formate was 1: 300: 300.

When the experiments were conducted with organic solvents, 0.75 mL of the organic solvent was added to the 0.75 mL of Ru/acetophenone solution (0.0273 g of Ru catalyst dissolved in 0.75 mL of acetophenone). After full mixing, the organic solution was transferred to the reactor with the 1.5 mL of aqueous sodium formate solution. The mole ratio of Ru catalyst: acetophenone: formate was 1: 150: 300.

The reaction was conducted at room temperature and ambient pressure for 24 h with or without an external electric field applied across the two phases. After reaction, 100 μL of liquid samples from the organic phase were taken out from the reactor and diluted to 1.5 mL with methanol prior to GC analysis. Solid products generated at the liquid-liquid interface were collected from the reactor and washed with chloroform and deionized water for three times to remove any organic compounds or catalysts attached on the solids. The aqueous solution obtained was then collected and dried with low pressure evaporation to generate the white solid sample for FTIR analysis.

2.2.4 Analytical methods and characterizations

Gas chromatography (GC)

Liquid samples were analyzed by gas chromatography (Agilent 6890N equipped with a J&W SCIENTIFIC DB-WAX capillary column, 15 m × 0.53 mm, and a flame ionization detector) under the following conditions: helium as carrier gas (5 mL/min), inlet and detector temperatures 250 °C, oven temperature 150 °C, and injection volume of 1 μL. The retention time of the six possible components (acetophenone, 1-phenylethanol, 1-cycolhexylethanol, ethylbenzene, 1-

cyclohexylethanone, and ethylcyclohexane) in the reaction system was determined using individual standards.

Fourier transform infrared spectroscopy (FTIR)

Solid samples were analyzed by Fourier transform infrared spectroscopy. The Fourier transform infrared spectra were obtained using a Nicolet™iS™10 FT-IR spectrometer equipped with a monolithic diamond ATR crystal (Thermo Fisher Scientific Inc., USA). Signals were collected in the range from 4000 cm^{-1} to 500 cm^{-1} with the resolution of 4 cm^{-1} and at 100 scans. Solid phase standards of sodium formate and sodium bicarbonate (both of p.a. purity grade) were analyzed directly using the ATR crystal. The blend of the two standards, with the mass ratio of 1:1, was carefully prepared with the use of an agate mortar and pestle and next investigated with the ATR crystal. Homogeneity of the mixture was tested by comparison of FTIR spectra for three different samples and no discrepancies between the examined spectra were observed.

2.3 Results and discussion

2.3.1 Reaction stoichiometry

The experiments were initiated with the application of a low electric potential of positive 15 V in a reaction comprising sodium formate solution and acetophenone with no organic solvent presented. No current was measured in the system during the reaction. After 24 h of reaction, the color of the organic phase turned to dark brown from a clear light brown color, and a layer of white solids was formed at the liquid-liquid interface region. GC analysis showed that 1-phenylethanol was the only organic product formed during the reaction, and no other organic intermediates or by-products were detected. FTIR analysis (**Figure 2.2**) indicated that the solids at the interface are a mixture of sodium formate and sodium bicarbonate, which suggests that

sodium formate was converted into sodium bicarbonate during the reduction of acetophenone. The solid product was identified as a mixture of sodium bicarbonate and sodium formate based on the following observations from the spectra: 1) a characteristic peak was observed at ca. 1000 cm^{-1} which corresponds to the C-OH stretch of sodium bicarbonate, 2) characteristic peaks at ca. 2710 cm^{-1}, 2830 cm^{-1} and 2950 cm^{-1} corresponds to sodium formate C-H bending vibrations, symmetric C-H vibrations, and asymmetric C-H vibrations respectively, 3) the characteristic peaks in the solid sample spectra are identical with the standards mixture spectra though with different peak intensities due to the different mass ratios.

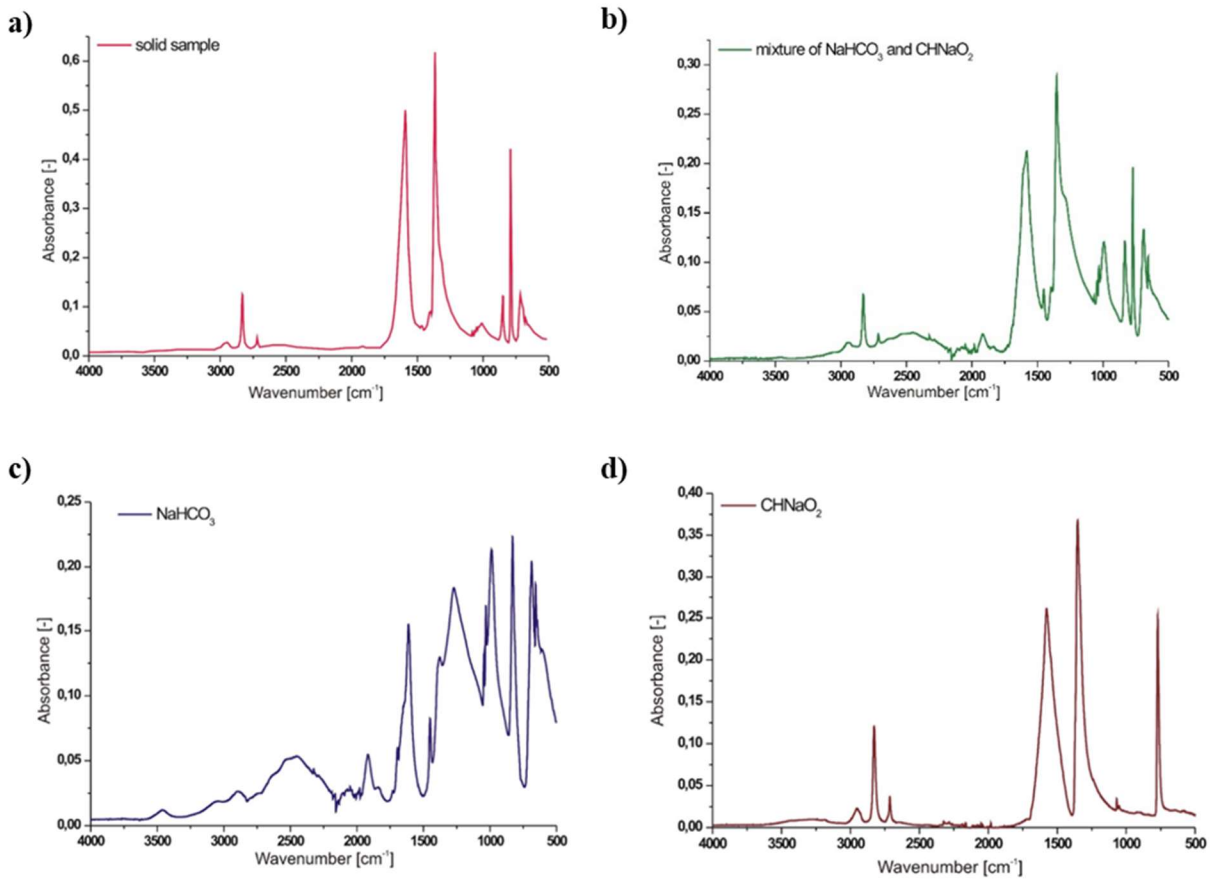

Figure 2.2 (a) FTIR spectra for the solid sample, (b) FTIR spectra for the 1:1 mixture of standard sodium formate and sodium bicarbonate, (c) FTIR spectra for the standard sodium bicarbonate, (d) FTIR spectra for the standard sodium formate.

The formation of sodium bicarbonate strongly suggested the participation of water in the reaction. Therefore, the reaction stoichiometry is balanced as equation (2-1).

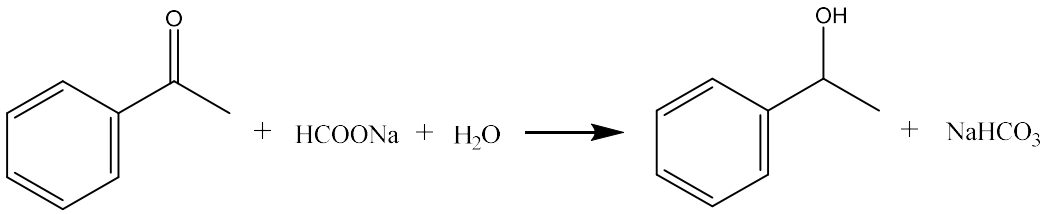

(2-1)

2.3.2 Direction of EEF

The effects of the direction of the applied electric fields on reaction performance were studied by comparison of the experiment with positive 15 V applied with a control experiment with no EEF applied and an experiment with negative 15 V EEF applied. No organic solvents were used in those experiments. The corresponding yields were summarized in **Figure 2.3**. As can be seen, when the EEF was applied in the positive orientation, a yield of about 13% was achieved. There was nearly a 3-fold increase in the yield of 1-phenylethanol at equivalent reaction time compared to that without electric field applied. Having demonstrated the intensification effect of EEF on the catalytic phase transfer hydrogenation of acetophenone, the EEF orientation was reversed, resulting in a dramatic inhibition of the reaction, with less than 1% of 1-phenylethanol produced. These results show strong evidence that the application of external electric fields could significantly influence reaction performance in a liquid biphasic system with reactive ions involved. It also suggests that the reaction performance could be potentially manipulated by controlling the orientation of the electric field.

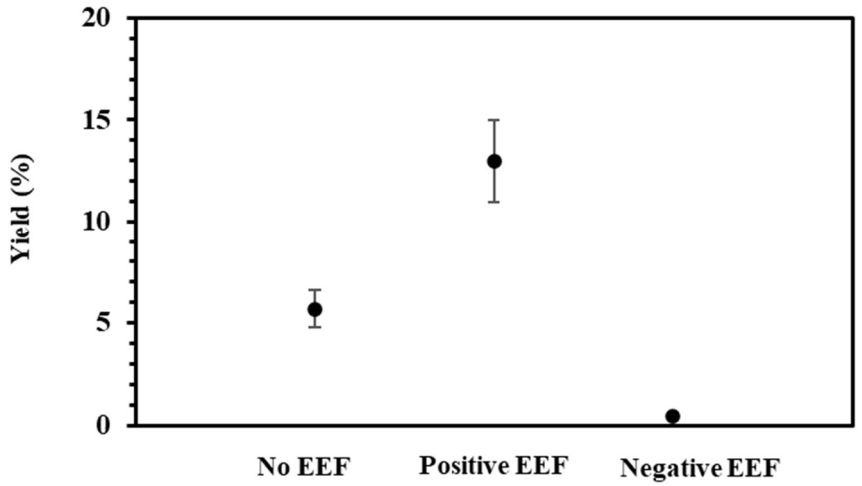

Figure 2.3 Yields of 1-phenylethanol under different electric field conditions (15 V positive OEEF, 15 V negative OEEF, and no OEEF).

2.3.2 Possible mechanism

Based on the above observation, one possible reason for the EEF induced intensification is the increased mass transfer rate of reactants to the interfacial region, as illustrated in **Figure 2.4**. A positive EEF could facilitate the continuous migration of the negatively charged formate to the interface at an accelerated rate. On the other hand, as suggested by Meijer and co-workers, a protonated 16-electron Ru complex (see **Figure 2.5**) was possibly formed during the reaction system as the real catalyst.[103] This cationic Ru complex is possibly enriched in the interfacial region due to the electrostatic force and it would rapidly interact with the negatively charged formate to generate the 18-electron Ru complex, thus accelerating the hydrogenation reaction by transferring the two hydrogen to the substrate. Possible reduction of the reaction barrier by EEF could also contribute to the increased 1-phenylethanol yield, as suggested by Shaik and co-workers,[104] which requires further investigation.

By comparison, when the EEF was applied in the reversed orientation, formate and the 16-electron Ru complex were assumed to be constrained in the aqueous and organic phases respectively, thus preventing the reaction.

It is, therefore, postulated that as the formate reached the interfacial boundary, it transferred a hydride to the protonated 16-electron Ru complex to form the 18-electron Ru complex with the release of CO_2. Following the mechanism proposed by Meijer and co-workers, a water molecule likely transfers a proton to the ketone substrate, generating OH^- ion.[105] The CO_2 further reacts with OH^- ion to form bicarbonate. As sodium bicarbonate has a very poor solubility in acetophenone and much lower solubility in water than sodium formate, while sodium formate is very concentrated in the aqueous phase (36.8% w/w, or 58.4 g/ 100 mL water), salting-out occurs resulting in the accumulation of the white solids at the interface. While this proposed mechanism may explain the observed phenomenon, further investigation is required to validate those assumptions.

In a mechanistic study by Wu et al.,[101] water was proposed to be important by participating in the catalytic cycle through different mechanisms. The observation in the designed reaction system further supported the importance of water in the transfer hydrogenation of acetophenone with aqueous sodium formate as hydrogen source. Furthermore, water may provide a hydrogen to the substrate, thus significantly changing the mechanism.

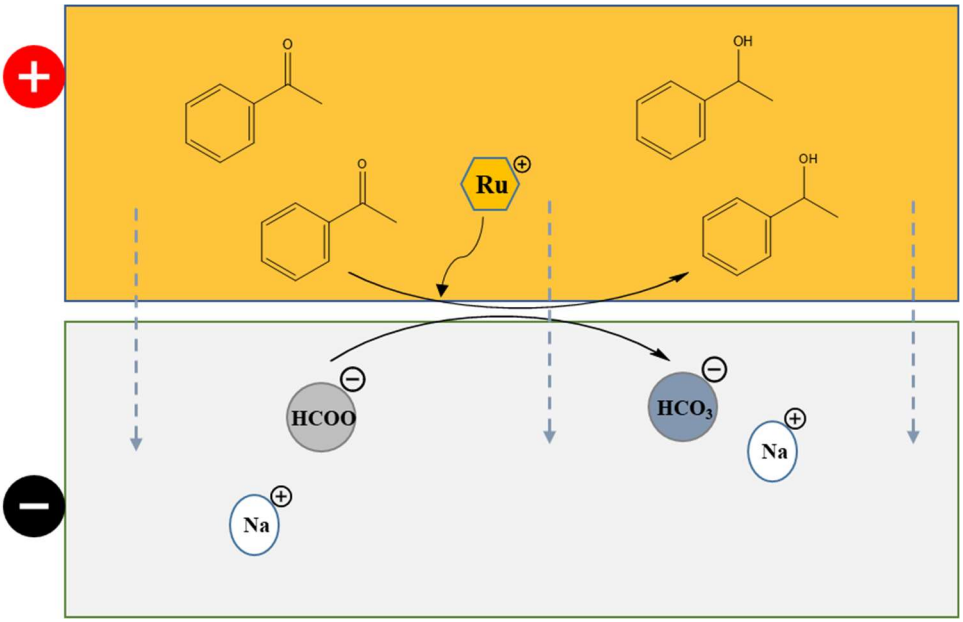

Figure 2.4 Proposed distribution and migration of ions/species in the two phases under a positive EEF.

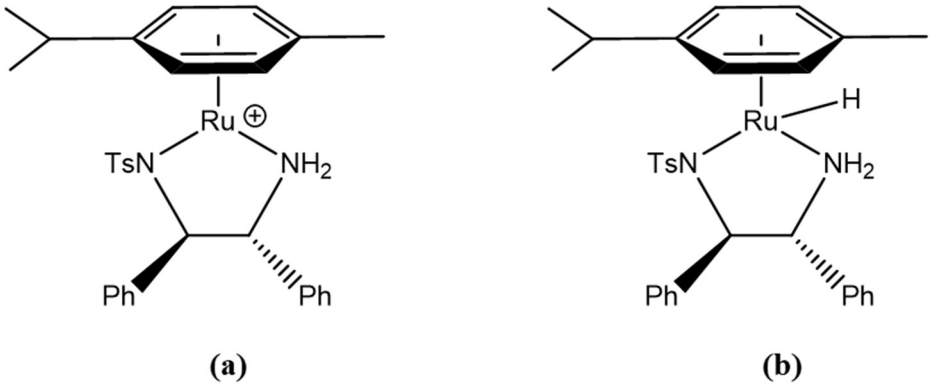

Figure 2.5 The (a) protonated 16-electron Ru complex and (b)18-electron Ru complex.

2.3.3 Organic solvents

The effects of organic solvents on the reaction performance were subsequently investigated with EEF applied. Addition of an organic solvent to the organic substrate can be important in phase

transfer catalysis reactions for promoting the interaction of reactive species in the organic phase. However, in the case when an external electric field is applied, the interactions between reactive species could be significantly different due to the presence of an applied electrostatic force. The difference in physical property of the organic phases could significantly change the strength or magnitude of the electrostatic force applied to the reaction ions, resulting in changes to the interactions between reactive species, which could further influence the reaction performance.

In this part, three commonly used organic solvents with different physical properties were preliminarily studied, as shown in **Figure 2.6** and **Table 2.1**. When non-polar solvent (n-pentane) was employed, the yield of 1-phenylethanol was obtained at 22.6% with a selectivity of about 60% after 24 h of reaction with positive 15 V applied. Toluene showed the poorest influence on acetophenone reduction with the lowest 1-phenyethanol yield and selectivity. However, when chloroform, which has the highest polarity among the three, was used as solvent, the highest 1-phenylethanol yield of 30.7% was achieved under the same reaction condition and the selectivity was as high as 87%.

One possible reason for the observed difference in product yields is the different response of the organic solvent molecules to the stabilization effect on their dipole moments by the oriented external electric field, as suggested by Shaik et al.[84] Once stabilized, the molecule dipole will be aligned opposite to the direction of the electric field. In other words, the molecules are polarized in a certain orientation under the influence of the applied electric fields. Accordingly, in the reaction system studied, when the positive EEF was applied, the resulting positive end of the solvent molecules would orient towards the interface. As chloroform has the largest dipole among the three solvents, it would be polarized to the largest extent, which makes the

chloroform phase most attractive to the negatively charged formate. Additionally, the highest solubility of water in chloroform may also contribute to the increased reaction yield.

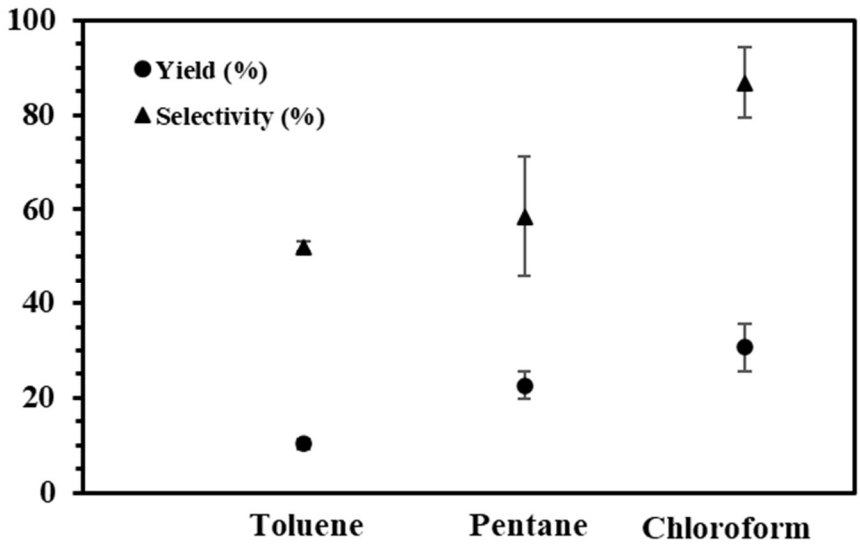

Figure 2.6 Yields and selectivity of 1-phenylethanol with different solvents used and 15 V of positive EEF applied.

The physical properties of the studied solvents are presented in **Table 2.1**. It suggests that the electrical conductivity of the organic solvents may also play an important role in the reaction performance. When the solvent is more conductive, there is less potential drop across the organic phase. As chloroform and n-pentane are about 6 orders of magnitude more conductive than toluene, a higher electric field strength would be maintained across the interface due to the smaller potential drop. This resulted in a larger electrostatic force to promote the migration of formate to the interfacial region and finally led to higher product yields. While toluene has a higher dipole moment than n-pentane, it is much less conductive and gives the lowest 1-phenylethanol yield, suggesting that electrical conductivity may be a dominant factor than dipole in influencing the migration of reactive species under EEFs. When comparing the different effects on reaction performance between chloroform and n-pentane, the higher yield achieved by

using chloroform may be attributed to the overall promoting effects by polarity, electrical conductivity, and solubility. This also suggests that the influence of organic solvents on phase transfer catalysis reaction is much more complicated when an external electric field is applied.

The viscosity of the solvents showed a negligible influence on the reaction performance. This is possibly due to the small difference between the viscosities and the dominant effect of electric field on the mass transfer rate. Overall, chloroform exhibited the best performance among the solvents studied on phase transfer hydrogenation of acetophenone under a low positive EEF of 15 V. Further studies are required to involve more solvents and to reveal their roles in phase transfer catalysis with application of EEFs.

Table 2.1 Physical properties of the studied organic solvents

Solvents	Polarity	Dipole (D)	Electrical conductivity (siemen/cm)	Viscosity (cP)	Mixture viscosity (cP)[a]
Toluene	9.9	0.4	8E-16	0.59	0.88
n-Pentane	0.9	0	2E-10	0.24	0.34
Chloroform	25.9	11	<1E-10	0.57	0.96

[a] Mixture viscosity was measured with a Brookfield Digital Rheometer (DV-III) at 22 °C with 0.5 mL of organic solvents and 0.5 mL of acetophenone.

2.3.4 Potential of EEF

Studies by Kaminski et al. have indicated that increased electric field potential led to improved mass transfer rates. Therefore, the influence of different EEF potential on the reaction performance was studied and the results are presented in **Figure 2.7**. Chloroform was used as solvent and positive electric fields were applied in those experiments. As shown in **Figure 2.7**, the yield of 1-phenylethanol increased by 5-fold and the selectivity increased by more than 2-

fold when the EEF potential increased from 0 V to 15 V. However, when the potential was increased to 30 V, no apparent increase of 1-phenylethanol yield or selectivity was observed.

The observed 1-phenylethanol production showed a non-linear dependence on the EEF potential, while the reason is unknown as the reaction condition was not optimized and the data are not sufficient to draw a conclusion. Further research is required to evaluate more EEF potential values and to elucidate the influence of electric potential upon mass transfer and reaction kinetics of the proposed reaction.

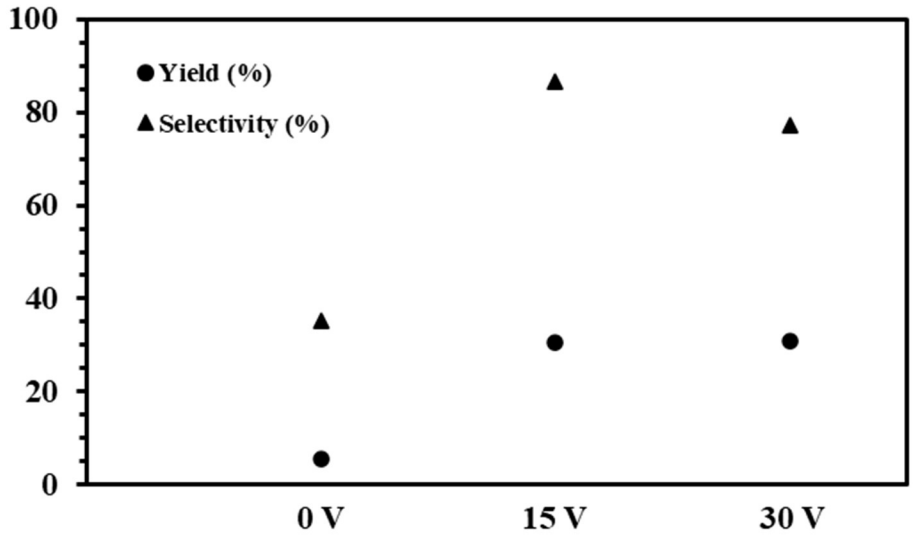

Figure 2.7 Yield and selectivity of 1-phenylethanol under different positive EEF potential with chloroform as solvent.

2.4 Conclusions

The work in this chapter successfully demonstrated the possibility of employing a low external electric field as a replacement of phase transfer catalyst in phase transfer catalysis reactions, particularly for the transfer hydrogenation of acetophenone with sodium formate as reductant. This idea was reported for the first time to the best of my knowledge. The study also

demonstrated experimentally that an EEF can act as promoter or inhibitor for the phase transfer hydrogenation depending on the orientation of the electric field, which suggests a great potential of external electric fields in controlling reaction rates. A mechanistic explanation was attempted to understand the insight of the intensification by a positive EEF based on published theoretical studies of the mechanism. The relatively low product yields are due to the unoptimized reaction conditions.

Overall, the intriguing preliminary findings in this chapter raise the interest to experimentally explore and fundamentally understand the science of electric field chemistry and its application on organic synthesis and catalysis. Further studies on reaction kinetics, product enantioselectivity, etc. will be conducted to better explore the roles of EEFs in the proposed reaction system.

Chapter III: Controlling Reaction Rate of Phase Transfer Hydrogenation of Acetophenone by Application of a Low External Electric Field

3.1 Introduction

The idea of controlling reaction rate and selectivity was originated from the pioneering work by Shaik and co-workers,[83,84,86,87,104,106,107] in which Diel-Alder addition reactions simulated by density functional theory (DFT) methods were reported to be accelerated when an external electric field was oriented along the "reaction axis". It was proposed that application of external electric fields along the reaction axis could enhance the electron flow, leading to a lower reaction barrier and stabilization of transition states and thus promoting the reactions.[83,86] Meanwhile, it was also proposed that the reaction enantioselectivity may be controlled by aligning the electric field along the dipole moment of the reactants.[87] However, attention was not directed at manipulating chemical reactions by application of external electric fields until it was evidenced in an experimental study by Aragones et al., in which a Diel-Alder addition reaction at the single-molecule level was accelerated by an electric field applied through a scanning tunnelling microscopy break-junction approach.[88] Since then, external electric fields have been regarded as smart reagents and catalysts for a range of chemical reactions, and significant efforts have been devoted to this area both theoretically and experimentally.[89,108-110]

While appealing and promising, these studies are only successfully conducted on molecular scale, and precise techniques, such as scanning tunneling microscope break junction (STMBJ) [88,111,112] or mechanically controllable break junction (MCBJ),[89,113,114] are usually required for operation and analysis. Challenges arise when applying those theories and methods to bulk scale

reactions. One of the major challenges is to align the electric field along the reaction axis while thousands of reactant molecules are randomly oriented in the reaction system. Another challenge is to maintain safety when a voltage as high as thousands of volts is applied to a lab-scale (or larger scales) reactor, as the required electric field strength is in the range of 10^7 to 10^9 V/m.[89,110] Due to those challenges, the significance of external electric fields on controlling chemical reactions on bulk scale remains understudied.

The preliminary work conducted in Chapter II provides an alternative way to simply manipulate the reaction rates by controlling the migration of reactive species in the system via the application of a low external electric field. The local concentration of the reactants could be altered by flipping the orientation of the external electric field, thus either promoting or inhibiting the reaction.

In this chapter, further studies are described based on the same model reaction (transfer hydrogenation of acetophenone with sodium formate) in a batch system to give more insights in the roles of external electric fields in reaction control. Studies on electrostatically influenced mass transfer, reaction kinetics, mechanism, product enantioselectivity, catalyst activity, etc. were discussed. Mathematical modeling and simulation using COMSOL Multiphysics software were conducted to support the experimental results.

3.2 Experimental section

3.2.1 Materials

All chemicals used in this work were purchased from commercial reagent suppliers and used without further purification: acetophenone (Sigma-Aldrich, 99%), sodium formate (Sigma-Aldrich, 99.0%), RuCl(p-cymene)[(S,S)-Ts-DPEN] (Sigma-Aldrich), 1-butanol (Sigma-Aldrich,

99.8%), 1-pentanol (Sigma-Aldrich, ⩾ 99%), 1-hexanol (Alfa Aesar, 99%), 1-heptanol (Sigma-Aldrich, 98%), 1-octanol (Sigma-Aldrich, ⩾ 99%).

3.2.2 Experimental apparatus and procedure

The transfer hydrogenation of acetophenone with sodium formate was studied in the same reactor as shown in Chapter II. The biphasic system was set up with a sodium formate/water solution as the more dense aqueous phase and acetophenone/organic solvents as the less dense organic phase in which the Ru complex (RuCl(p-cymene)[(S,S)-Ts-DPEN]) was dissolved. As stated before, the reactor was constructed of highly insulating glass with a cylindrically symmetrical geometry. Two planar electrodes of equal dimensions were coaxially located at each end of the reactor. The electrical field was assumed to be linear and uniform in both radial and vertical direction with negligible space charge migration and wall effects under the low applied voltages which were used. The inner diameter of the reactor was 20 mm. The distance between the two electrode surfaces was 10 mm.

The organic solvents studied here were different from those used in Chapter II, which were 1-butanol, 1-pentanol, 1-hexanol, 1-heptanol, and 1-octanol. Low DC voltage external electric fields from a high voltage power supply (PASCO SF-9585A) was applied across the two phases without agitation. Stainless steel or titanium electrodes were used. To avoid salting-out that occurred in the preliminary work, sodium formate with lower concentration was used. In a single experimental study, 0.34 g of sodium formate was fully dissolved in 1.5 mL of deionized water, while 117 μL of acetophenone was mixed with 1.5 mL of organic solvent to dissolve 0.0064 g Ru catalyst. The mole ratio of Ru catalyst: acetophenone: sodium formate was 1: 100: 500. The reactions were conducted at room temperature and ambient pressure with positive or negative electric fields applied during reaction. The orientations of the electric field were defined in the

same way as discussed in Chapter II. A positive orientation was defined as the direction of the electric field when the anode is placed in the organic phase with the cathode in the aqueous phase. The conversion of acetophenone, total yield of 1-phenylethanol, and enantioselectivity of (S)-1-phenylethanol were determined by gas chromatography using a chiral column.

3.2.3 Analytical methods and characterizations

Gas chromatography

10 μL of liquid samples from the organic phase were withdrawn after each reaction and diluted to 1.5 mL with methanol for gas chromatography analysis. An Agilent 6890N gas chromatograph equipped with a CP-Chirasil-Dex CB column (25m×0.25 mm) and a flame ionization detector was used to identify reaction products and determine enantioselectivity under the following conditions: helium as carrier gas (3 mL/min), inlet and detector temperature 250 °C, oven temperature 115°C. The retention time of the chiral 1-phenylethanol products ((S) and (R) 1-phenylethanol) was determined respectively based on the peak areas, the Ru catalyst used, and the reference retention time from literatures.

The enantioselectivity of the (S)-1-phenylethanol is determined as,

$$\%ee = (S - R)/(S + R) \times 100$$

where *S* and *R* represent the moles of (S)-1-phenylethanol and (R)-1-phenylethanol, respectively.

Nuclear magnetic resonance (NMR) spectroscopy

Four samples were prepared for NMR analysis. Sample 1 was prepared by dissolving 5.8 mg of RuCl(p-cymene)[(S,S)-Ts-DPEN] in 500 μL of MeOH-d4 (Cambridge Isotopes). Sample 2 was obtained by dissolving 6.4 mg of RuCl(p-cymene)[(S,S)-Ts-DPEN] in a mixture of 1.5 mL 1-butanol and 117 μL acetophenone. Samples 3 and 4 were collected from reactions under positive and negative 15 V of electric potential respectively after 24 h using titanium electrodes and 1-

butanol as solvent. 500 μL of each liquid sample were pipetted into a 5 mm NMR tube (Wilmad Lab-Glass, Vineland, NJ). All NMR spectra were acquired on a 500 MHz Bruker AVIII spectrometer equipped with a cryogenically cooled X-channel observe probe. All data was analyzed using MestreNova NMR software (Santiago De Compostela, Spain).

X-ray florescence (XRF)

A handheld XRF analyzer (Olympus, Delta Professional) with Ru anode and silicon drift detector was used for fast determination of the metal contents in the degradation products of stainless steel electrode. These solid samples were collected from the interface after reaction and dried prior for analysis. Precious metal mode with a targeted collimator was employed during analysis. All samples were scanned three times and analyzed with the workstation setup.

3.3 Theoretical modeling and simulation

The transport of the charged reactive species, referred to as electromigration in the present study, was modeled based on the Nernst-Plank equation.[115-117] The molar flux of species *i*, *Ji*, is expressed in Equation (3-1), describing the diffusion by concentration difference and migration by electrostatic force. The convection term is not included due to the fact that the experiments were conducted in a quiescent hydrodynamic environment.

$$J_i = -D_i \nabla c_i - \frac{D_i z_i F}{RT} c_i \nabla \Phi \tag{3-1}$$

where D_i is the diffusion coefficient (m^2/s), c_i is the ion concentration (mol/m^3), z_i is the valence number, F is the Faraday constant, R is the gas constant, T is the absolute temperature (K), and Φ is the electric potential (V).

The Wilke-Chang equation (Equation (3-2))[118] was applied to estimate the mutual diffusion coefficient of acetophenone and the Ru catalyst in 1-butanol, where M_B refers to the molecular

weight of solvent, μ_B is the viscosity of solvent, V_A is the molar volume of the solute. A value of unity was used for the empirical parameter φ.

$$D_{AB} = \frac{7.4\times10^{-8}(\varphi M_B)^{1/2}T}{\mu_B V_A^{0.6}} \tag{3-2}$$

The electric field in the domain was described by the Poisson differential equation[118]:

$$\nabla \cdot (\varepsilon_0 \varepsilon_r \nabla \Phi) = -\rho_v \tag{3-3}$$

where ε_0 is the dielectric constant of the free space, ε_r is the relative permittivity of materials, ρ_v is the electric space charge density.

Figure 3.1 illustrates the model geometry of the reactor and the accounted species in the two phases. Simulation was conducted to understand the mass transfer of reactive species in the proposed reaction system, assuming no reaction nor flux at/across the interface. Therefore, the boundary condition was set up in equations (3-4).

$$\text{At } z = L, -\nabla J_i = 0 \tag{3-4}$$

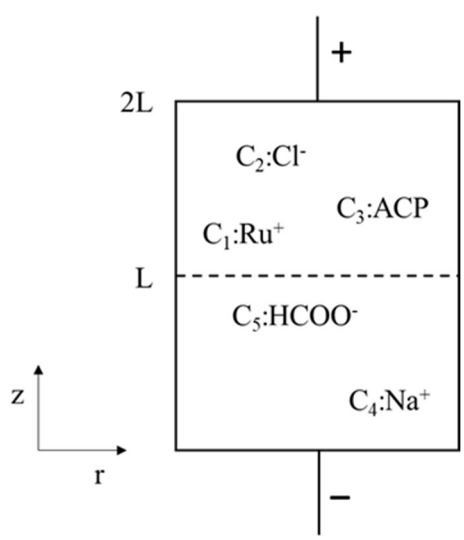

Figure 3.1 Model geometry. L = 0.5 cm. ACP is short for acetophenone.

The equations were solved using the finite element method in COMSOL Multiphysics 5.4, with defined initial concentrations, charge numbers, and mutual diffusion coefficient values. Concentration profiles of Ru catalyst and formate at the interface were calculated under various external electric fields.

3.4 Results and discussion

3.4.1 Solvent effects

The effects of the different organic solvents used in conjunction with the acetophenone reactant were first studied as their different physical and chemical properties could significantly affect the reaction performance, especially when an external electric field is applied. Five primary alcohols, namely 1-butanol, 1-pentanol, 1-hexanol, 1-heptanol, and 1-octanol as organic solvents were investigated. The choices were made based on the principles of green chemistry on one hand, on the other hand, the selected solvents should be immiscible with water and have distinguishable density difference in order to maintain a stable biphasic reaction system. A number of different organic solvents were tested, and these five primary alcohols stood out for their low environmental impacts and the abilities to generate a stable interface with water.

The experimental results are presented in **Figure 3.2**, showing total conversion values and product yields. **Table 3.1** lists the physical and chemical properties of the five solvents. No corresponding aldehyde by-products were detected by GC analysis after the reactions, which confirmed the role of sodium formate as hydrogen source and the concept of phase transfer hydrogenation. As we can see, addition of 1-butanol resulted in the best performance in promoting the transfer hydrogenation of acetophenone with or without external electric fields. When 15 V of positive DC voltage was applied, the conversion and yield were almost doubled

compared to those with no electric field applied, reaching 84.7% and 76.8% respectively after 24 h of reaction. The conversion and yield decreased gradually with the increase of the molecular weight of these homologous alcohol solvents regardless of applied electric fields.

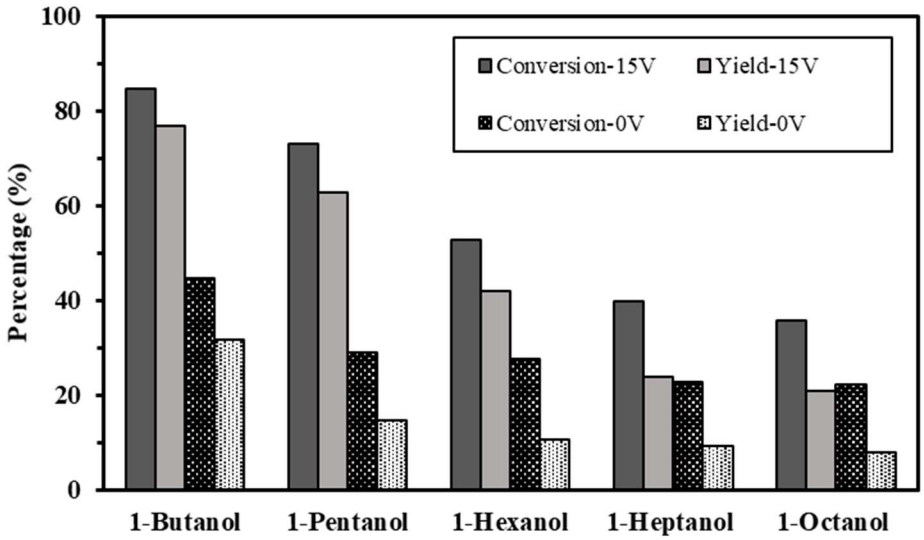

Figure 3.2 Acetophenone conversion (mol%) and 1-phenelethanol yields (mol%) under 0 V or 15 V of positive external electric field for 24 h with different organic solvents and stainless steel electrodes.

One possible reason for the significantly different performance may be their respective solubilities in water. Compared to the other solvents, 1-butanol has the highest solubility in water, which initially promotes the interaction between the reactants at the interface to the most extent, resulting in the highest conversion and reaction rate (more than 2-fold faster than that with 1-octanol as solvent). On the other hand, these alcohols are protic solvents, which possess the ability to generate protons by dissociation. With the largest dielectric constant value among the studied solvents, 1-butanol has the greatest potential to be polarized to generate protons under an external electric field. These protons could further promote the dissociation of the neutral Ru compound (RuCl(p-cymene)[(S-S)-Ts-DPEN]) to form the cationic Ru complex

(species **2** in **Figure 3.5**) by removing the chloride ion, therefore accelerating and promoting the generation of the catalysts and ultimately increasing the production rate. While the dipole moment and electrical conductivity might be important in electrostatically promoted reactions according to the previous investigation in Chapter II, the differences of these properties between the five solvents are small. Accordingly, it is difficult to attribute the differences in reaction performance to dipole moment and conductivity in the present study.

Table 3.1 Properties of the studied organic solvents.

Solvent	Electrical conductivity (ns/cm)	Solubility in water (25°C/mass%)[119]	Dipole(D)[119]	Dielectric constant (20°C)[119]
1-butanol	60[120]	7.3	1.66	17.84
1-pentanol	41[121,122]	2.14	1.7	15.13[a]
1-hexanol	--	0.59	--	13.03
1-heptanol	--	0.164	--	11.75
1-octanol	66[120]	0.046	1.76	10.3

a: This value was obtained at 25°C.

3.4.2 Electric field potential

Various values of positive external electric field potential were applied to determine their effects on mass transfer and kinetics in the proposed reaction system. The conversion of acetophenone under different values of positive external electric field, recorded at different times are shown in **Figure 3.3**. The data in this Figure are only for the acetophenone/1-butanol mixture using stainless steel electrodes. It was observed that the initial reaction rates increased with the increase of electric field potential. The conversion of acetophenone in the presence of an applied voltage of 100 V was observed to reach 44.5% after a reaction time of 2 hours, which is nearly 4-fold of the conversion attained at 15 V. However, at longer reaction times, the rate of increase

was observed to decline. The decline was greater at the higher voltages. For example, after 8 h, a higher conversion was achieved at 15 V compared to the values observed at 30 V and 50 V. The total conversion at 15 V reached 84.7% after 24 h which is about 20% higher than that at 30 V and 40% higher than that at 50 V.

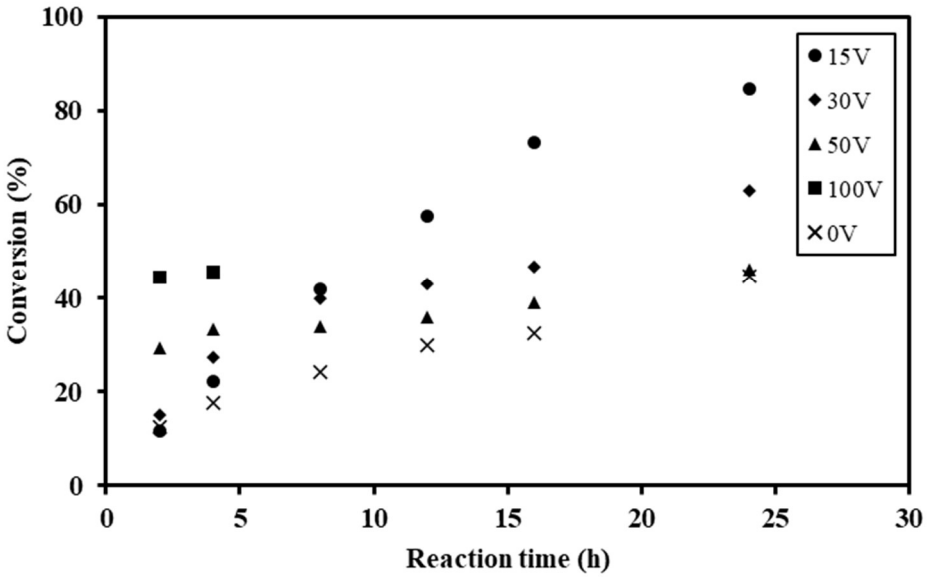

Figure 3.3 Acetophenone conversion (mol%) under different positive external electric field for 24 h with stainless steel electrodes and 1-butanol as solvent.

The increase in conversion with increased electric field potential in the first few hours is consistent with the increased mass transfer of charged reactive species controlled by external electric fields. This is supported by the simulation results in **Figure 3.4**. As we can see, the rates of electromigration of both formate and Ru catalyst were increased with the increase of voltage at the beginning. The enhancement of reaction rates observed under higher electric fields is consistent with the accelerated transportation rates of both formate anions and the cationic Ru catalysts to the liquid-liquid interface, resulting in more rapid reactions compared to those with lower electric fields applied. The simulation results also suggested that the equilibrium concentration of Ru catalyst at the interface decreased with increased voltage, which explains the

corresponding lower conversion at longer reaction times when higher electric fields were applied. Additionally, as suggested by Pavlova et al.,[105] a negatively charged alkoxide intermediate could be formed during the reaction. As the reaction continues, a portion of these alkoxide anions could be attracted and constrained to the region close to the anode electrode, preventing these reactive species from migrating to the interface region and thus retarding the reaction rates. This inhibition is greater when a greater electrostatic force is applied, leading to the lower reaction rate as observed at an elevated electric field potential after longer reaction times.

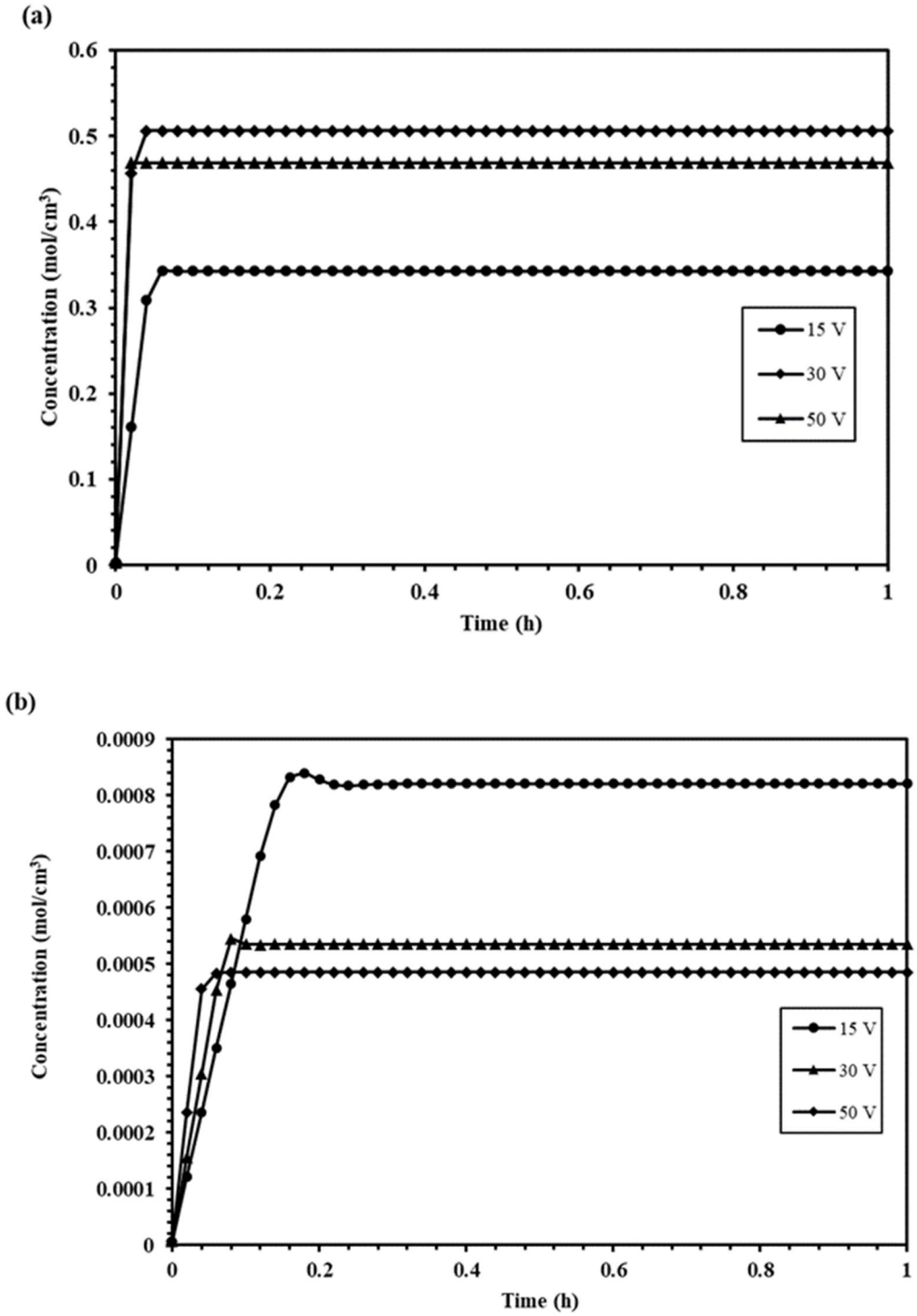

Figure 3.4 Simulated concentration profiles at the interface under various electric fields. (a) concentration profile of formate ions, (b) concentration profile of Ru catalyst.

On the other hand, an external electric field induced current flow in the reaction system along with degradation of the stainless steel anode electrode (immersed in the organic phase) were observed. Additionally, gas bubbles of unknown composition were generated on the cathode. The degradation of the electrode was confirmed by weight loss measurement (see Cases 1, 2 and 3 in **Table 3.2**). The degradation products which formed a thin layer of black slurry at the liquid-liquid interface were characterized by XRF analysis. The analysis showed that the slurry consisted mainly of Fe, Ni, and Cr with a small amount of Ru. For reactions under higher electric potentials, higher current flows and greater degradation rates of the anode electrode were observed as shown in **Table 3.2** (Cases 1, 2, and 3). The decomposition of the electrode is consistent with galvanic corrosion, in which hydrogen is produced at the cathode with the corrosion occurring at the anode. At higher electric potentials, stronger galvanic corrosion effects would be expected, leading to greater electrode degradation rates. With more metal ions released from the degradation process, higher current flows would be observed due to increased conductivity of the system. The degradation products formed as a slurry layer at the interface could block the interface thus decelerating the reaction by inhibiting the mass transfer to the interface. At higher electric potential, a higher degradation rate was observed, leading to a higher blocking coverage of the interface and finally leading to a lower reaction rate and conversion.

To eliminate the negative effects of electrode degradation and clarify the inhibiting effects of high electric potential, chemically stable titanium electrodes were employed as replacements of stainless steel electrodes, and the results are recorded as Cases 4, 5, and 6 in **Table 3.2**, compared to those with stainless steel electrodes (Cases 1, 2, and 3). For experiments with different electric potential applied, the average degradation rate of titanium electrodes is less than 0.1% w/w, and no apparent black slurry was observed. Although there was negligible evidence

of titanium electrode degradation, reaction performance showed the same trend as observed in the experiments using stainless steel electrodes, when the applied electric potential was increased. This suggests that the electrode degradation plays a minimal role in the changes of reaction performance, thus strongly suggesting the influence of electrostatic forces on the controllable migration of Ru catalyst and alkoxide ions being the main reason for the reaction deactivation and the importance of external electric fields in controlling reaction rates. Furthermore, in spite of apparent reaction deactivation, a constant product ((S)-1-phenylethanol) enantioselectivity was achieved. This is evidence that there was no catalyst decomposition during the reaction under positive external electric fields, which may further suggest that the deactivation is most likely due to the influenced migration of reactive species.

Table 3.2 Summary of experiments under various positive external electric fields.

Case	Voltage (V)	Time (h)	Electrode	Current (mA)	Weight loss (% w/w)	Yield (%)	ee (%)
0	0	24	--	N/A	~0	49.8	94.6
1	15	24	SS	1.2	3.5	76.8	93.5
2	30	24	SS	1.7	4.3	55.5	93.4
3	50	24	SS	2.6	4.4	32.6	93.3
4	15	24	Ti	0.2	0.085	67.4	94.5
5	30	24	Ti	0.5	0.085	60.1	94.5
6	50	24	Ti	1.6	0.09	26.6	94.5
7	30-8h + 15-16h		Ti	0.2	0.09	67.5	94.5
8	30-4h + 15-20h		Ti	0.2	0.02	63.9	94.3
9	50-4h + 15-20h		Ti	0.2	0.1	47.1	94.3

A further set of experiments was conducted to investigate the reaction performance when the applied electrical potential was varied over the course of the reaction. With reference to **Table 3.2**, the data shown in the last three rows list the results of these experiments, labelled Cases 7, 8,

and 9. In case 7, after reacting for 8 h under 30 V, the electric potential was switched to 15 V for another 16 h of reaction. The reaction yield reached 67.5%, increased by 7.4% compared to that with solely 30 V applied for 24 h (Case 5). In case 8 and 9, 30 V or 50 V were applied for 4 h respectively followed by application of 15 V for 20 h. In these two cases, the yields of 1-phenylethanol increased when comparing to those with solely 30 V or 50 V applied for 24 h. These results suggest that the reaction could be externally controlled by simply switching the applied electric potential over the course of the reaction.

3.4.3 Proposed mechanism and kinetics study

Based on the observations, a stepwise mechanism for the phase transfer hydrogenation of acetophenone with aqueous formate as hydrogen source and RuCl(p-cymene)[(S,S)-Ts-DPEN] as catalyst under an external electric field is proposed in **Figure 3.5**. The cationic Ru complex **2** is generated by removal of chloride after compound **1** dissolves in 1-butanol. Following the formation, species **2** undergoes electromigration to the interface where a hydride is transferred to **2** from a formate to generate Ru-hydride species **3**, with the release of CO_2.[101] Instead of transferring both hydrogen to the substrate concertedly,[94] only the hydride on Ru-H in complex **3** is transferred to acetophenone with the proton on the NH_2 moiety retained,[105] resulting in the regeneration of species **2** and the formation of the corresponding alkoxide intermediate due to the stabilization of water by hydrogen bonding.[105] This hydride transfer step is proposed as the rate-limiting step. Finally, the alkoxide quickly picks up a proton from water to form the product,[105] and the generated hydroxide further reacts with CO_2 to form bicarbonate as observed in the study in Chapter II.

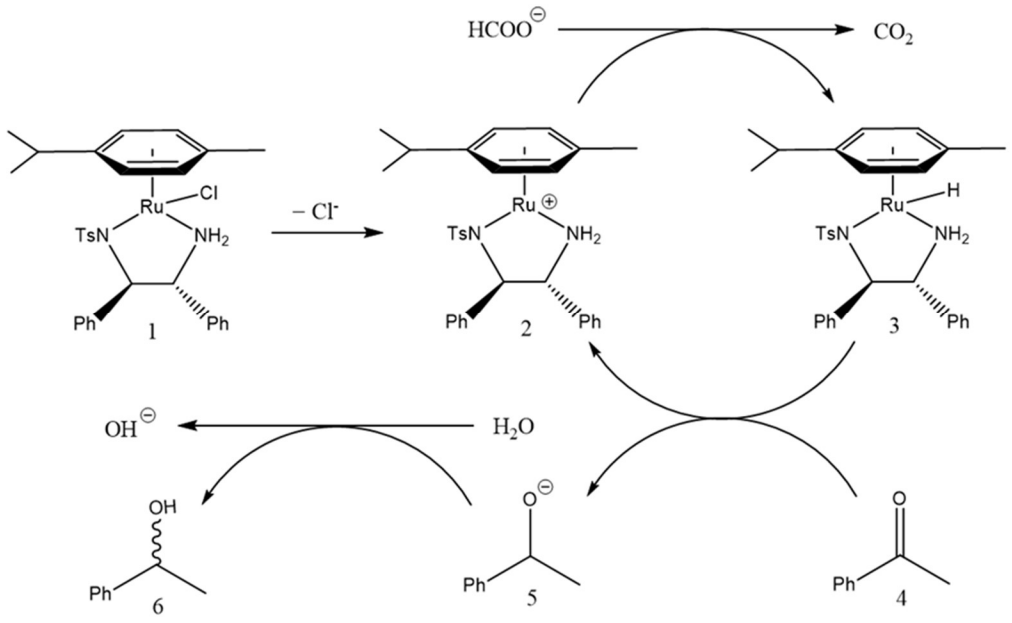

Figure 3.5 Proposed mechanism for the phase transfer hydrogenation of acetophenone with aqueous formate as hydrogen source and Ru-TsDPEN catalyst. **1**: neutral Ru pre-catalyst (RuCl(p-cymene)[(S-S)-Ts-DPEN]), **2**: cationic Ru catalyst (Ru^+(p-cymene)[(S-S)-Ts-DPEN]), **3**: Ru-hydride catalyst (RuH(p-cymene)[(S-S)-Ts-DPEN]), **4**: acetophenone, **5**: corresponding alkoxide of acetophenone, **6**: 1-phenylethanol.

The stoichiometry and rate expression consistent with the proposed mechanism are summarized in Equations (3-5) - (3-11), assuming that the coordination of formate with species **2** to form a formato intermediate and its decarboxylation to generate species **3** are reversible and equilibrated prior to hydrogen transfer,[101] where K_1 is the equilibrium constant, and k_1, k_2, k_3 are the respective reaction rate constants. *ACP* and *ACPH*$^-$ represent acetophenone and its corresponding alkoxide, while 1-*PE* refers to 1-phenylethanol and [*Ru*] represents the total concentration of catalyst. As CO_2 rapidly reacts with hydroxide to form bicarbonate during the reaction, the concentration of CO_2 in the system is expected to be small, therefore the rate expression can be further simplified as a second order kinetics over the concentration of catalyst and substrate (Equation (3-11)). This is consistent with the study by Wu et al.[101] and with the above observation which showed that the reaction rates were limited by the concentration of Ru

catalyst and the alkoxide at the interface region. Both of these concentrations were affected by the electromigration under the influence of external electric fields. These observations suggest an important impact of electric fields on kinetics of interfacial reactions involving reactive ions.

$$2 + HCOO^{-} \overset{K_1}{\leftrightarrow} 3 + CO_2 \tag{3-5}$$

$$3 + ACP \overset{k_1}{\rightarrow} 2 + ACPH^{-} \tag{3-6}$$

$$ACPH^{-} + H_2O \overset{k_2}{\rightarrow} 1 - PE + OH^{-} \tag{3-7}$$

$$CO_2 + OH^{-} \overset{k3}{\rightarrow} HCO_3^{-} \tag{3-8}$$

Overall: $$HCOO^{-} + ACP + H_2O \rightarrow 1 - PE + HCO_3^{-} \tag{3-9}$$

Rate expression: $$r = \frac{K_1 k_1 [Ru][ACP][HCOO^{-}]}{[CO_2] + K_1[HCOO^{-}]} \tag{3-10}$$

When $[CO_2] \ll K_1[HCOO^{-}]$, $$r = k_1[Ru][ACP] \tag{3-11}$$

3.4.4 Electric field polarity and product enantioselectivity

As shown in **Table 3.2**, the enantioselectivity of (S)-1-phenylethanol remained constant when electric fields were applied in the positive orientation. Since the orientation of EEF was proved to be important for controlling reaction rates in the study in Chapter II, a reversed external electric field was then applied to the reaction system. The results are presented in **Table 3.3**. In these cases, the reactions were inhibited when the electric potential was applied in the negative orientation compared to that without electric fields applied, which further confirmed the idea of controlling mass transfer and reaction rates by external electric fields, in accord with the findings in Chapter II.

However, the yield of 1-phenylethanol increased with the increased negative electric field potential, which was unexpected, since larger inhibiting electrostatic forces should result in

lower reaction rates and conversion. Those unexpected increases are likely attributed to the significant increase in the current flow in the reaction system. As shown in **Figure 3.6**, the increase in negative electric field potential led to an increase in the current flow, which increased the instability of the reaction system. Increase in current flow is consistent with the local temperature increase due to joule heating, which may counteract some of the inhibiting effects caused by higher negative electrostatic forces and finally promote the reactions.

Table 3. 3 Summary for experiments with various negative external electric fields applied.

Voltage (V)	Time (h)	Electrode	Average current (mA)	Yield (%)	ee (%)
0	24	--	N/A	49.8	94.6
-5	24	Ti	1.0	16.9	91.0
-10	24	Ti	6.2	22.4	86.0
-15	24	Ti	8.9	23.0	66.1
-20	24	Ti	15.0	45.6	82.9
-30	24	Ti	44.0	48.4	75.2

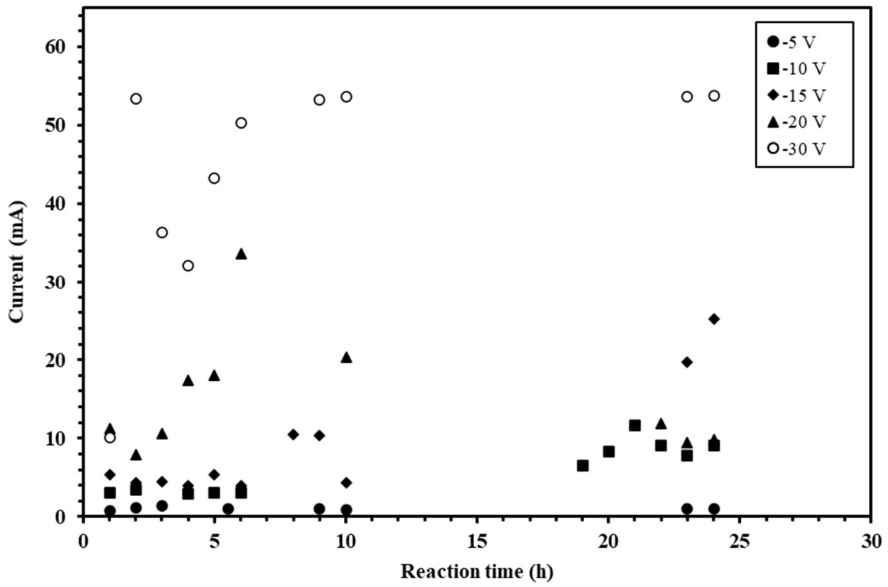

Figure 3.6 Current flow at different reaction time under various negative external electric fields.

On the other hand, with the increase of the negative electric potential, decrease in (S)-1-phenylethanol enantioselectivity was observed. However, these changes in the enantioselectivity are probably not due to the ability of EEF on controlling reaction selectivity but are more likely attributed to the catalyst decomposition. **Figure 3.7** showed the NMR analysis for the identification of the chiral Ru catalyst structure in the system before and after reactions. Samples 1 (spectrum A) and 2 (spectrum B) were obtained by dissolving the fresh Ru catalysts in CD_3OD and reaction mixture (1-butanol and acetophenone mixture) respectively, and peaks from the Ru catalyst are clearly present at approximately 6.57 and 6.79 ppm. For sample 3 (spectra C), collected from the reaction run under positive 15 V for 24 h, small signals (due to the low initial concentration and difficulty of detection in 1H NMR spectra) for the Ru catalyst can be seen. However, the NMR spectra for sample 4, collected from the reaction run under negative 15 V for 24 h, showed no signals for the Ru catalyst. While the apparent decomposition of the Ru catalyst is strongly correlated with the use of the negative electric fields, the mechanism of decomposition has not been elucidated. NMR experiments conducted with deuterated acetophenone in the presence of deuterated butanol are expected to provide more insight into the decomposition mechanism of the catalyst but are beyond the scope of the present research.

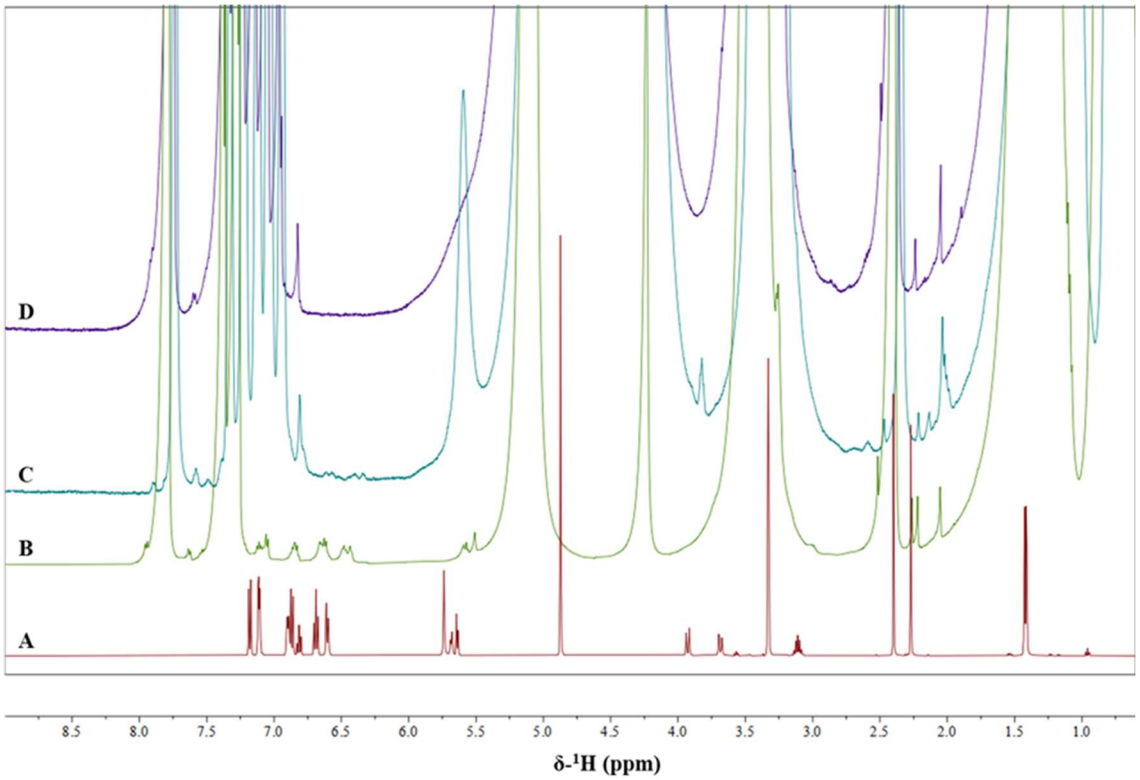

Figure 3.7 Stack plot of 1D 1H NMR spectra of samples 1 (A), 2 (B), 3 (C) and 4 (D). To highlight the minor species, spectra B was expanded vertically by 8 times, and spectra C and D were expanded by 24 times.

3.5 Conclusions

In this chapter, the control of reaction rates by application of low external electric fields for the catalytic transfer hydrogenation of acetophenone was demonstrated. The influence of applied electric fields on reaction performance was evaluated experimentally and the controllable mass transfer of reactive species by electric fields was further supported by simulation results. Significant improvements in reaction conversion and yield were achieved at low values of positive voltage relative to a control of zero volts, with an optimum voltage of positive 15 V. Increases beyond this value to positive 30 V and 50 V showed significant reduction in performance at longer reaction times due to lower equilibrium concentration of Ru catalyst at the interface and possible formation and migration of the alkoxide intermediate during reaction. The

degradation products from the electrolytic corrosion of the stainless steel electrodes did not significantly impact the hydrogenation reaction. The influence of different EEF values on the concentrations of reactive species at the interface was suggested as the main reason for the differences in reaction performance. Enantiomeric excess values were measured, and no significant changes were observed with variation in the positive voltage values. A mechanism and reaction rate expression were proposed based on the observations, suggesting the importance of external electric fields in influencing reactions with reactive ions involved.

The direction of the applied electric field was proved to be important as both reaction conversion and enantioselectivity were significantly reduced when the electric field was in the negative orientation. Meanwhile, a monotonic increase in conversion was observed as voltage increased from -5 V to -50 V due to possible temperature increase resulted from the increase of current. Catalyst decomposition by the influence of negative voltages was concluded as the main reason for reduced enantioselectivity, as implied from the NMR analysis.

The field strength in this study is in the scale of kilovolts per meter (e.g. 1500 V/m, 3000 V/m, or 5000 V/m), which is 4 to 6 order smaller than those (10^7 to 10^9 V/m) applied in the experiments at molecular level, indicating a much lower energy consumption. It is likely that scale up of the proposed reaction system in a larger reactor, based on geometrical similarity of the reactor and electrodes with the same symmetry, would result in similar enhancements. It is worth noting that differences in electrode geometry or aspect ratio in a scaled-up reactor would give rise to significant differences in the distribution of electrical field strength and thus reaction conditions and performance. Given the importance of bulk scale applications, further experimental and simulation studies would be necessary for in-depth study of the effects of reactor and electrode geometry on reaction performance.

Overall, this work extends the scope for controllable synthesis of organic reactions conducted in two phase liquid systems and raises an opportunity to approach green engineering with minimal energy consumption for mass transfer limited reactions. It is also important for understanding the influence of external electric fields on mass transfer and kinetics in biphasic liquid systems used for organic synthesis and interfacial catalysis on macroscale.

Chapter IV: An Electrospray-Based Flow Reaction System for Intensified Transfer Hydrogenation of Acetophenone

4.1 Introduction

In Chapters II and III, the application of a low external electric field has been successfully demonstrated as an efficient tool for process intensification and manipulation of the phase transfer hydrogenation of acetophenone in a batch liquid biphasic system. However, the reaction time is long due to the small interfacial area constrained in the tube reactor, which needs to be improved to achieve faster reaction rates. As has been discussed in Chapter I, application of an external electric field to generate an electrospray has been demonstrated as a feasible and efficient approach for generation of fine droplets in liquid biphasic systems to increase interfacial areas. This technique has the advantage of easy set-up compared with, for example, microreactors. It also offers the potential for lower energy consumption compared with dispersion by mechanical stirring. Therefore, in this chapter, a flow reaction system based on electrospray is established to increase the interfacial area between the two liquid phases, thus achieving higher conversions in shorter reaction times.

Among the limited studies on the application of electrospray on liquid-liquid biphasic reactions, the improvements in reaction performance are mainly attributed to the increased interfacial areas. However, other parameters, such as electric field induced current flow, catalyst activity under an electric field, and composition of the two phases may also influence the reaction performance yet are not investigated nor fully understood.

Hence, the aim of the work described in this chapter is to achieve two goals, 1) achieving high conversion for the studied reaction system in short reaction times, 2) providing more insight

for the fundamental understanding of electrospray in intensifying reaction performance in liquid biphasic reaction systems.

In the studied reaction system, the aqueous sodium formate solution is highly conductive, serving as the dispersed phase, while the organic phase consisting of acetophenone and other solvents is of low conductivity, serving as the continuous phase. By continuously spraying the aqueous sodium formate solution into the organic phase and recycling it at the outlet of the reactor, a continuously flowing reaction system was established. The magnitude and polarity of applied electric fields, the flow rate and concentration of dispersion phase, and the composition of continuous phase were studied to evaluate their influence on reaction performance.

4.2 Experimental Section

4.2.1 Materials

All chemicals used in this work were purchased from commercial reagent suppliers and used without further purification: acetophenone (Sigma-Aldrich, 99%), sodium formate (Sigma-Aldrich, 99.0%), RuCl(p-cymene)[(S,S)-Ts-DPEN] (Sigma-Aldrich), toluene (Sigma-Aldrich, anhydrous, 99.8%), 1-butanol (Sigma-Aldrich, 99.8%).

4.2.2 Experiment apparatus

The experimental arrangement is comprised of the reactor located inside an isolated cabinet equipped with interlock protection to prevent access in the presence of high voltages, shown in **Figure 4.1**. The electric field was applied to the reactor from a high voltage power supply unit (Glassman high voltage unit, XP power). The aqueous feed was metered to the reactor using a peristaltic pump (Fisherbrand™ Variable-Flow Peristaltic Pumps) located outside of the cabinet together with the power unit to ensure safe manipulation of voltages and pumping speeds.

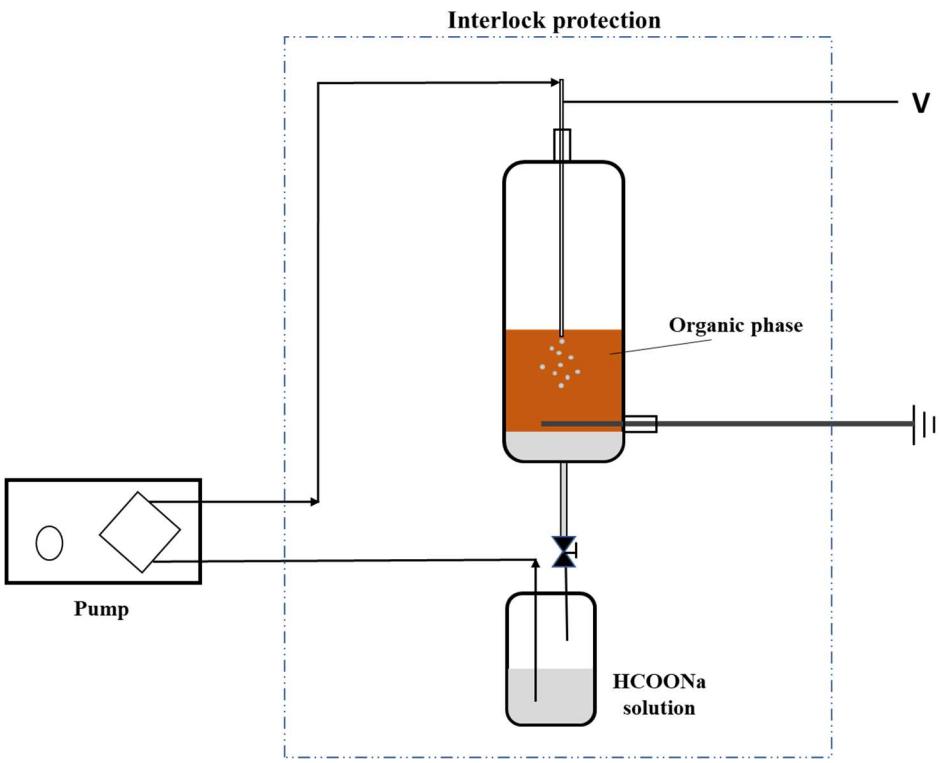

Figure 4.1 Sketch of the experiment setup for the continuous electrospray reaction system.

The reactor used here is different from the one used in Chapters II and III. It was also constructed of highly insulating glass but with a lower electrode located horizontally through the wall of the reactor and an outlet at the base of the reactor controlled by a valve. An upper electrode (a stainless steel nozzle) was inserted coaxially at the top of the reactor. The configuration in this reactor is not symmetrical in geometry and thus the electrical field was not assumed to be linear or uniform in either radial or vertical direction under the high applied voltages which were used. The inner diameter of the reactor was 30 mm. The distance between the two electrodes was 30 mm (for reactions with 30 mL of organic solvent used). The high voltage power supply was designed to cut out at a low current threshold, typically 6 mA, for safety concerns. The interlock system ensures the power supply to be automatically shut down if

the door of the cabinet was opened during high voltage operation. An extract fan was installed on the top of the cabinet to prevent possible accumulation of organic vapors.

4.2.3 Experimental procedure

The transfer hydrogenation of acetophenone with sodium formate as hydrogen source was studied in the aforementioned reactor with different volumes (20 mL or 30 mL) and compositions of organic phase. The organic phase was a mixture of toluene and 1-butanol with different volumetric ratios of 1-butanol. A typical reaction was conducted with addition of 30 mL of organic solvent (volumetric ratio of 1-butanol as 16.7%), to which 585 μL of acetophenone (1.67E-4 mol/mL) was added with 0.032 g of the Ru catalyst (1.67E-6 mol/mL) dissolved to form the continuous organic phase. An aqueous sodium formate solution of 20 mL with a concentration of 0.0025 mol/mL was sprayed through a stainless-steel nozzle into the organic phase at various flow rates and under different electric fields. The mole ratio of Ru catalyst: acetophenone: sodium formate was 1: 100: 1000. A positive electric field is generated when the nozzle is connected to the power source and the bottom electrode is earthed, while a negative electric field is generated when the connections are reversed. The nozzle was made from a length of 316 stainless steel tubing with an inner diameter of 0.61 mm and outer diameter of 2.4 mm. Electric field voltages in the magnitude of 0 kV to 4 kV were studied. The reactions were run for 1 or 2 hours. After reaction, samples from the organic phase were withdrawn and centrifuged to separate out the aqueous holdup retained in the organic phase. After centrifugation, a small amount of the organic sample was collected and diluted with methanol before it was analyzed by gas chromatography.

4.2.4 Analytical methods and characterizations

Gas chromatography

For a reaction involving 30 mL of organic solvent, 40 μL of organic samples were collected and diluted to 1.5 ml with methanol for gas chromatography analysis. For experiments in which 20 mL of organic solvent were used, 25 μL of the organic samples were analyzed. An Agilent 6890 N gas chromatograph equipped with a CP-Chirasil-Dex CB column (25 m × 0.25 mm) and a flame ionization detector was used to identify reaction products and to determine enantioselectivity under the following conditions: helium as carrier gas (3 ml/min), inlet and detector temperature 250 °C, oven temperature 115 °C.

Droplet size measurement

In this study, detailed droplet size measurements were not included. Examination of video footage, however, suggests a strong dependence of droplet size upon operating voltage with transitions from dripping mode flow (~1800 μm at 1 kV) to cone-jet mode flow (150-300 μm non-spherical at 1.3 kV) to fine mist (< 25 μm at 3 kV), consistent with observations in other systems reported in the literature.[123] The lack of more rigorous droplet size distribution data is deemed reasonable, as the correlations between the droplet size and electric fields and flow rates of dispersed phase are well established by other researchers.[74,77,79]

4.3 Results and discussion

4.3.1 Magnitude and polarity of applied electric fields

The influence of the magnitude and polarity of the applied electric fields was studied with 30 mL of organic solvent consisting of 16.7% v/v 1-butanol. The results are summarized in **Figure 4.2**. With this organic mixture as continuous phase, negligible current flow was detected during the

reaction, thus minimizing the influence of joule heating on the reaction performance. When a positive voltage of 1 kV was applied, conversion and yield values were found comparable to those without an external electric field applied. This was explained by the fact that a dripping mode of electrospray with discrete droplet formation[123,124] was observed when 1 kV of voltage was applied. The slight decrease in droplet size and increase in drop velocity under this condition, compared to the case with no electric field applied, was not considered as a significant influence on either the interfacial area or the reaction performance. Further increase in the applied voltage to 1.3 kV resulted in a cone-jet mode of droplet formation[123,124] with significant reduction in drop size. When the voltage was increased to 2 kV, formation of an emulsion started to be observed. Once a stable emulsion was generated, the conversion and yield increased with the increase in the magnitude of the applied electric field. This may be explained by the decrease in droplet size and the resulting increase in interfacial area. Circulation of the emulsion droplets in the continuous organic phase was also observed, which may further promote mass transfer at the interfacial region.

It is interesting to note that the polarity of the applied electric field did not make a difference to the reaction performance when comparing the experiments which were operated respectively with positive and negative voltages of 3 kV applied. This observation contrasts with the findings in other electrospray systems observed by other researchers,[81,82] suggesting a complex dependence of observed reaction rate upon both droplet size and field-induced modification of intrinsic kinetics. On the other hand, the electrospray system in the present work was significantly different from the reported systems in composition and phases, which added more complexity to elucidate the role of electric field polarity in influencing droplet size and reaction performance. Additionally, the observation regarding the direction of electric field on reaction

performance is different from the observation in the quiescent batch system studied in Chapters II and III, in which the reaction was either promoted or inhibited depending on the orientation of the applied electric fields. This difference may be explained by the different migration distance required for reactive species across the interfacial boundary and the different electrostatic forces acting on reactive species in the two systems with different geometries.

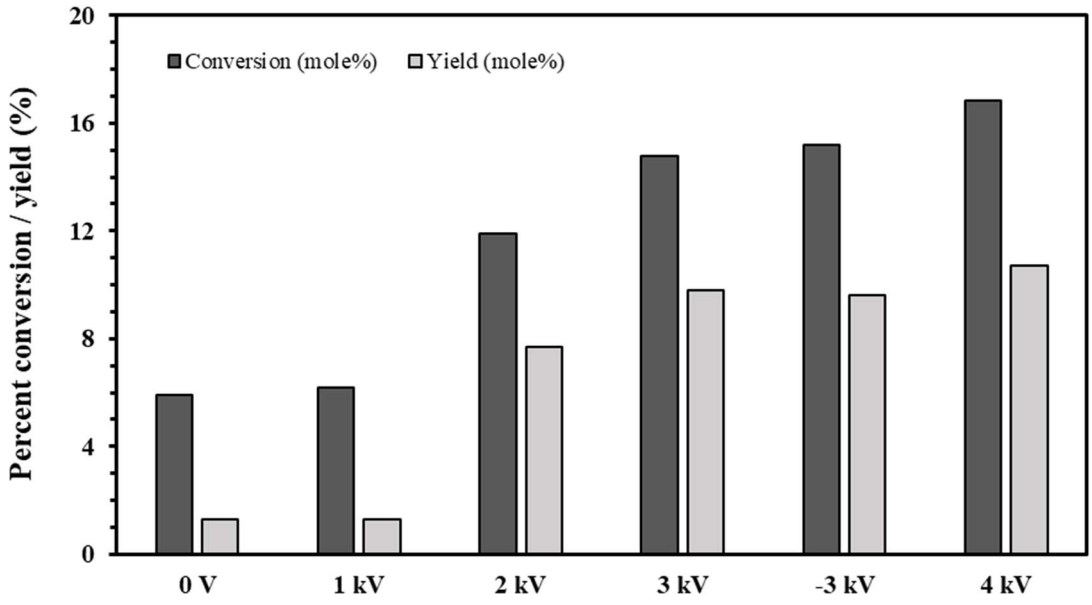

Figure 4.2 Reaction conversions and product yields under various electric field conditions. The concentration of sodium formate solution was 0.0025 mol/mL, and the flow rate of dispersed phase was 0.82 mL/min.

4.3.2 Flow rates and concentration of dispersed phase

Studies have shown that flow rate and conductivity of the dispersed phase have major effects on the droplet chargeability,[125] which influences the droplet size. Generally, the decrease in flow rate and increase in conductivity of the sprayed liquid lead to increased droplet charge and reduced drop size.[126] This could be significant particularly for reactions that are limited by mass transfer due to low interfacial areas.

In this work, various flow rates and conductivities of the aqueous dispersed phase were studied. It was observed that a decreased flow rate resulted in an improved reaction performance, as summarized in **Figure 4.3**. This observation correlated well with the studies by others showing that smaller droplet size was obtained at lower flow rate,[79] thus resulting in increased surface area and enhanced reaction conversion. The flow rate of dispersed phase through the charged nozzle may influence the droplet size in three possible aspects. First, the flow rate through the electrical charged nozzle controls the effective contact time of the elements in the dispersed phase with the source of electrostatic charge. The greater the flow rate the shorter the contact time. Since the acquisition of surface charge by the forming drops at the nozzle is time dependent,[127,128] higher flow rate will result in less charge acquisition, which in turn reduces the likelihood of drop breakup during the electrospray and results in larger drop size. Second, when the flow rate is smaller, the velocity of emission of the dispersed phase from the nozzle is smaller, resulting in a smaller inertial force applied on the droplet surface. As a consequence, the influence of electrostatic force on the droplet formation may be dominant, leading to higher disruption of the droplet surface. A third factor is that increase in velocity of the dispersed phase will reduce the residence time of the formed drops in the reactor which will negatively impact the conversion.

The influence of sodium formate concentration and, accordingly, aqueous solution conductivity were studied. Measurements made at each of the concentrations guaranteed an excess of the stoichiometric ratio of sodium formate to acetophenone. It is interesting to see that the overall conversion in the 2 h reaction time was virtually unaffected by the concentration or conductivity of the dispersed phase. The increase in sodium formate concentration apparently increased the driving force for mass transfer of formate to the interface and yet no difference in

reaction rate was observed, suggesting that the equilibrium concentration of formate in organic phase may be too small for the flux to change. On the other hand, the aqueous sodium formate solution with the studied concentrations may be too conductive so that increase in the conductivity makes no difference on the surface charge acquisition, thus resulting in similar droplet size and similar reaction rates.

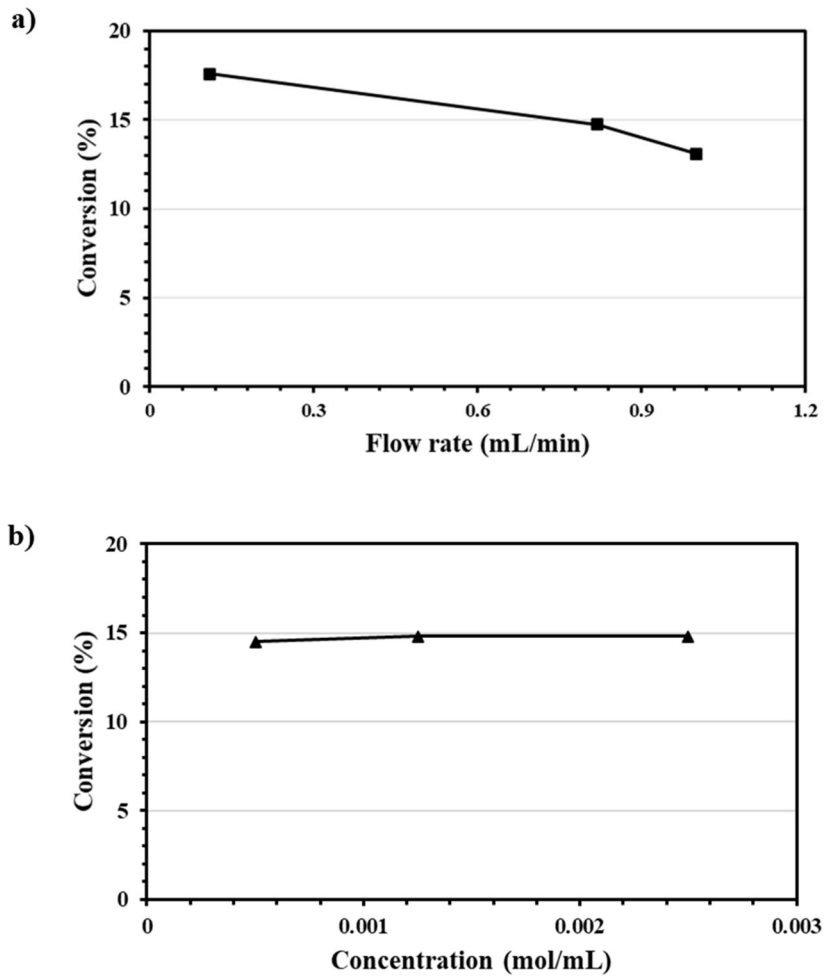

Figure 4.3 (a) Reaction conversion at various flow rates of the dispersed phase. Reactions were conducted with 3 kV applied with sodium formate solution of 0.0025 mol/mL and 30 mL of organic solvent consisting of 16.7% v/v 1-butanol in toluene. (b) reaction conversion with different concentration of sodium formate in the dispersed phase. Reactions were conducted with 3 kV applied with the flow rate of dispersed phase as 0.82 mL/min and 30 mL of organic solvent consisting of 16.7% v/v 1-butanol in toluene.

4.3.3 Composition of continuous phase

Composition of the continuous phase is important as different composition would result in different conductivities of the continuous phase and different partition with the dispersed phase, which would further influence the reaction performance. The effects of different composition and volume of the continuous phase on reaction performance were studied and summarized in **Table 4.1**. These experiments were performed with sodium formate concentration of 0.0025 mol/mL and the flow rate of dispersed phase at 0.82 mL/min.

It should be noted that the composition of the continuous phase varied by modifying the volumetric ratio of 1-butanol to toluene. As toluene is highly electrically resistant (8E-16 S/m)[129] while 1-butanol has a relatively high conductivity (6E-6 S/m),[120] the increase in the volumetric ratio of 1-butanol increased the conductivity of the continuous phase. When 1-butanol was solely present as the organic phase, a high electric field could not be maintained due to high current flow, therefore no electrospray could be generated. In contrast, when toluene was solely used as the organic phase, a stable electrospray was achieved while a poor reaction performance was observed due to the severe coalescence of droplets on the inner wall of the reactor. As a result, the experiments were conducted with a reasonable range of toluene/1-butanol ratios to tune the properties of the continuous phase.

As shown by comparison of Cases 1 and 2 in **Table 4.1**, when the volumetric ratio of 1-butanol increased, there was almost a 2-fold increase in both conversion and yield after a reaction time of 2 h. Meanwhile, the change in the composition resulted in a significant increase in current flow, which induced an elevated temperature by joule heating. Further increasing the volumetric ratio of 1-butanol to 50% resulted in a significant increase in the conductivity of the continuous phase which limited the maximum applied voltage to be less than 3 kV. Therefore,

the reaction with 50% v/v of 1-butanol in the organic phase was conducted with an applied voltage of 1.5 kV. While the applied voltage was much lower, an emulsion was also generated, and it was observed that a 20% increase in both conversion and yield was attained in a reduced reaction time (1 h of reaction) compared to Case 1 and Case 2. These results demonstrated the importance of the continuous phase composition in determining reaction performance. When the continuous phase is of higher conductivity, a lower voltage is required to generate electrostatic dispersion. Three parameters may contribute to the improved reaction performance: temperature, electric current, and partitioning between the continuous and the dispersed phase due to the solubility of 1-butanol in water.

To distinguish the effects of the three parameters, Cases 4 and 5 were designed to study the effects of temperature solely while Cases 6 to 8 were conducted to study the effects of partitioning between the two phases. It was shown that the increase in temperature resulted in the increase in conversion and yields (Cases 1, 4, and 5). However, only a slight increase was observed despite the significant increase in temperature, suggesting that the reaction was not in the intrinsic kinetics region and therefore temperature may not have a dominant influence on the reaction performance. Cases 6 to 8 were conducted in a batch reactor with vigorous stirring. As can be seen, the conversion and yields were almost identical in the stirred system and the sprayed system with a voltage of 3 kV applied (Cases 1 and 6), suggesting a similar level of mass transfer limitation in the two systems. Similar to that observed in Cases 4 and 5, conversion and yields increased by only a few percent when the volumetric ratio of 1-butanol increased from 16.7% to 50%, which suggests that the partitioning between the two phases is not the governing factor in determining the reaction performance. It is therefore proposed that the electric current may play a significant role in achieving high reaction rates in the electrospray system, possibly due to the

current promoted electrons transfer between the reactants. Further experimental design and studies are required to elucidate its role and effects.

On the other hand, comparison of Cases 1-3 with Cases 6-8 suggested that the electrospray system is superior to the batch system in achieving higher selectivity (yield/conversion) while slightly reducing enantioselectivity. It was also observed that increase in temperature led to a decrease in enantioselectivity (Cases 1, 4, and 5).

Further optimization of reaction conditions was conducted, and it was shown that when the organic volume was reduced to 20 mL (Case 9), 71% conversion was achieved in 1 h of reaction time with a relatively lower electric field applied. If compared to the quiescent batch system with external electric fields applied in Chapters II and III, the reaction time was significantly reduced from 24 h to 1 h while the reaction volume was increased by 13.3 times, showing a great improvement in reaction rate achieved by electrospray. When compared to the stirred batch system studied by Wu et al.,[97] comparable conversion (71% vs 76%) was achieved while the reaction volume was increased by 20 times.

Table 4.1 Reaction performance with different organic composition and reaction conditions.

Case	Condition	Organic volume (mL) and 1-butanol volumetric ratio (v/v%)	Current (mA)	T (°C)	Time (h)	Conversion (mole%)	Yield (%)	ee(%)
1	3 kV	30 mL (16.7)	0.03	23	2	14.8	9.8	89.4
2	3 kV	30 mL (33.3)	0.8	35[a]	2	27.5	22.0	90.3
3	1.5 kV	30 mL (50)	5.9	68[a]	1	35.2	28.6	88.3
4	3 kV	30 mL (16.7)	0.05	40[b]	2	17.6	14.6	87.6
5	3 kV	30 mL (16.7)	0.08	70[b]	2	19.7	15.5	84
6	1100 rpm	30 mL (16.7)	--	23	2	14.6	9.4	91
7	1100 rpm	30 mL (33.3)	--	23	2	17.1	11.8	91.5
8	1100 rpm	30 mL (50)	--	23	2	20.9	12.7	92.6
9	2 kV	20 mL (50)	5.4	75[a]	1	71.0	69.7	85.7

a: temperature increase caused by joule heating.

b: a heating tape was used to increase the temperature.

4.3.4 Catalyst activity

Catalyst activity under a high external electric field is an important parameter to evaluate. The effects of high voltage electric fields on the catalyst activity were studied using stirred batch reaction experimental data as a benchmark. As shown in **Table 4.2**, the conversion and yield increased gradually with the increase of reaction time when 3 kV of external electric field was applied. This is consistent with the trend in conversion and yield in the batch system, suggesting that the high voltage may not deactivate the catalyst. The constant enantioselectivity values observed provided further evidence of this.

Table 4.2 Reaction performance in an electrospray system and a batch system at different reaction times.

Case	Condition	Time (h)	Conversion (%)	Yield (%)	ee (%)
1	3 kV	1	12.1	6.2	89.0
2	3 kV	2	14.8	9.8	89.4
3	3 kV	3	19.1	12.3	89.6
4	3 kV	4	21.2	14.3	90.2
5	1100 rpm	1	14.0	6.6	90.0
6	1100 rpm	2	14.6	9.4	91.0
7	1100 rpm	3	19.3	10.9	90.7
8	1100 rpm	4	25.8	10.7	91.0
9	*	2+2	9.5	2.2	86.6

* The reaction was conducted as follows: no acetophenone used in the organic phase in the first 2 h, then the reaction was run for another 2 h with acetophenone added. The other reaction conditions were the same as Case 2. The catalyst was present for the whole 4 h.

However, when the experiment was conducted without acetophenone substrate in the first 2 hours followed by the addition of acetophenone for another 2 hours of reaction, as shown in Case 9, the production of 1-phenylethanol was significantly suppressed with a reduced enantioselectivity. This may suggest that when the substrate is absent, the catalyst could be deactivated by the high electric field, while when the substrate is present, it may bond with the catalyst in a way to prevent it from deactivation.

4.4 Conclusions

In this chapter, a flow reaction system for the phase transfer hydrogenation of acetophenone was successfully established by the application of an electrospray. It was found that the polarity of electric field is insignificant in influencing the reaction performance in the electrospray system. The electric current flow observed during the reaction was suggested as an important factor in

the improvement of the reaction performance, while further study is necessary for in-depth understanding of its role. The influence of the high voltage electric field on the catalyst activity is intriguing, which also requires further clarification. It was concluded that the application of an external electric field in an electrospray system may not only enhance interfacial areas but may also result in other effects, including current flow and catalyst deactivation, both of which would further influence the reaction performance. The mechanism explaining these effects are yet to be fully elucidated.

However, a quantitative correlation of droplet size and reaction performance along with characterization of the influence of conductivities of both phases and electric current on the droplet size were not studied, which should be elucidated in future work. The conductivity of both phases has a major influence on the magnitude of electrostatic charge retained on the produced droplets, hence on the electrical forces which they experience. The electrical forces which act on both the droplet formation and motion have a major effect on drop size and trajectory, thus influencing mass transfer. The current conclusions and future work will lead to novel applications of electrospray in organic synthesis.

In summary, the electrospray-based flow reaction system showed excellent performance for the biphasic transfer hydrogenation of acetophenone. In comparison to the studied batch systems,[97,99] the reaction volume is increased by up to 20 times, showing great potential for large scale applications. This work provides an alternative for continuous synthesis of organic compounds in two liquid phase systems and is believed to be important for understanding the roles of external electric fields in organic synthesis and phase transfer catalysis.

Chapter V: Conclusions and Perspectives of Future Work

5.1 Conclusions

In this thesis, the intensification of phase transfer hydrogenation of acetophenone in liquid biphasic systems by application of external electric fields was studied in both a batch reactor and a flow reactor. This work demonstrated the importance of external electric fields in promoting mass transfer and reaction performance for organic synthesis and catalysis reactions. The application of external electric fields to liquid biphasic systems provides a promising alternative approach for achieving sustainable chemistry and engineering.

The work described here revealed the different roles of the applied external electric fields in batch systems versus continuous systems. Specifically, the improvement in reaction performance in a batch system was attributed to the intensified mass transfer by the controllable migration of reactive species under the applied electrostatic forces. The idea of employing external electric fields to act as a phase transfer catalyst is proposed for the first time to the best of my knowledge. In an electrospray system, the enhanced reaction conversion and yields resulted not only from the increased interfacial area but may also from the induced current flow in the system. It was concluded that the role of external electric fields in an electrospray system may not only enhance interfacial areas but may also result in other effects, for example, current flow, and catalyst deactivation, which were not fully understood previously.

Overall, this work extended the scope of controllable synthesis of organic compounds in liquid biphasic systems, and it is believed to be important as an original contribution to the field of electric field chemistry for understanding the roles of external electric fields in influencing mass transfer and kinetics from both chemistry and engineering perspectives.

5.2 Further work

5.2.1 Droplet size and charge measurements in an electrospray system

Though the droplet size in an electrospray system has been extensively studied and some correlations have been established, it is still important and worthy of analysis as a complement to this work. For example, vigorous studied on the dependence of droplet size on the continuous phase conductivity should be conducted as it is poorly understood. The droplet size measurement should be co-analyzed with the charge acquisition on the droplet surface. It is important to understand the correlations between the surface charge and the droplet size in the studied electrospray system. Since the conductivity of both dispersed phase and continuous phase could influence the surface charge thus further influence drop size, relations among them should be developed to provide more insights into the enhanced reaction performance.

To study the surface charge on an individual charged droplet, an electrospray in a dripping mode will be employed with an electrometer to measure the coulombic charge on a single droplet, as shown in **Figure 5.1**.[130] The charge is measured when the droplet gets in contract with the conductive collecting plate connected with a electrometer. A dynamic laser scattering instrument is coupled to measure the droplet size and velocity. The charge and size of a single droplet generated in air will be measured first as a control experiment, as the conductivity of air is relatively small. Then the generation of the dripping mode electrospray will be conducted in the studied biphasic system with different organic phase compositions/conductivities or different aqueous phase concentrations/conductivities. The dependence of the droplet charge on the conductivity of both phases may be concluded by comparing the measured charge and size of an individual droplet generated in the biphasic systems with those in the control experiments. Proper calibrations with theoretical equations may also be required.

Additionally, the droplet size and velocity distribution in the reaction system can be measured by dynamic laser scattering, which could provide more insights to understand the observations of different reaction performance influenced by different operating conditions.

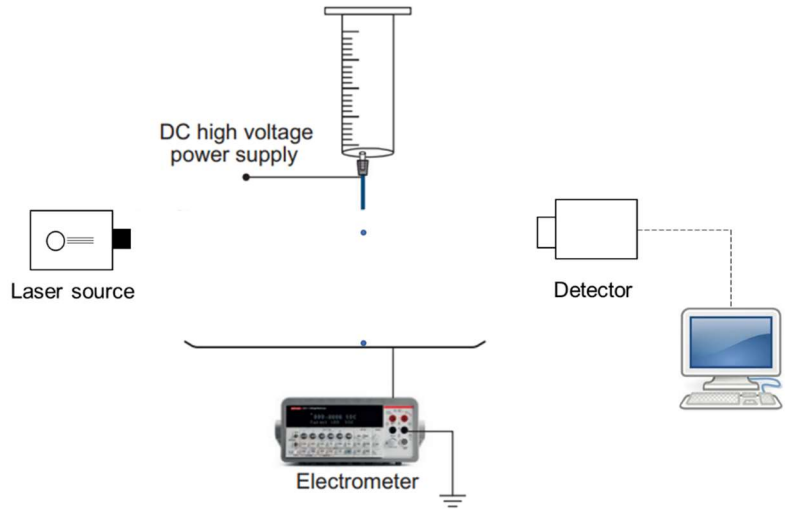

Figure 5.1 Experimental setup for droplet charge, size, and velocity measurement.

5.2.2 Evaluation of the importance of current flow

The effects of the induced current flow in the system were not elucidated, and further research is necessary to understand its role. Experiments may be designed to control the organic composition and temperature with current flow as the only variable in a jacked glass reactor. For example, for reactions involving an organic mixture of 30 mL with 16.7% v/v 1-butanol, a screening of different salts should be conducted to find a salt that can dissolve in this organic mixture while not participating in the reaction. Upon dissolution in the organic phase, a current could be induced by application of an external electric field. The generated heat could be simultaneously removed by the cooling water flowing through the jacket. By changing the

concentration of the salt in the organic phase, different magnitudes of current flow could be generated when a fixed electric field is applied.

The major challenge for these experiments is the solubility of the salt in toluene. Toluene is relatively nonpolar and most inorganic salts are not soluble in it. Therefore, a wide range of salts may be tested. Dicyclohexylammonium hydrochloride may be a potential candidate, which requires experimental validation. Alternatively, some hydrophobic ionic liquids may be possibly used as an addition into the organic phase to alter the ion concentration in the continuous phase thus changing the current flow.

5.2.3 Extension of reaction scopes

In this work, the reaction has only focused on the hydrogenation of acetophenone. In order to extend the application of external electric fields on promoting organic synthesis reactions, other ketones used as substrates should be studied. **Figure 5.2** summarized some of the commonly used ketone substrates for transfer hydrogenation reactions catalyzed by Ru catalysts.[98]

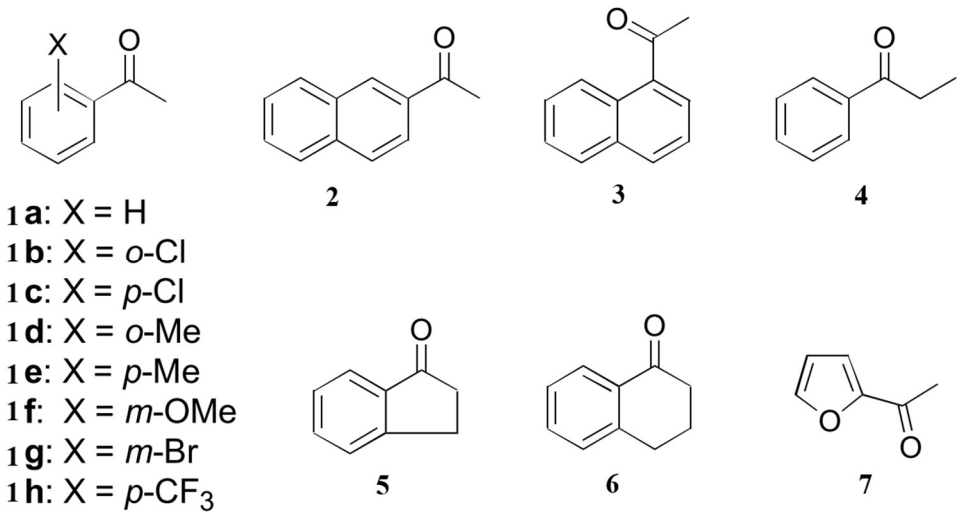

Figure 5.2 A list of ketone substrates.

On the other hand, this method could be extended to other phase transfer catalysis reactions. Reactions with particular interest are the oxidation reactions of alcohols with hydrogen peroxide as oxidant. Transformation of alcohols to value-added products by oxidation is important in chemical industry. Using hydrogen peroxide as oxidant offers a green approach by reducing waste generation compared to conventional metal or organic oxidants. In a typical hydrogen peroxide alcohol oxidation reaction, hydrogen peroxide and catalysts are dissolved in the aqueous phase while the alcohol substrate forms the organic phase. Tungsten-based salts, for example Na_2WO_4,[131] and polyoxometalates[56] are commonly used as catalysts. These catalyst species are negatively charged, which could be transferred to the aqueous-organic interface by an applied external electrostatic force. Therefore, the oxidation of alcohols by hydrogen peroxide can served as a model reaction system to study the wide applications of external electric fields on organic synthesis.

5.2.4 New reactor design

Loscertales et al. developed a technique, as shown in **Figure 5.3**, for micro or nano scale encapsulation via electrified coaxial liquid jets.[132] In that study, two liquids were flowed coaxially under the application of a high electric field, resulting in a small core-shell structure with one liquid coated by the other liquid. This methodology is potentially attracting for the intensification of liquid biphasic reactions.

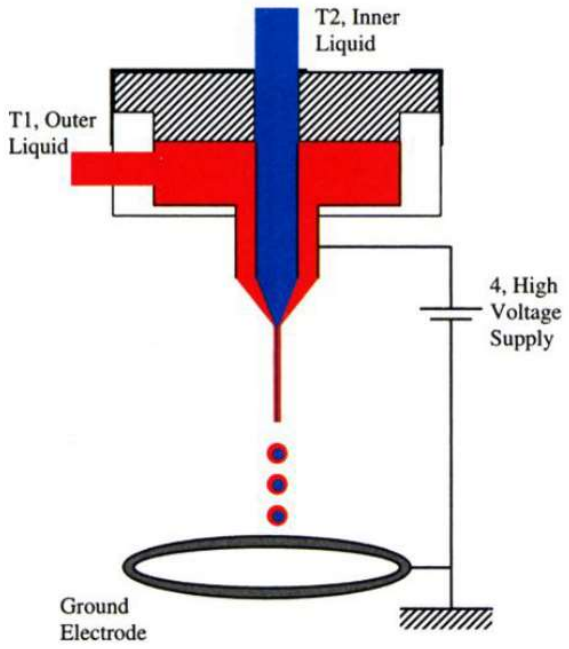

Figure 5.3 Experiment setup for the electrified coaxial liquid jet.

For example, if we apply this method to the transfer hydrogenation of acetophenone with aqueous sodium formate solution, fine droplets with acetophenone phase covered by aqueous phase could be generated by flowing the organic phase though the inner tube while the water phase flowing through the outer tube. Each of those generated small droplets could be considered as a fine reactor, which would significantly increase the mass transfer and reaction rates. It will also be interesting to explore the mass transfer phenomenon inside the small droplets by studying the core-shell interfacial disturbance and the inner circulation. To the best of my knowledge, the method has only been used for particle size control applications. Therefore, it is very promising to apply this technique to organic synthesis for process intensification.

Reference

1. Letan R. Liquid-liquid processes. In: Kreith F, Boehm RF (eds). *Direct-Contact Heat Transfer*. Springer, Berlin, Heidelberg; 1988; 83-118.

2. Hanson C. *Recent Advances in Liquid-Liquid Extraction*. 1st ed. Oxford, New York: Pergamon Press; 1971.

3. Cañadas R, González-Miquel M, González EJ, Díaz I, Rodríguez M. Overview of neoteric solvents as extractants in food industry: A focus on phenolic compounds separation from liquid streams. *Food Research International.* 2020; 136: 109558.

4. Hutchings MJ, Ahmed-Omer B, Wirth T. Liquid-liquid biphasic reactions. In: Wirth T (ed). *Microreactors in Organic Chemistry and Catalysis*. 2nd ed. Wiley-VCH; 2013; 197-219.

5. Reichardt C, Welton T. *Solvents and Solvent Effects in Organic Chemistry*. 4th ed. Hoboken: John Wiley & Sons; 2011.

6. Welton T. Solvents and sustainable chemistry. *Proceedings of the Royal Society A: Mathematical, Physical and Engineering Sciences.* 2015; 471(2183): 20150502.

7. Clarke CJ, Tu W-C, Levers O, Bröhl A, Hallett JP. Green and sustainable solvents in chemical processes. *Chemical Reviews.* 2018; 118(2): 747-800.

8. Keil FJ. Process intensification. *Reviews in Chemical Engineering.* 2018; 34(2): 135-200.

9. Guajardo N, Carlesi C, Schrebler R, Morales J. Applications of liquid/liquid biphasic oxidations by hydrogen peroxide with ionic liquids or deep eutectic solvents. *ChemPlusChem.* 2017; 82(2): 165-176.

10. Reddy PN, Padmaja P, Subba Reddy BV, Rambabu G. Ionic liquid/water mixture promoted organic transformations. *RSC Advances.* 2015; 5(63): 51035-51054.

11. Makosza M. Phase-transfer catalysis. A general green methodology in organic synthesis. *Pure and Applied Chemistry*. 2000; 72: 1399-1403.

12. Mąkosza M, Fedoryński M. Phase transfer catalysis. *Catalysis Reviews.* 2003; 45(3-4): 321-367.

13. Starks CM. Phase-transfer catalysis. I. Heterogeneous reactions involving anion transfer by quaternary ammonium and phosphonium salts. *Journal of the American Chemical Society.* 1971; 93(1): 195-199.

14. Makosza M. Two-phase reactions in the chemistry of carbanions and halocarbenes. A useful tool in organic synthesis. *Pure and Applied Chemistry.* 1975; 43(3-4): 439-462.

15. Freedman HH. Industrial applications of phase transfer catalysis (PTC): past, present and future. *Pure and Applied Chemistry.* 1986; 58: 857-868.

16. O'Donnell MJ, Bennett WD, Wu S. The stereoselective synthesis of .alpha.-amino acids by phase-transfer catalysis. *Journal of the American Chemical Society.* 1989; 111(6): 2353-2355.

17. Ooi T, Maruoka K. Recent advances in asymmetric phase-transfer catalysis. *Angewandte Chemie International Edition.* 2007; 46(23): 4222-4266.

18. Shirakawa S, Maruoka K. Recent Developments in asymmetric phase-transfer reactions. *Angewandte Chemie International Edition.* 2013; 52(16): 4312-4348.

19. Kaneko S, Kumatabara Y, Shirakawa S. A new generation of chiral phase-transfer catalysts. *Organic & Biomolecular Chemistry.* 2016; 14(24): 5367-5376.

20. Maruoka K. Practical aspects of recent asymmetric phase-transfer catalysis. *Organic Process Research & Development.* 2008; 12(4): 679-697.

21. Shi Q, Lee Y-J, Kim M-J, Park M-K, Lee K, Song H, Cheng M, Jeong B-S, Park H-G, Jew S-S. Highly efficient polymer supported phase-transfer catalysts containing hydrogen bond inducing functional groups. *Tetrahedron Letters.* 2008; 49(8): 1380-1383.

22. Chinchilla R, Mazón P, Nájera C. Asymmetric synthesis of α-amino acids using polymer-supported Cinchona alkaloid-derived ammonium salts as chiral phase-transfer catalysts. *Tetrahedron: Asymmetry.* 2000; 11(16): 3277-3281.

23. Ooi T, Uematsu Y, Kameda M, Maruoka K. Conformationally flexible, chiral quaternary ammonium bromides for asymmetric phase-transfer catalysis. *Angewandte Chemie International Edition.* 2002; 41(9): 1551-1554.

24. Murakami Y, Takeda Y, Minakata S. Diastereoselective aziridination of chiral electron-deficient olefins with N-chloro-N-sodiocarbamates catalyzed by chiral quaternary ammonium salts. *The Journal of Organic Chemistry.* 2011; 76(15): 6277-6285.

25. Patterson DE, Xie S, Jones LA, Osterhout MH, Henry CG, Roper TD. Synthesis of 4-fluoro-β-(4-fluorophenyl)-l-phenylalanine by an asymmetric phase-transfer catalyzed alkylation: synthesis on scale and catalyst stability. *Organic Process Research & Development.* 2007; 11(3): 624-627.

26. Khoo KS, Leong HY, Chew KW, Lim J-W, Ling TC, Show PL, Yen H-W. Liquid biphasic system: a recent bioseparation technology. *Processes.* 2020; 8(2): 149.

27. Iqbal M, Tao Y, Xie S, et al. Aqueous two-phase system (ATPS): an overview and advances in its applications. *Biological Procedures Online.* 2016;18(1):18.

28. Ruiz-Ruiz F, Benavides J, Aguilar O, Rito-Palomares M. Aqueous two-phase affinity partitioning systems: current applications and trends. *Journal of Chromatography A.* 2012; 1244: 1-13.

29. Santos JHPM, Capela EV, Boal-Palheiros I, Coutinho JAP, Freire MG, Ventura SPM. Aqueous biphasic systems in the separation of food colorants. *Biochemistry and Molecular Biology Education.* 2018; 46(4): 390-397.

30. Khoo KS, Tan KL, Lee SY, Show PL. Organic solvent-based liquid biphasic system. In: Show PL, Lee SY, Chew KW (eds). *Liquid Biphasic System*. Elsevier; 2021: 39-50.

31. Chia SR, Khoo ZS, Chew KW, Show PL. Ionic liquid-based liquid biphasic system. In: Show PL, Lee SY, Chew KW (eds). *Liquid Biphasic System*: Elsevier; 2021: 51-71.

32. Leong YK, Lee VSS, Show PL. Surfactant/detergent-based liquid biphasic system. In: Show PL, Lee SY, Chew KW (eds). *Liquid Biphasic System*: Elsevier; 2021: 73-84.

33. Ferreira AM, Cláudio AFM, Válega M, et al. Switchable (pH-driven) aqueous biphasic systems formed by ionic liquids as integrated production-separation platforms. *Green Chemistry.* 2017; 19(12): 2768-2773.

34. Ferreira AM, Passos H, Okafuji A, et al. An integrated process for enzymatic catalysis allowing product recovery and enzyme reuse by applying thermoreversible aqueous biphasic systems. *Green Chemistry.* 2018; 20(6): 1218-1223.

35. Balan V. Current challenges in commercially producing biofuels from lignocellulosic biomass. *ISRN Biotechnology.* 2014; 2014: 463074.

36. Alonso DM, Hakim SH, Zhou S, et al. Increasing the revenue from lignocellulosic biomass: maximizing feedstock utilization. *Science Advances.* 2017; 3(5): e1603301.

37. Chen Z, Bai X, Lusi A, Jacoby WA, Wan C. One-pot selective conversion of lignocellulosic biomass into furfural and co-products using aqueous choline chloride/methyl isobutyl ketone biphasic solvent system. *Bioresource Technology.* 2019; 289: 121708.

38. Zhang X, Bai Y, Cao X, Sun R. Pretreatment of Eucalyptus in biphasic system for furfural production and accelerated enzymatic hydrolysis. *Bioresource Technology.* 2017; 238:1-6.

39. Saha B, Abu-Omar MM. Advances in 5-hydroxymethylfurfural production from biomass in biphasic solvents. *Green Chemistry.* 2014; 16(1): 24-38.

40. Adamiak W, Jedraszko J, Nogala W, et al. A simple liquid-liquid biphasic system for hydrogen peroxide generation. *The Journal of Physical Chemistry C.* 2015; 119(34): 20011-20015.

41. von Keutz T, Cantillo D, Kappe CO. Enhanced mixing of biphasic liquid-liquid systems for the synthesis of gem-dihalocyclopropanes using packed bed reactors. *Journal of Flow Chemistry.* 2019; 9(1): 27-34.

42. Stankiewicz AI, Moulijn JA. Process intensification: transforming chemical engineering. *Chemical Engineering Progress.* 2000; 96(1): 22-34.

43. Van Gerven T, Stankiewicz A. Structure, Energy, synergy, time-the fundamentals of process intensification. *Industrial & Engineering Chemistry Research.* 2009; 48(5): 2465-2474.

44. Weatherley LR. *Intensification of Liquid–Liquid Processes*. Cambridge: Cambridge University Press; 2020.

45. Haswell SJ, Middleton RJ, O'Sullivan B, Skelton V, Watts P, Styring P. The application of micro reactors to synthetic chemistry. *Chemical Communications.* 2001; (5):391-398.

46. Šalić A, Tušek A, Zelić B. Application of microreactors in medicine and biomedicine. *Journal of Applied Biomedicine.* 2012; 10(3): 137-153.

47. Bojang AA, Wu H-S. Design, Fundamental Principles of Fabrication and Applications of Microreactors. *Processes.* 2020; 8(8): 891.

48. Fletcher P, Haswell S. Downsizing synthesis. *Chemistry in Britain.* 1999; 35(11): 38-41.

49. Wilhite BA. Unconventional microreactor designs for process intensification in the distributed reforming of hydrocarbons: a review of recent developments at Texas A&M University. *Current Opinion in Chemical Engineering.* 2017; 17: 100-107.

50. Sattari A, Hanafizadeh P, Hoorfar M. Multiphase flow in microfluidics: from droplets and bubbles to the encapsulated structures. *Advances in Colloid and Interface Science.* 2020; 282: 102208.

51. Joanicot M, Ajdari A. Droplet Control for Microfluidics. *Science.* 2005; 309(5736): 887-888.

52. Yan Z, Tian J, Wang K, Nigam KDP, Luo G. Microreaction processes for synthesis and utilization of epoxides: a review. *Chemical Engineering Science.* 2021; 229: 116071.

53. Deng N-N, Wang W, Ju X-J, Xie R, Weitz DA, Chu L-Y. Wetting-induced formation of controllable monodisperse multiple emulsions in microfluidics. *Lab on a Chip.* 2013; 13(20): 4047-4052.

54. Jaritsch D, Holbach A, Kockmann N. Counter-current extraction in microchannel flow: current status and perspectives. *Journal of Fluids Engineering.* 2014; 136(9): 091211.

55. Wang K, Li L, Xie P, Luo G. Liquid–liquid microflow reaction engineering. *Reaction Chemistry & Engineering.* 2017; 2(5): 611-627.

56. Peer M, Weeranoppanant N, Adamo A, Zhang Y, Jensen KF. Biphasic catalytic hydrogen peroxide oxidation of alcohols in flow: scale-up and extraction. *Organic Process Research & Development.* 2016; 20(9): 1677-1685.

57. Shang M, Noël T, Wang Q, Hessel V. Packed-bed microreactor for continuous-flow adipic acid synthesis from cyclohexene and hydrogen peroxide. *Chemical Engineering & Technology.* 2013; 36(6): 1001-1009.

58. Ji J, Zhao Y, Guo L, Liu B, Ji C, Yang P. Interfacial organic synthesis in a simple droplet-based microfluidic system. *Lab on a Chip.* 2012; 12(7): 1373-1377.

59. Jovanović J, Hengeveld W, Rebrov EV, Nijhuis TA, Hessel V, Schouten JC. Redispersion microreactor system for phase transfer-catalyzed esterification. *Chemical Engineering & Technology.* 2011; 34(10): 1691-1699.

60. Karan D, Khan SA. Mesoscale triphasic flow reactors for metal catalyzed gas-liquid reactions. *Reaction Chemistry & Engineering.* 2019; 4(7): 1331-1340.

61. Weeranoppanant N. Enabling tools for continuous-flow biphasic liquid-liquid reaction. *Reaction Chemistry & Engineering.* 2019; 4(2): 235-243.

62. Nieves-Remacha MJ, Kulkarni AA, Jensen KF. Hydrodynamics of liquid-liquid dispersion in an advanced-flow reactor. *Industrial & Engineering Chemistry Research.* 2012; 51(50): 16251-16262.

63. Zhang Y, Born SC, Jensen KF. Scale-up investigation of the continuous phase-transfer-catalyzed hypochlorite oxidation of alcohols and aldehydes. *Organic Process Research & Development.* 2014; 18(11): 1476-1481.

64. Mandrelli F, Buco A, Piccioni L, et al. The scale-up of continuous biphasic liquid/liquid reactions under super-heating conditions: methodology and reactor design. *Green Chemistry.* 2017; 19(6): 1425-1430.

65. Mo Y, Lin H, Jensen KF. High-performance miniature CSTR for biphasic C-C bond-forming reactions. *Chemical Engineering Journal.* 2018; 335: 936-944.

66. Weatherley LR. Electrically Driven Intensification of Liquid-Liquid Processes. In: Weatherley LR (ed). *Intensification of Liquid-Liquid Processes*. Cambridge: Cambridge University Press; 2020: 211-268.

67. Shin W-T, Yiacoumi S, Tsouris C. Electric-field effects on interfaces: electrospray and electrocoalescence. *Current Opinion in Colloid & Interface Science.* 2004; 9(3): 249-255.

68. Tsouris C, Neal SH, Shah VM, Spurrier MA, Lee MK. Comparision of liquid-liquid dispersions formed by a stirred tank and electrostatic spraying*. *Chemical Engineering Communications.* 1997; 160(1): 175-197.

69. Cross J. *Electrostatics: principles, problems and applications*. Bristol: Bristol: Hilger; 1987.

70. Tsouris C, DePaoli DW, Feng JQ, Scott TC. Experimental investigation of electrostatic dispersion of nonconductive fluids into conductive fluids. *Industrial & Engineering Chemistry Research.* 1995; 34(4): 1394-1403.

71. Petera J, Weatherley LR, Hume AP, Gawrysiak T. A finite element algorithm for particle/droplet trajectory tracking, tested in a liquid-liquid system in the presence of an external electric field. *Computers & Chemical Engineering.* 2007; 31(11): 1369-1388.

72. Scheele GF, Meister BJ. Drop formation at low velocities in liquid-liquid systems: Part I. prediction of drop volume. *AIChE Journal.* 1968; 14(1): 9-15.

73. Takamatsu T, Yamaguchi M, Katayama T. Formation of single charged drops in liquid media under a uniform electric field. *Journal of Chemical Engineering of Japan.* 1982; 15(5): 349-355.

74. Kamiński K, Krawczyk M, Augustyniak J, Weatherley LR, Petera J. Electrically induced liquid-liquid extraction from organic mixtures with the use of ionic liquids. *Chemical Engineering Journal.* 2014; 235: 109-123.

75. Hume AP, Weatherley LR, Petera J. Trajectories of charged drops in a liquid-liquid system. *Chemical Engineering Journal.* 2003; 95(1): 171-177.

76. Petera J, Strzelecki W, Agrawal D, Weatherley LR. Charged droplet and particle-mixing studies in liquid-liquid systems in the presence of non-linear electrical fields. *Chemical Engineering Science.* 2005; 60(1): 135-149.

77. Kim H, Luo D, Link D, Weitz DA, Marquez M, Cheng Z. Controlled production of emulsion drops using an electric field in a flow-focusing microfluidic device. *Applied Physics Letters.* 2007; 91(13): 133106.

78. Sato M, Saito M, Hatori T. Emulsification and size control of insulating and/or viscous liquids in liquid-liquid systems by electrostatic dispersion. *Journal of Colloid and Interface Science.* 1993; 156(2): 504-507.

79. Young CJ, Poole-Warren LA, Martens PJ. Combining submerged electrospray and UV photopolymerization for production of synthetic hydrogel microspheres for cell encapsulation. *Biotechnology and Bioengineering.* 2012; 109(6): 1561-1570.

80. Kaufman EN, Harkins JB, Rodriguez M, Tsouris C, Selvaraj PT, Murphy SE. Development of an electro-spray bioreactor for crude oil processing. *Fuel Processing Technology.* 1997; 52(1): 127-144.

81. Weatherley LR, Rooney D. Enzymatic catalysis and electrostatic process intensification for processing of natural oils. *Chemical Engineering Journal.* 2008; 135(1): 25-32..

82. Ido Y, Kobara H, Tominaga K-i, Wakisaka A. A reactor system using electrospray in the liquid phase and its application in selective cyclosiloxane synthesis. *Industrial & Engineering Chemistry Research.* 2017; 56(16): 4878-4882.

83. Shaik S, Mandal D, Ramanan R. Oriented electric fields as future smart reagents in chemistry. *Nature Chemistry.* 2016; 8: 1091-1098.

84. Shaik S, Ramanan R, Danovich D, Mandal D. Structure and reactivity/selectivity control by oriented-external electric fields. *Chemical Society Reviews.* 2018; 47(14): 5125-5145.

85. Che F, Gray JT, Ha S, Kruse N, Scott SL, McEwen J-S. Elucidating the roles of electric fields in catalysis: a perspective. *ACS Catalysis.* 2018; 8(6): 5153-5174.

86. Meir R, Chen H, Lai W, Shaik S. Oriented electric fields accelerate Diels-Alder reactions and control the endo/exo selectivity. *ChemPhysChem.* 2010; 11(1): 301-310.

87. Wang Z, Danovich D, Ramanan R, Shaik S. Oriented-external electric fields create absolute enantioselectivity in Diels-Alder reactions: importance of the molecular dipole moment. *Journal of the American Chemical Society.* 2018; 140(41): 13350-13359.

88. Aragonès AC, Haworth NL, Darwish N, et al. Electrostatic catalysis of a Diels-Alder reaction. *Nature.* 2016; 531: 88-91.

89. Huang X, Tang C, Li J, et al. Electric field-induced selective catalysis of single-molecule reaction. *Science Advances.* 2019; 5(6): eaaw3072.

90. Fujii A, Hashiguchi S, Uematsu N, Ikariya T, Noyori R. Ruthenium(II)-catalyzed asymmetric transfer hydrogenation of ketones using a formic acid-triethylamine mixture. *Journal of the American Chemical Society.* 1996; 118(10): 2521-2522.

91. Haack K-J, Hashiguchi S, Fujii A, Ikariya T, Noyori R. The catalyst precursor, catalyst, and intermediate in the RuII-promoted asymmetric hydrogen transfer between alcohols and ketones. *Angewandte Chemie International Edition in English.* 1997; 36(3): 285-288.

92. Noyori R, Hashiguchi S. Asymmetric transfer hydrogenation catalyzed by chiral ruthenium complexes. *Accounts of Chemical Research.* 1997; 30(2): 97-102.

93. Noyori R, Yamakawa M, Hashiguchi S. Metal-ligand bifunctional catalysis: a nonclassical mechanism for asymmetric hydrogen transfer between alcohols and carbonyl compounds. *The Journal of Organic Chemistry.* 2001; 66(24): 7931-7944.

94. Ohkuma T, Utsumi N, Tsutsumi K, Murata K, Sandoval C, Noyori R. The hydrogenation/transfer hydrogenation network: asymmetric hydrogenation of ketones with chiral η6-arene/N-tosylethylenediamine-ruthenium(II) catalysts. *Journal of the American Chemical Society.* 2006; 128(27): 8724-8725.

95. Sandoval CA, Ohkuma T, Muñiz K, Noyori R. Mechanism of asymmetric hydrogenation of ketones catalyzed by BINAP/1,2-diamine−ruthenium(II) complexes. *Journal of the American Chemical Society.* 2003; 125(44): 13490-13503.

96. Ikariya T, Murata K, Noyori R. Bifunctional transition metal-based molecular catalysts for asymmetric syntheses. *Organic & Biomolecular Chemistry.* 2006; 4(3): 393-406.

97. Wu X, Li X, Hems W, King F, Xiao J. Accelerated asymmetric transfer hydrogenation of aromatic ketones in water. *Organic & Biomolecular Chemistry.* 2004; 2(13): 1818-1821.

98. Li X, Chen W, Hems W, King F, Xiao J. Asymmetric transfer hydrogenation of ketones with a polymer-supported chiral diamine. *Tetrahedron Letters.* 2004; 45(5): 951-953.

99. Li X, Wu X, Chen W, Hancock FE, King F, Xiao J. Asymmetric transfer hydrogenation in water with a supported Noyori−Ikariya catalyst. *Organic Letters.* 2004; 6(19): 3321-3324.

100. Wu X, Xiao J. Aqueous-phase asymmetric transfer hydrogenation of ketones - a greener approach to chiral alcohols. *Chemical Communications.* 2007; (24): 2449-2466.

101. Wu X, Liu J, Di Tommaso D, et al. A multilateral mechanistic study into asymmetric transfer hydrogenation in water. *Chemistry - A European Journal.* 2008; 14(25): 7699-7715.

102. Wang L, Ma H, Song L, Li L, Wang Y, Wang H. Transfer hydrogenation of acetophenone in an organic-aqueous biphasic system containing double long-chain surfactants. *RSC Advances.* 2014; 4(4): 1567-1569.

103. Pavlova A, Rösler E, Meijer EJ. Mechanistic aspects of using formate as a hydrogen donor in aqueous transfer hydrogenation. *ACS Catalysis.* 2016; 6(8): 5350-5358.

104. Ramanan R, Danovich D, Mandal D, Shaik S. Catalysis of methyl transfer reactions by oriented external electric fields: are gold-thiolate linkers innocent? *Journal of the American Chemical Society.* 2018; 140(12): 4354-4362.

105. Pavlova A, Meijer EJ. Understanding the role of water in aqueous ruthenium-catalyzed transfer hydrogenation of ketones. *ChemPhysChem.* 2012; 13(15): 3492-3496.

106. Shaik S, de Visser SP, Kumar D. External electric field will control the selectivity of enzymatic-like bond activations. *Journal of the American Chemical Society.* 2004; 126(37): 11746-11749.

107. Hirao H, Chen H, Carvajal MA, Wang Y, Shaik S. Effect of external electric fields on the C-H bond activation reactivity of nonheme iron-oxo reagents. *Journal of the American Chemical Society.* 2008; 130(11): 3319-3327.

108. Cassone G, Pietrucci F, Saija F, Guyot F, Saitta AM. One-step electric-field driven methane and formaldehyde synthesis from liquid methanol. *Chemical Science.* 2017; 8(3): 2329-2336.

109. Cassone G, Sponer J, Sponer JE, Pietrucci F, Saitta AM, Saija F. Synthesis of (d)-erythrose from glycolaldehyde aqueous solutions under electric field. *Chemical Communications.* 2018; 54(26): 3211-3214.

110. Cassone G, Sofia A, Rinaldi G, Sponer J. Catalyst-free hydrogen synthesis from liquid ethanol: an ab initio molecular dynamics study. *The Journal of Physical Chemistry C.* 2019; 123(14): 9202-9208.

111. Xu B, Tao NJ. Measurement of single-molecule resistance by repeated formation of molecular junctions. *Science.* 2003; 301: 1221-1223.

112. Venkataraman L, Klare JE, Nuckolls C, Hybertsen MS, Steigerwald ML. Dependence of single-molecule junction conductance on molecular conformation. *Nature.* 2006; 442(7105): 904-907.

113. Frisenda R, Janssen VAEC, Grozema FC, van der Zant HSJ, Renaud N. Mechanically controlled quantum interference in individual π-stacked dimers. *Nature Chemistry.* 2016; 8(12): 1099-1104.

114. Schwarz F, Kastlunger G, Lissel F, et al. Field-induced conductance switching by charge-state alternation in organometallic single-molecule junctions. *Nature Nanotechnology.* 2016/02/01 2016;11(2):170-176.

115. Bier M, Palusinski OA, Mosher RA, Saville DA. Electrophoresis: mathematical modeling and computer simulation. *Science.* 1983; 219(4590): 1281-1287.

116. Levine ML, Cabezas H, Bier M. Transport of solutes across aqueous phase interfaces by electrophoresis. Mathematical modeling. *Journal of Chromatography.* 1992; 607(1): 113-118.

117. Zhu HT, Yang B, Gao CJ, Wu YQ. Ion transfer modeling based on Nernst-Planck theory for saline water desalination during electrodialysis process. *Asia-Pacific Journal of Chemical Engineering.* 2020; 15: e2410.

118. Petera J, Weatherley LR, Rooney D, Kaminski K. A finite element model of enzymatically catalyzed hydrolysis in an electrostatic spray reactor. *Computers & Chemical Engineering.* 2009; 33(1): 144-161.

119. Rumble JR. *CRC handbook of chemistry and physics*. 100th ed. Boca Raton: CRC Press; 2019.

120. Gañán-Calvo AM, López-Herrera JM, Rebollo-Muñoz N, Montanero JM. The onset of electrospray: the universal scaling laws of the first ejection. *Scientific Reports.* 2016; 6(1): 32357.

121. Prego M, Cabeza O, Carballo E, Franjo CF, Jime´nez E. Measurement and interpretation of the electrical conductivity of 1-alcohols from 273 K to 333 K. *Journal of Molecular Liquids.* 2000; 89(1): 233-238.

122. Prego M, Rilo E, Carballo E, Franjo C, Jiménez E, Cabeza O. Electrical conductivity data of alkanols from 273 to 333 K. *Journal of Molecular Liquids.* 2003; 102(1): 83-91.

123. Cloupeau M, Prunet-Foch B. Electrohydrodynamic spraying functioning modes: a critical review. *Journal of Aerosol Science.* 1994; 25(6): 1021-1036.

124. Cloupeau M, Prunet-Foch B. Electrostatic spraying of liquids: main functioning modes. *Journal of Electrostatics.* 1990; 25(2): 165-184.

125. Maski D, Durairaj D. Effects of electrode voltage, liquid flow rate, and liquid properties on spray chargeability of an air-assisted electrostatic-induction spray-charging system. *Journal of Electrostatics.* 2010; 68(2): 152-158.

126. Post SL, Roten RL. A review of the effects of droplet size and flow rate on the chargeability of spray droplets in electrostatic agricultural sprays. *Transactions of the ASABE.* 2018; 61(4): 1243-1248.

127. Stewart G, Thornton JD. Charge and velocity characteristics of electrically charged droplets. Part I. theoretical considerations. *Institution of Chemical Engineers Symposium Series.* 1967, 26, 29-36.

128. Stewart G, Thornton JD . Charge and velocity characteristics of electrically charged droplets. Part II. preliminary measurements of droplet charge and velocity. *Institution of Chemical Engineers Symposium Series.* 1967; 26: 37-41.

129. Smallwood IM. Toulene. In: Smallwood IM (ed). *Handbook of Organic Solvent Properties*. Oxford: Butterworth-Heinemann; 1996: 39-41.

130. Kim H-H, Kim J-H, Ogata A. Time-resolved high-speed camera observation of electrospray. *Journal of Aerosol Science.* 2011; 42(4): 249-263.

131. Noyori R, Aoki M, Sato K. Green oxidation with aqueous hydrogen peroxide. *Chemical Communications.* 2003; (16): 1977-1986.

132. Loscertales IG, Barrero A, Guerrero I, Cortijo R, Marquez M, Gañán-Calvo AM. Micro/nano encapsulation via electrified coaxial liquid jets. *Science.* 2002; 295(5560): 1695-1698.

Appendix I: Retention times for different compounds in a nonchiral GC column.

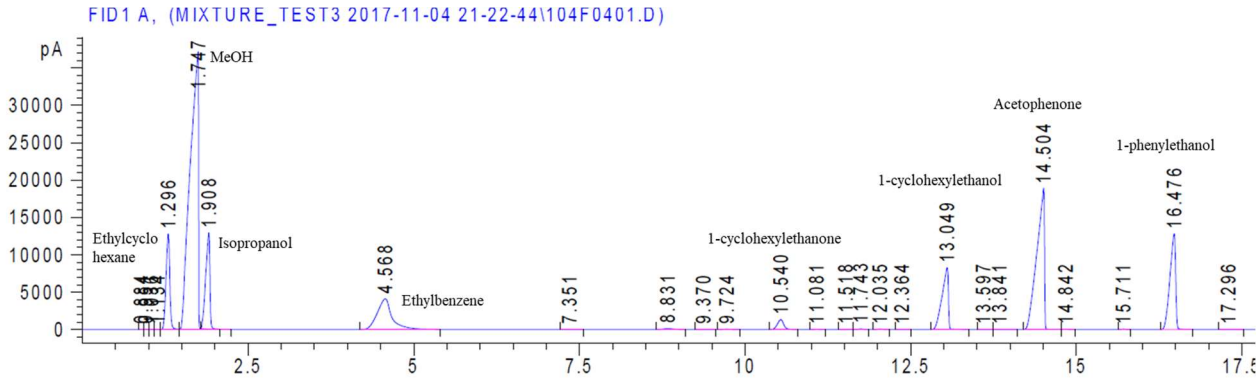

Appendix II: GC spectrum of a 24 h reaction sample from a batch reactor with 1-butanol as organic solvent.

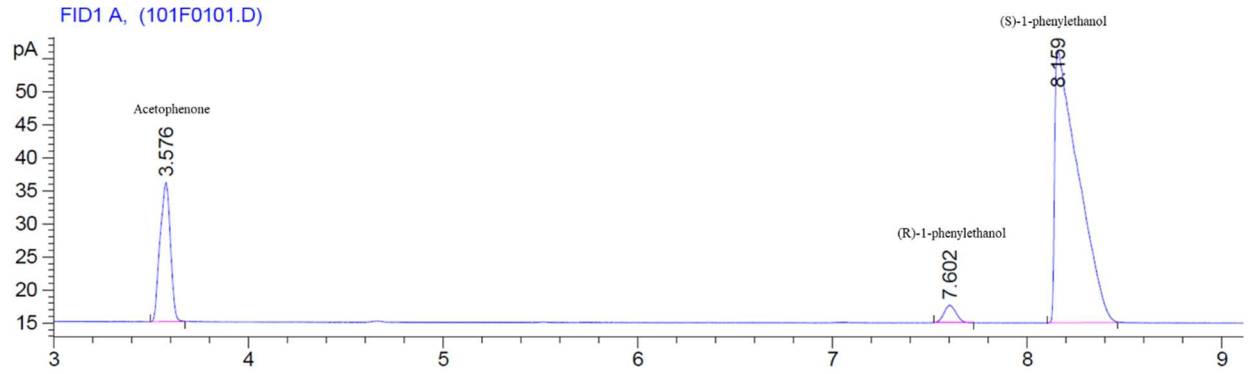

Appendix III: GC spectrum of a 1 h reaction sample from the electrospray system with 20 mL of organic phase (10 mL toluene and 10 mL 1-butanol) and 2 kV of voltage applied.

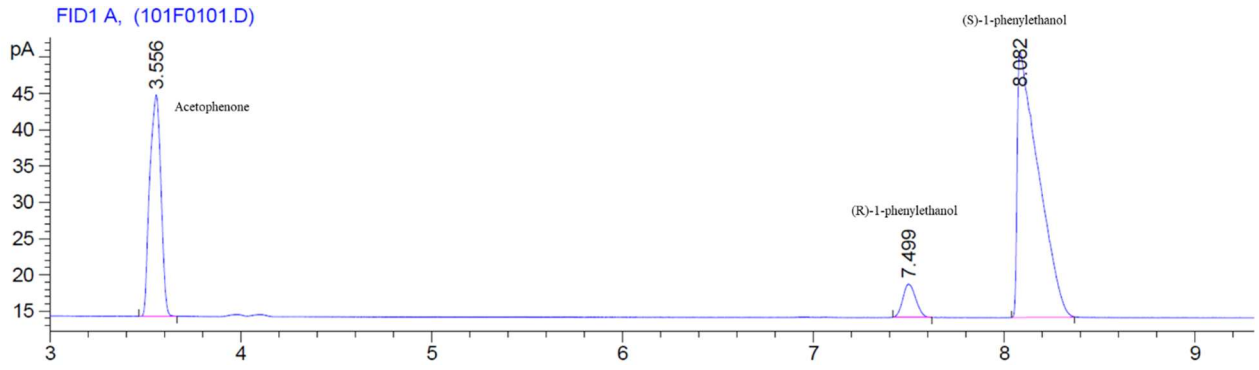

Appendix IV: XFR analysis data of the black slurry from stainless steel electrode decomposition.

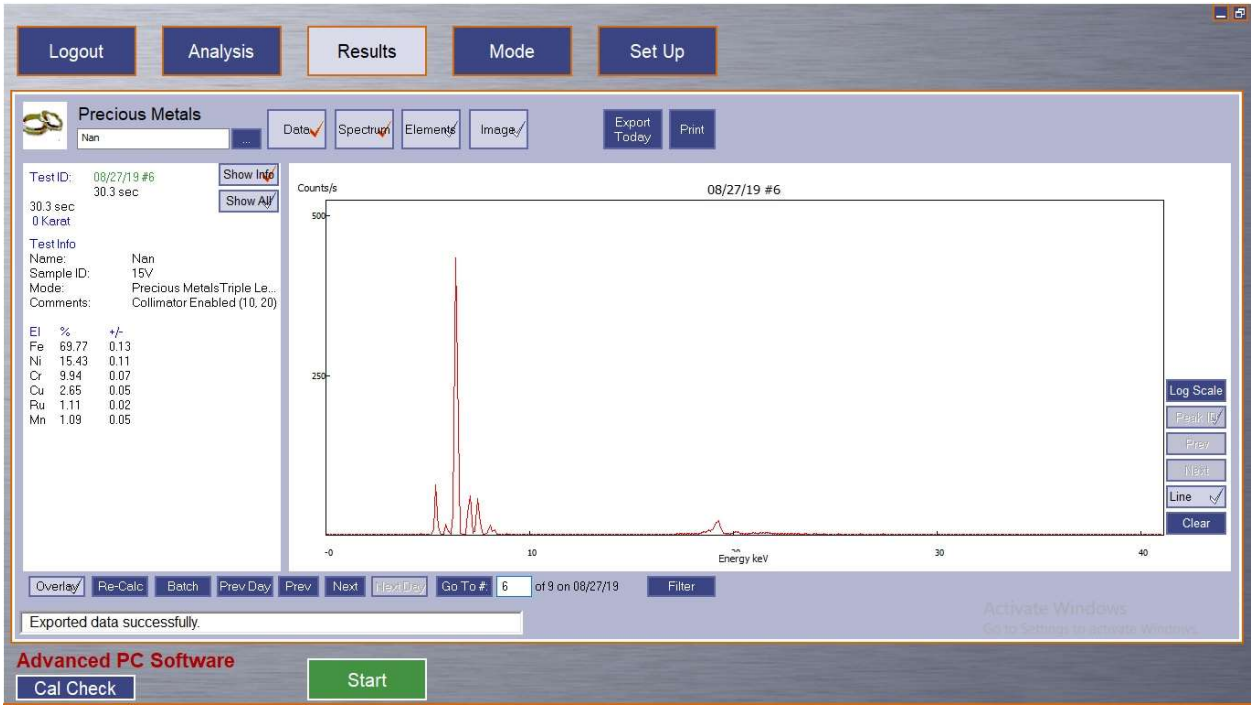

Appendix V: Reactor used for the batch reactions in Chapter II and III.

Appendix VI: Reactor used for the continuous reaction in Chapter IV.

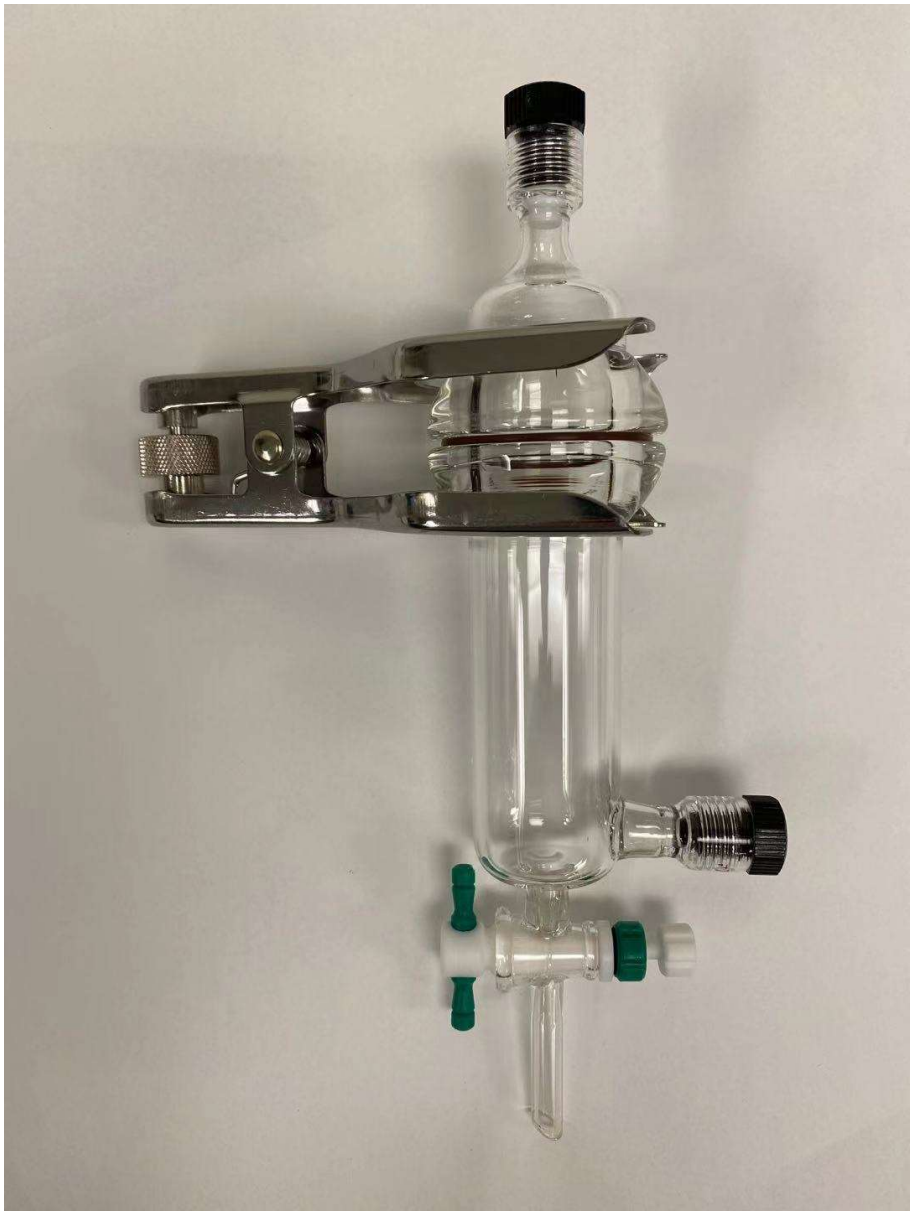

Appendix VII: Simulation of the concentrations of reactive species at the liquid interface under 15 V in COMSOL Multiphysics 5.4

(1) Component and Physics

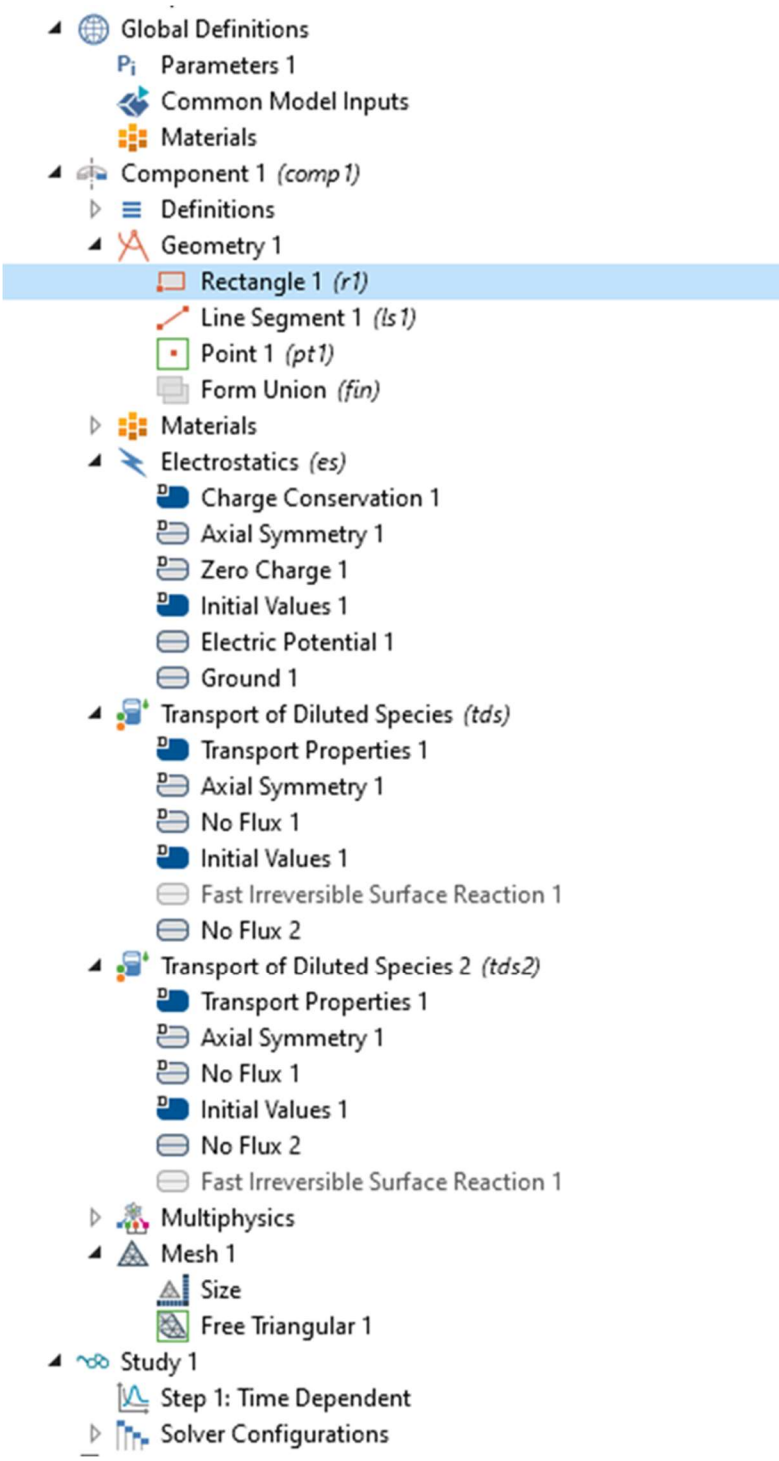

(2) Geometry

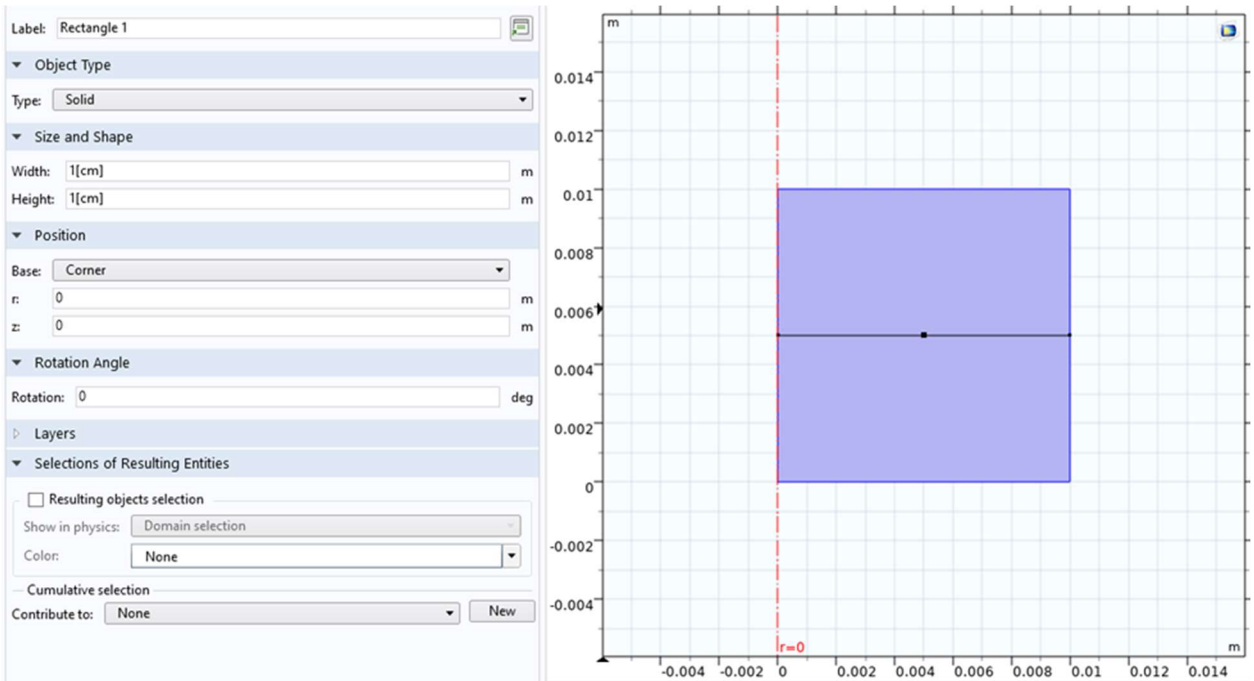

(3) Parameters in Global Definitions

Parameters

Name	Expression	Value	Description
F	96485.3[C/mol]	96485 C/mol	
V	1.5[cm^3]	1.5E-6 m^3	
A	3.24[cm^2]	3.24E-4 m^2	
k	1.10[cm^3/mol/s]	1.1E-6 m^3/(s·...	

(4) Water in Materials

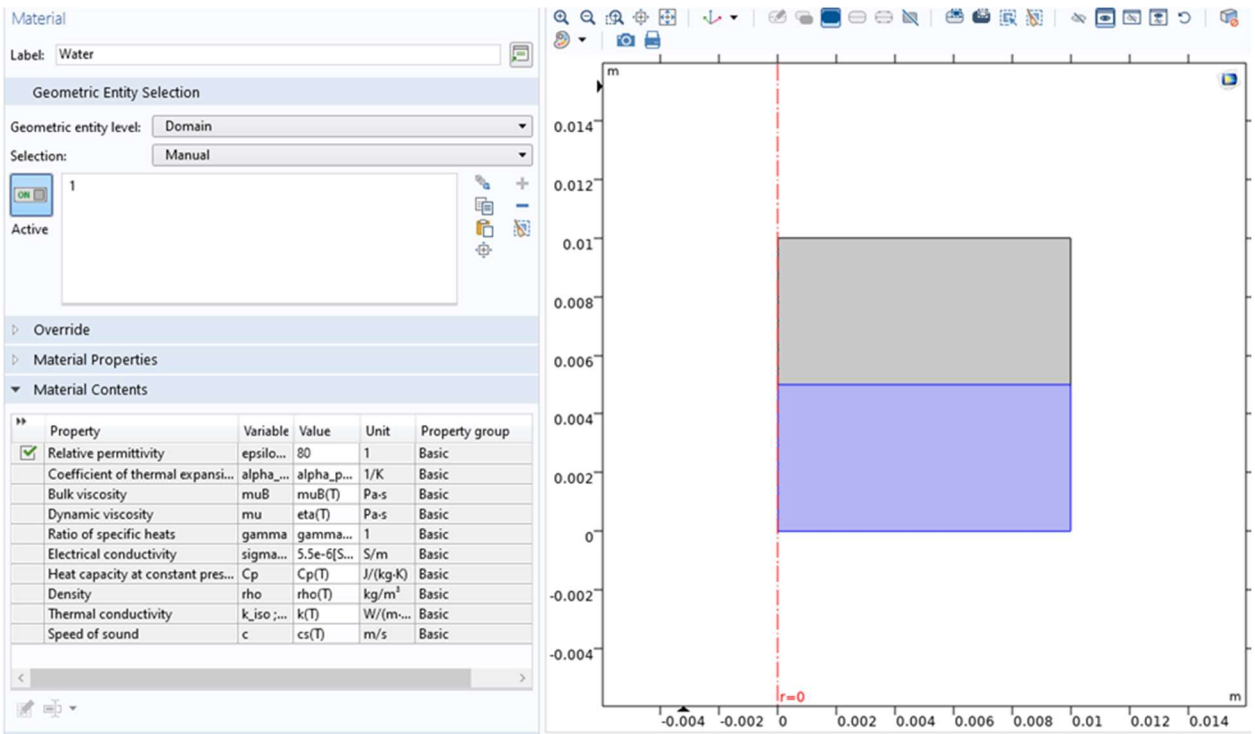

(5) 1-butanol in Materials

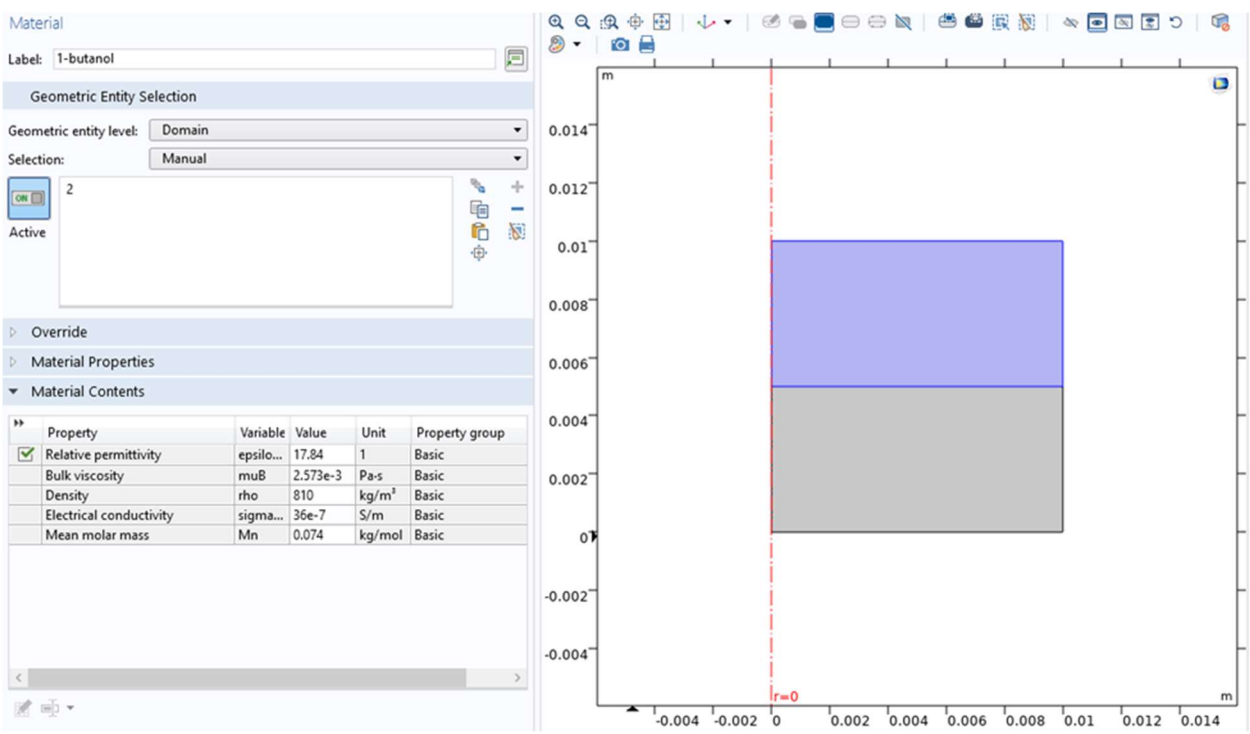

(6) Electrostatics Physics

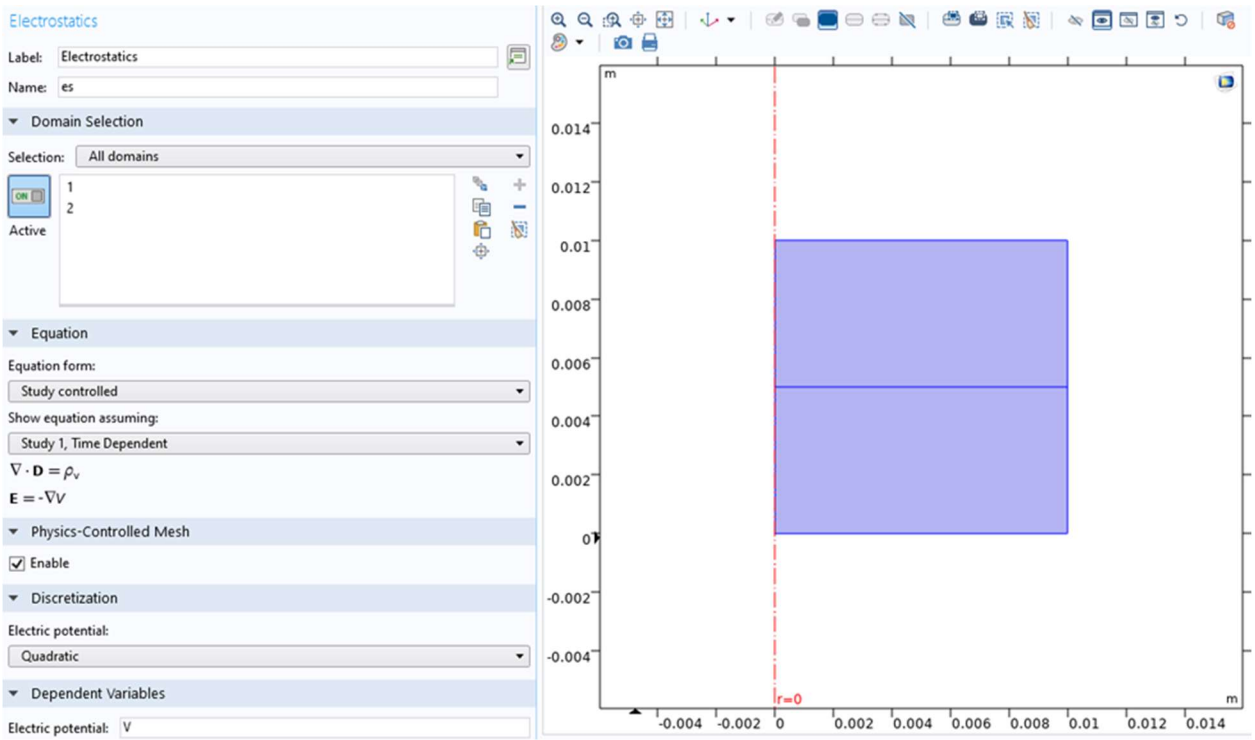

(7) Boundary condition 1 in electrostatics physics

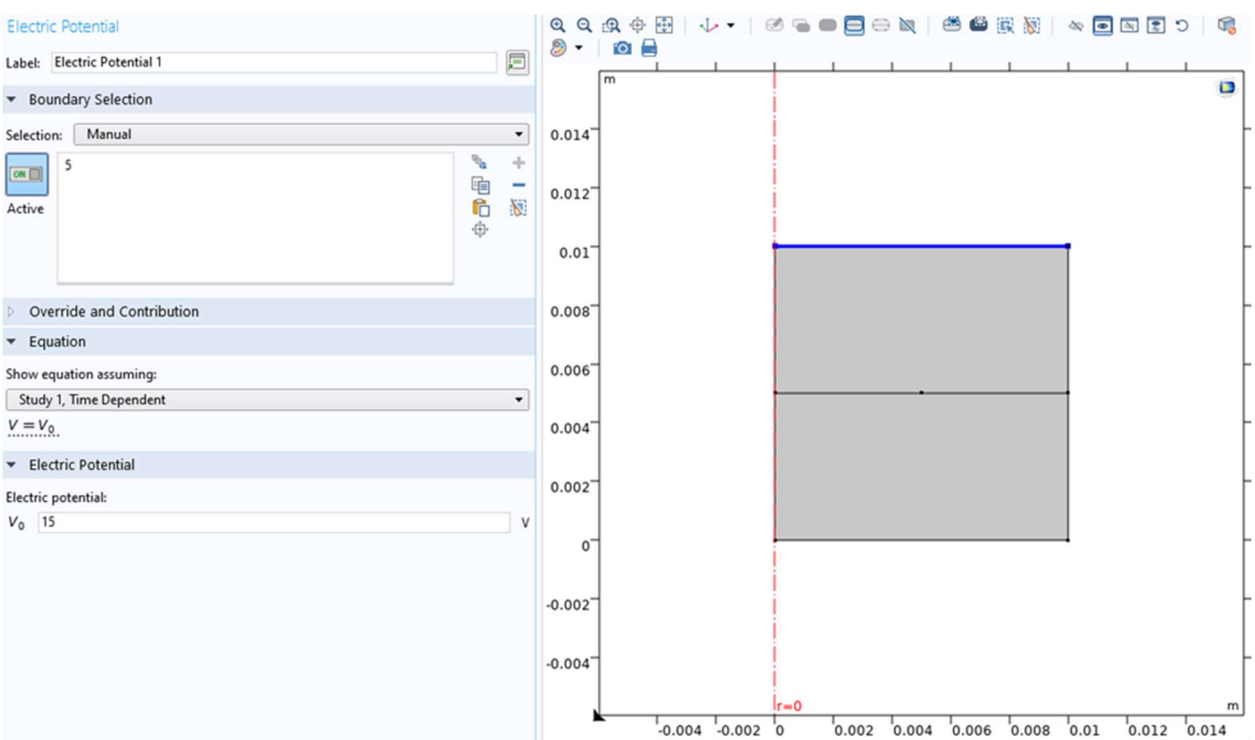

(8) Boundary condition 2 in electrostatics physics

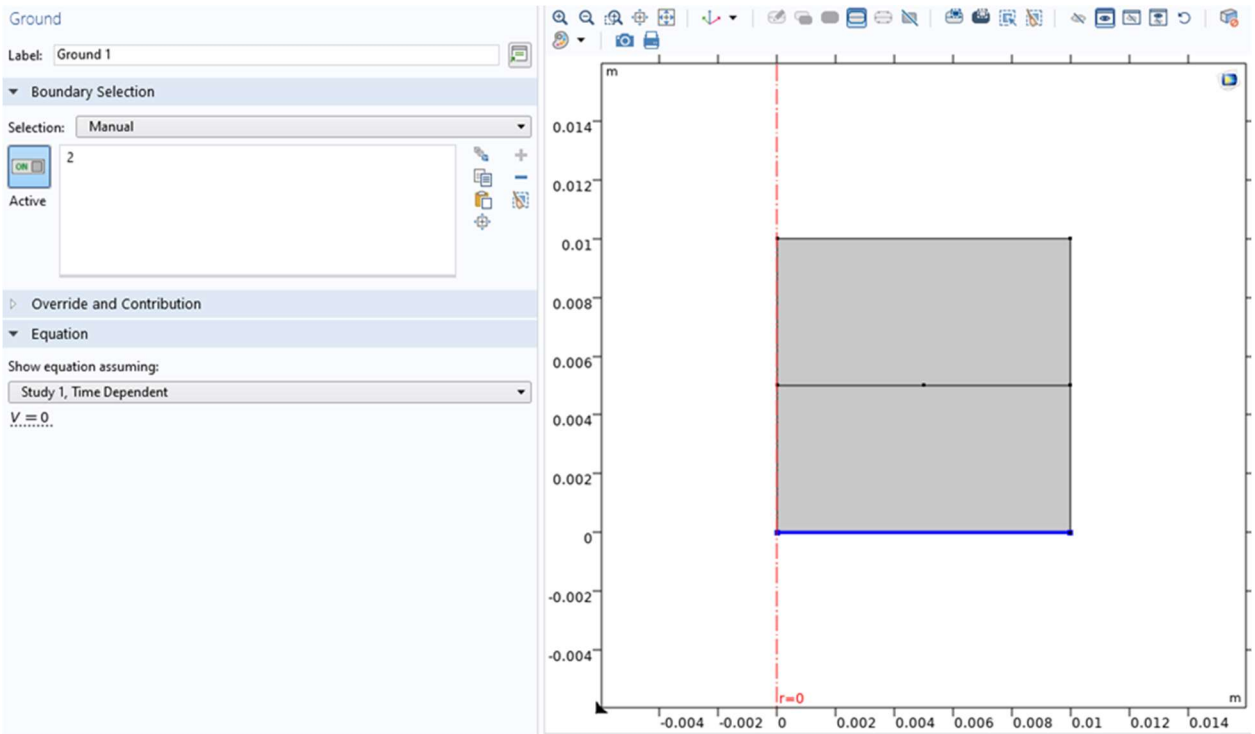

(9) Transport of Diluted Species in organic phase

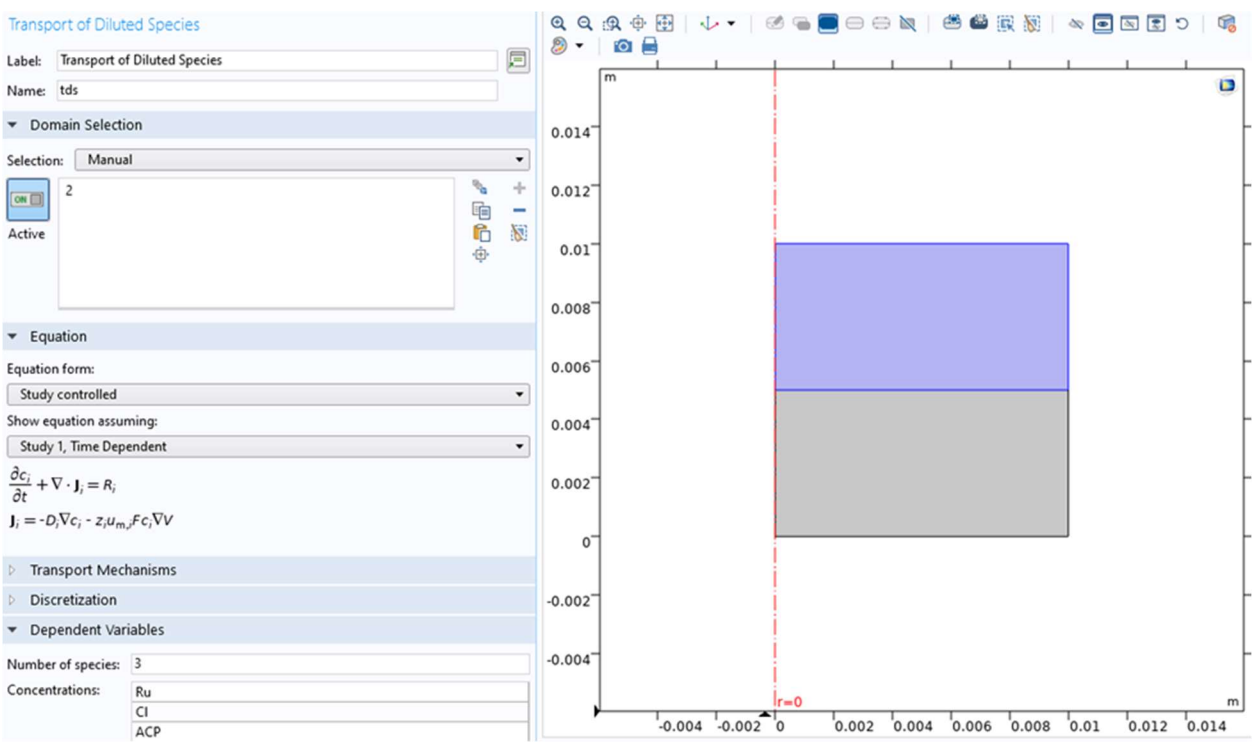

(10) Transport of Diluted Species in aqueous phase

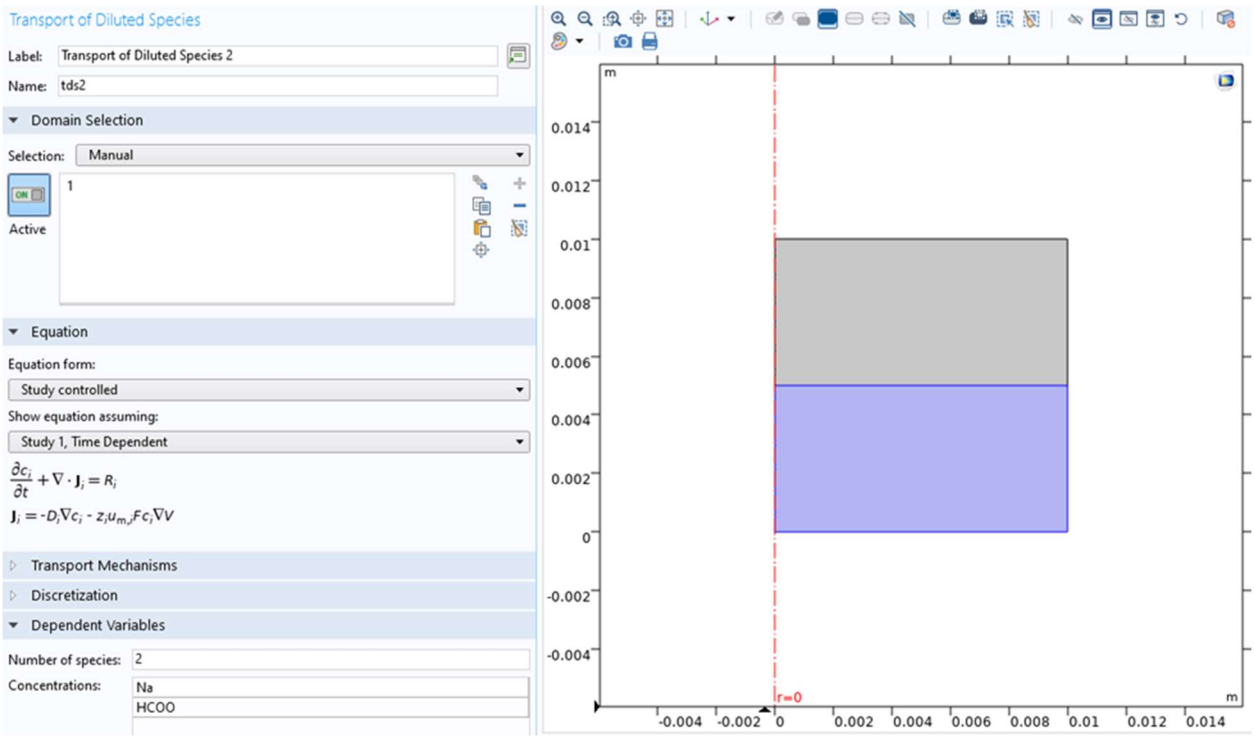

(11) Mesh Size

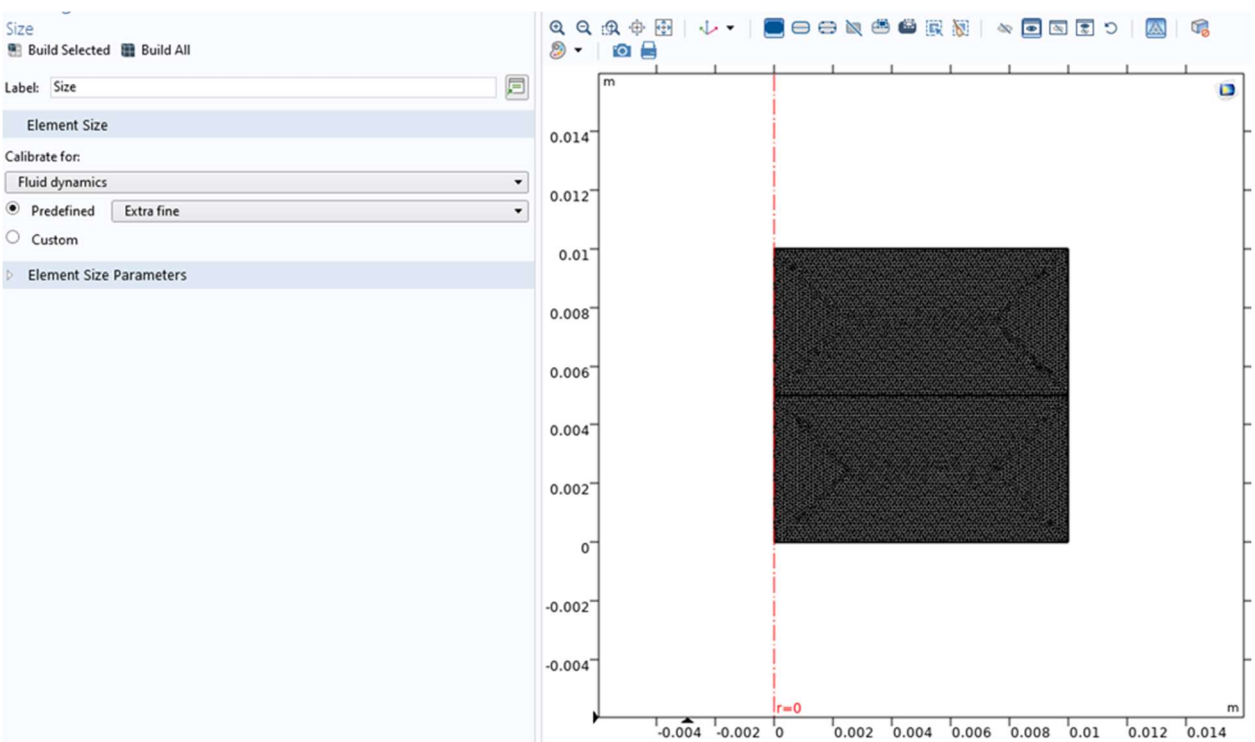

(12) Time dependent simulation

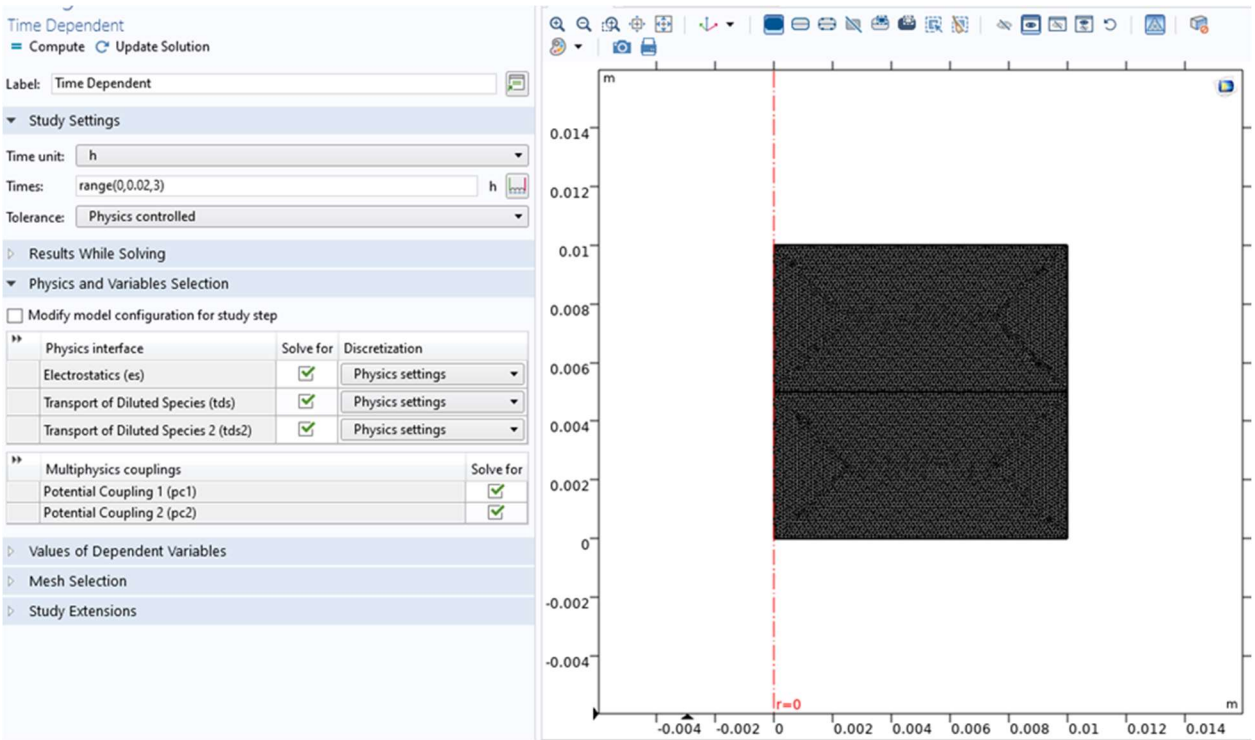

List of Publications, Presentations and Awards

Publications

1. **N. Wang**, A. M. Allgeier, L. R. Weatherley. An electrospray-based flow reaction system for intensified transfer hydrogenation of acetophenone. (In preparation)
2. **N. Wang**, A. M. Allgeier, L. R. Weatherley. Controlling reaction rate of phase transfer hydrogenation of acetophenone by application of low external electric field. *AIChE Journal*, 67:e17079, **2021**.
3. **N. Wang**, K. Kaminski, J. Petera, A. M. Allgeier, L. R. Weatherley. Electrostatically enhanced catalytic phase transfer hydrogenation of acetophenone under low external electric field. *Chemical Engineering Journal*, 374, 1096-1101, **2019**.
4. J. Dou, Z. Sun, A.A. Opalade, **N. Wang**, W. Fu, F. Tao. Operando chemistry of catalyst surfaces during catalysis, *Chemical Society Reviews*, 46, 2001-2027, **2017**.
5. Y. Tang, L. Nguyen, Y. Li, **N. Wang**, F. Tao. Surface of a catalyst in a gas phase, *Current Opinion in Chemical Engineering*, 12, 52-61, **2016.**

Awards

2021 Kansas Corn Next Generation Scholarship (Kansas Corn Commission)

2020 Doctoral Student Research Fund Award (University of Kansas)

Presentations

1. 2019 AIChE Annual Meeting, Poster presentation, November 10 - 15, Orlando, FL
2. 2019 AIChE Spring Meeting, Poster presentation, March 31 - April 4, New Orleans, LA
3. 2018 AIChE Annual Meeting, Poster presentation, October 28 - November 2, Pittsburgh, PA
4. 2016 ACS Midwest Regional Meeting, Poster presentation, October 26 - 28, Manhattan, KS